AD-763 499

GLASSY CARBONS

Edward E. Hucke

Michigan University

Prepared for:

Advanced Research Projects Agency

June 1973

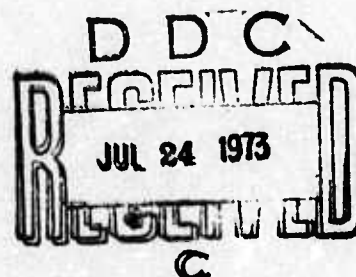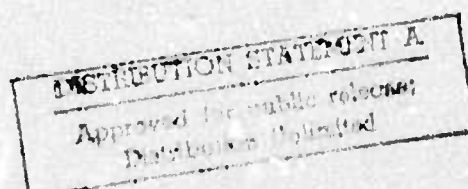Semi-Annual Progress Report

for the Period January 1, 1973 to June 30, 1973

Glassy Carbons

June 1973

Sponsored by
Advanced Research Projects Agency
ARPA Order No. 1824

Department of Materials and Metallurgical Engineering

GLASSY CARBONS

Semi-Annual Progress Report for the Period
January 1, 1973 to June 30, 1973

June 1973

ARPA Order Number: 1824
Program Code Number: 1D10
Contractor: The Regents of the University of Michigan
Effective Date of Contract: 1 June 1973
Amount of Contract: $150,000
Contract Number: DAHC15-71-C-0283
Principle Investigator: Professor Edward E. Hucke
                        Department of Materials & Metallurgical
                                    Engineering
                        The University of Michigan
                        Ann Arbor, Michigan 48104
                        (313) 764-3302

The views and conclusions contained in this document are those of the author and should no be interpreted as necessarily representing the official policies, either expressed or implied, of the Advanced Research Projects Agency or the U.S. Government.

TABLE OF CONTENTS

SUMMARY

Measurements of the physical and mechanical properties
of a large number of glassy carbon samples produced from con-
trolled pyrolysis of furfural alcohol resins has demonstrated
that the structure can be tailored very substantially. The
ability to control properties such as density and fine structure
leads to interesting and potentially useful mechanical, physical,
and chemical properties. Section thickness in excess of 2 inches
have been achieved in very fine pored ($<100\overset{\circ}{A}$) glassy carbons in
processing times of less than six days.

The carbon's fine structure determined by electron micro-
scopy, electron diffraction and X-ray diffraction is not homo-
geneous on a size scale below 100 Angstroms. The material is
paracrystalline with the crystallite size ranging from $10\text{-}100\overset{\circ}{A}$
depending on processing, and with some very crystalline features
occasionally existing in sizes up to $500\overset{\circ}{A}$.

Thermodynamic measurments of the configurational enthalpy
and entropy of various glassy carbons relative to graphite con-
firms that their structures are significantly different. Com-
parison of the measured values with calculated entropies shows
that there must be substantial disorder existing within the solid
carbon rather than its structure being merely microcrystalline
graphite. The thermodynamic measurements also yield a measure
of the fraction of surface sites covered by oxygen which is
found to be higher for glassy carbons than for graphite.

Helium, xylene, mercury intrusion, small angle X-ray scattering, surface area analysis, and scanning electron microscopy show the pore structure of glassy carbons may be either isolated or interconnected, and in a size range from $5\overset{\circ}{A}$ to 50 microns. Mechanical strength has an approximate inverse relation to the pore size. The pore structure allows a decrease in density, as well as the opportunity to vary mechanical properties and provide chemical filtering and absorption appliances with substantial strength.

GLASSY CARBONS

I.   Introduction

This report covers work carried out during the period
January 1973 to June 1973.   Results of the previous contract
periods are summarized in three previous semi-annual reports.[1,2,3]
Since various property evaluations are being carried out simul-
tanesouly, the data tables included in this report are cumu-
lative and nave been revised to reflect additional samples as
well as corrected in certain instances where more reliable
measurements were obtained.   Cumulative data tables are given
in Appendix A.

Glassy carbons have already been shown to have an unusual
set of properties, particularly with respect to inertness and
high strength to weight ratio.   These attributes, together with
the ready availability and high temperature capability of carbon
naturally lead to potential applications in a wide variety of
extreme conditions, such as reentry shields and sliding seals.
Aside from mechanical applications, the unusual inertness in the
human body has lead to various biomedical applications, while
its electrical properties have shown experimental promise as a
semi-conductor switch[4], and its molecular sieve properties
suggest applications in chemical separations[5].

Glassy carbon is still a new material and at present is

costly and available commercially only in thin sections. The
high cost and section limitation both stem from the need to use
very long pyrolysis cycles in order to obtain material without
cracks. A major objective of this research has been to achieve
larger section bodies with rapid processing times.

All of the glassy carbons are made from a variety of
polymers and gaseous precursors and are hard, strong and light;
but many subtle variations exist and considerable tailoring of
properties is possible. A major difficulty in comparing the
various carbon materials is that no simple criteria are avail-
able to distinguish one from the other. In general, many of
the physical and mechanical properties show significant differ-
ences and one can give a comparison of one material with another
only by specifying a complete property set. All of the properties
derive ultimately from the structure and therefore it is important
to be able to elucidate, control, and specify the structure of
the material. The lack of a well-defined crystalline structure
severely complicates matters since not only are the usual micro-
structural features (.1 to 100 microns) important, but also
variations in the ultrastructure (3 to 100 Angstroms) are en-
countered. Even a seemingly straight-forward property such as
real density becomes elusive because it can vary on the size
scale of the order of 50Å.

With an understanding of structural variations possible,
extension in the range of properties achievable can be made.
From data previously available in the literature and the early

results of this program[2,3], it has become obvious that "glassy carbon" is not a single material, since even though it contains essentially only carbon atoms, its structure can be varied at all size levels. It seems more appropriate to think of glassy carbon as a material that may have short range atomic coordination with a variable state of crystallinity; but in addition, where rather large fractions of thermally stable voids can be arranged at size levels from 5 Angstroms to 50 microns. This accounts for the low density and extremely wide variation in properties that can be achieved. The incorporation of voids into materials is not unique. However, it is unique to have up to 30% void remain stable in material at temperatures close to sublimation when the pore size is well below 100 Angstroms.

The porosity is often on such a fine scale and so stable that it must be considered as a feature of the crystal structure. The pore structure may be completely closed giving the material a gas impermeability or interconnected yielding sieve-like properties.

In addition to the pore structure, previous results[3,6,7] have shown the presence of a small amount of very crystalline regions ranging upwards in size to a micron. The regions are well crystallized graphite and other crystalline polymorphs of carbon.

The bulk of the structure also possesses some crystal- linity on a scale of the order of 100 Angstroms or less, but the perfection of the crystallites is very poor by usual standards;

and while the crystalline perfection may improve after heating to very high temperature, a well-defined graphitic structure is not achieved without unusual methods. The structure is better described as para-crystalline in the sense used to describe certain polymers. In fact, the glassy carbon structures are best considered polymers with vanishing contents of other than carbon atoms. The carbon structures are related to the polymer structures from which they evolve during pyrolysis. This observation follows from the differences obtainable in structure and properties of carbons after heating to 3000°C by merely changing the thermal history of the polymer in a temperature range below 100°C where polymer structure is being formed. Thus, even though most of the atoms present in the precursor polymer are later removed, the resulting carbon inherits part of the structure.

The present study is largely concerned with structures obtainable together with the simultaneous measurement of certain key physical and mechanical properties. It is desired to achieve in different samples as wide a variation in structure and properties as possible.

The materials are being investigated from the viewpoints of the solid structure and the pore structure, which of course are related. Since significant differences can be induced in both over a size range of more than four orders of magnitude, no single technique is sufficient. Instead, combined techniques must be used. Each is discussed in the following sections of the report. Representative property measurements are being

-4-

carried out in conjunction with the structural examinations.

Due to the large number of samples processed, complete structural and property evaluations are not attempted on every sample. Apparent density, real density, wide angle X-ray diffraction, scanning electron microscopy, and strength measurements are made on every suitable sample. Small angle X-ray scattering, selected area electron diffraction, transmission electron microscopy, thermodynamic analysis, surface area analysis, mercury porosimetry, electrical resistivity, hardness, modulus of elasticity, and internal friction are carried out on a selected small number of samples.

II.   Materials Preparation

During this report period over 380 samples of glassy carbon were prepared with over 100 different processing conditions. The work has continued to concentrate on furfural alcohol and a furfural alcohol resin, Durez 16470 as a carbon yielding material, with para-toluene sulfonic acid (PTSA) as the polymerization catalyst. A single sample made from an experimental heat setting resin (Hercules H-54) has also been produced by molding according to the manufacturer's recommendations. While glassy carbons are obtained in all cases, the yield of good material and response varies for each system. Thus far, the best results have been obtained with the Durez-PTSA system, although this may be due only to the greater experience with this system.

Catalyst levels from 2 to 20% by weight based on the monomer or resin content have been explored. Temperatures for addition of the catalyst and subsequent curing time and temperatures have been varied from several minutes to several weeks with temperatures from -11°C to 150°C. In all cases where a particularly interesting set of properties has been found, a duplicate set of specimens has been made to check reproducibility. In general, reproducibility is fair, but only if meticulous care is exercised to exactly reproduce all conditions. Standard sample cylinders approximately 5 cm in diameter and 20 cm in length have been adopted. Samples up to 15 cm in diameter have been produced from coarser pored material, while a few samples of 5 cm have been made from very fine pored (<100Å) material. The latter samples are far thicker than any other similar material previously reported even though the pyrolysis time of 6 days is much shorter than usual commercial practice.

The yield of crack free material has continued to improve due mainly to increased care in catalyst addition and prevention of trapped bubbles prior to and during casting. The presence of bubbles has been found to cause cracking in the subsequent pyrolysis of the samples.

In order to yield good material, it has been necessary to perform the hardening of the resin systems with a minimum temperature gradient throughout the piece, which often requires cooling after addition of the catalyst. The length of time curing, curing temperature and catalyst level have been varied over wide ranges

-6-

in order to vary structure.

The single-most important factor in obtaining crack free materials in pyrolysis is obtaining a uniform slow heating rate. While heating rates have been varied from 5 to 50°C per hour in the range of room temperature to 1000°C, the yield of crack free material is much greater at the slower rates. Rates up to 200°C per hour appear to cause no difficulty in heating material previously pyrolyzed to at least 700°C. Both flowing nitrogen and reduced pressure pyrolysis have been employed. Thus far, flowing nitrogen appears to yield less difficulty with respect to cracking.

On selected samples, carbon recovery and shrinkage data have been gathered. In both cases the data are comparable with those of the literature, namely a carbon recovery based on the total resin weight of about 55% and linear shrinkage of about 29%. However, differences in both shrinkage and recovery of about 10% can be noticed with varying of curing and pyrolysis schedule.

The Hercules resin H-54 gave a particularly high carbon recovery of 90.9% based on the original resin weight and a very small shrinkage (8.7%). For these reasons this resin merits further study.

Rather subtle differences exist in the cured resins which result in different properties after pyrolysis. Thus far no satisfactory means for quantitatively studying the resin have been developed. Exploratory work using scanning calorimetry has been initiated in an effort to see if the differing final results can be detected from the thermal changes occuring in the polymer stages.

The single-most important processing variable is the
maximum pyrolysis temperature (HTT) which has long been known
to affect the structure and properties. However, all the other
processing variables have some influence even though at this time
the data show no clear-cut correlations. Part of the difficulty
in finding a correlation is undoubtedly due to the fact that the
exothermic polymerization causes heating of parts of the sample
above the temperatures of intended control. It is also probable
that many of the effects noted in mechanical properties may be
due to the existence of very fine cracks or possibly residual
macroscopic stresses in specimens that appear to be macroscopically
sound. In this case, a particular processing change may appear to
cause a large effect on the properties, but may only aid in
yielding a more flaw free sample.

III.   Structural Studies

While the eventual goal of this study is to correlate
structure at various stages of the process with properties, the
results thus far are largely drawn from samples taken at only
two processing stages. The first stage corresponds to a maximum
temperature exposure in the range 650-1000°C, while the second
stage is that formed at about 2000°C. Some samples have been
examined at HTT between 1000°C and 2300°C, since for given pro-
cessing conditions maximum values of mechanical properties were
noted in this range.

The techniques chosen for structural examination fall

into two broad categories with respect to the information yielded. The first yields information predominantly about the state of the solid make-up of the structure, while the second deals mainly with the void structure. In the first category this study is employing bright field and dark field transmission electron microscopy, electron diffraction, wide angle X-ray diffraction and scanning and electron microscopy. The last two methods also yield information on pore structure.

Additional techniques used to establish the pore sturcture are small angle X-ray scattering, helium pycnometry, mercury porosimetry, and surface adsorption.

An attempt is also being made to gain structural information through a precise measurement of the thermodynamics of the equilibrium

$$C_{graphite} = C_{glassy}$$

Since the effort required to carry out the above techniques varies substantially, a complete set of data is collected on a limited number of samples after screening with more routine tests.

A. Solid Structure

X-ray Studies

Several useful measures of the state of non-graphitizing carbons can be derived from wide angle X-ray diffraction. The usual data for $d(002)$, L_c, $d(10)$, and L_a have been measured for

a sample from each processing condition with the results reported in Table 1 of the appendix. The procedures are the same as previously reported[2]. The "crystallite size" parameters, L_c and L_a are in reality only line broadening parameters and can not be literally interpreted as the size of graphite crystals, since the analysis considers only size broadening of highly crystalline material and ignores strain effects[8] and the possibility of a distribution of layer spacings. However, these parameters are useful for comparing different samples of glassy carbon and they do correspond very roughly to a paracrystalline size determined by electron diffraction and microscopy.

The results obtained to date are similar to others in that they show an increasing L_c and L_a, and decreasing d(002) as the pyrolysis temperature is raised. One such example of this variation can be seen in Figure 3. These results are consistent with the idea that the structure is based on imperfect layers from 15 to 50 Angstroms thick with a layer spacing significantly larger than graphite (3.35Å).

As previously reported, a large number of samples, but not all, show multiple reflections within the (002) line giving the impression of a multiple phase material. These samples have been designated as 2P, 3P or NVS in Table 1 where other than a smooth broad 002 peak exists. These results give strong support for the behavior postulated by Houska and Warren[9] for carbon blacks where they concluded nearest-neighbor pairs of layers assume the ordered graphite relation independently. Layer spacings

of 3.35Å and 3.44Å exist presumably corresponding to ordered
and disordered pairs, respectively. In the present study the 2P
or 3P samples show very good agreement with these values. There
is a strong tendency toward multiple reflections with higher
pyrolysis temperature, and some correlation with longer curing
times and higher catalyst concentration. However, there are many
reversals and no satisfactory reason can now be offered to ex-
plain why this behavior is sometimes present and sometimes not.
It is possible that sharp lines are always present in the (002)
but that their intensity is too low to allow resolution in all
but exceptional cases. The electron diffraction results support
this finding.

The only clear-cut correlation between the X-ray data
and any processing variable or measured property exists with HTT.
While additional correlations may be possible, it appears at
present that the X-ray data are not very sensitive indicators
of the structural differences that influence the measured proper-
ties. The table below indicates the relation of L_c to pyrolysis
temperature.

HTT °C	Lc, Angstroms
700	15-18
1300-1450	18-26
1500-1700	19-29
2000-2300	25-110

However, for a given HTT, a variation outside the experimental
uncertainty exists for samples with no other apparent processing
differences.

Electron Microscopy and Diffraction

Transmission electron microscopy (TEM) is being used
to examine the microstructure of selected glassy carbon samples.
Samples for direct TEM and selected area electron diffraction
(SAED) are prepared essentially the same way reported earlier[1,2,3].

No new features have been observed by any of the electron
microscopic techniques, although any additional examples of all
those reported previously[3] have been encountered. It may be
concluded that all the glassy carbons thus far examined are
quite heterogeneous on a size range below 100Å. The various tech-
niques used yield structural parameters that are at least approx-
imately consistant within themselves and with the wide angle
X-ray data.

A large portion of the material is very disordered and
appears to be granular on a size range of 20 to 60Å. The size
and crystalline perfection of these areas increases with HTT but
never very closely approaches graphite. The granular material
is arranged in platelets (150-500Å) and in a few cases rod-like
morphology. In addition there is a small but definite amount
of very crystalline material which sometimes is larger than 500Å.
Of this crystalline fraction, most gives a well-defined graphite
pattern while some give patterns definitely not assignable to
graphite. These areas are detectable well before any evidence
is seen in X-ray diffraction patterns. In general, these findings
parallel those of Whittaker[7], and give a hint to the cause of the
variability of properties achievable in the material.

-12-

Thermodynamics

The measurements of the Gibb's free energy change for the equilibrium

$$C_{Graphite} = C_{Glassy}$$

have shown encouraging results as a means of structurally differentiating various glassy carbons. This measurement as a function of temperature allows the evaluation of both the configurational enthalpy and entropy. The first gives a measure of the energies of missing atoms, strained bonds and similar defects while the second relates to the disorder relative to perfect crystalline graphite[1,2,3,10].

The measurement currently employed measures electrically the difference between graphite and glassy carbon maintained in their respective equilibrium oxygen partial pressures at a given temperature. It has been demonstrated that the cell yields a precise value for the equilibrium

$$CO_2(g) + C_{Graphite} = 2CO(g)$$

when one side of the cell is held at a known oxygen partial pressure, i.e., air. It was also previously shown that the cell gave near zero output with the same graphite on both sides and gave the expected linear free energy versus temperature relation when an unknown glassy carbon was used on one side. The equilibrium could be attained on either heating or cooling and was stable in the temperature range studied, 700°-1025°C. Additional

examples of this behavior are given in Fig. 1 for a commercial carbon and for an experimental resin (H-54) supplied by the Hercules Chemical Company. The lines shown are least square fits. The configurational entropy and enthalpy are the slope and intercept at zero absolute temperature, respectively.

Values for all the samples thus far analyzed are included in Table 4 and presented in graphical form in Fig. 2. On this plot the origin represents perfect crystalline hexagonal graphite. It is quite apparent that the various glassy carbons are remarkably different in thermodynamic properties. It should be pointed out that the earlier fused salt runs are less precise and subject to some uncertainties due to electrolyte evaporation and other experimental problems. At least several additional runs are planned in order to further check consistency of results between the two kinds of cell.

The graphite used for the reference is UCC-grade AGSR. Run ZC-15 shows a trial run using a stress recrystallized graphite. In this case the EMF was 1 mv or less throughout the temperature range giving rise to a rather large experimental uncertainty. Both ΔH and ΔS, while small, are opposite in sign from the expected result. Refinements in experimental apparatus and technique may yield more information on this point.

The measurements are for the free energy of carbon saturated with oxygen at a total pressure of 1 atmosphere. For many of the samples the oxygen partial pressures under these condidtions are below 10^{-18} atmospheres. These conditions are

FIGURE 1

FIGURE 2

-16-
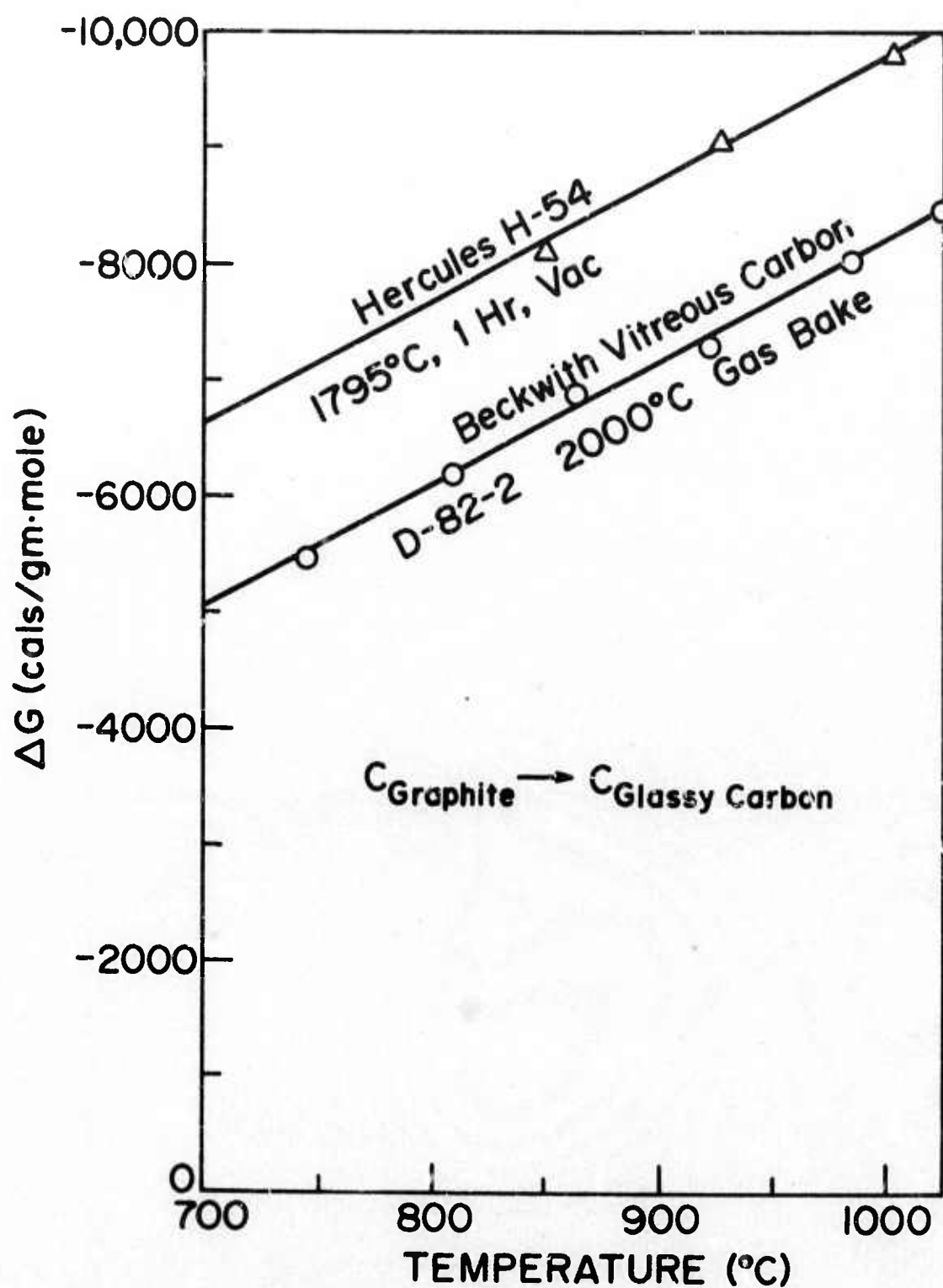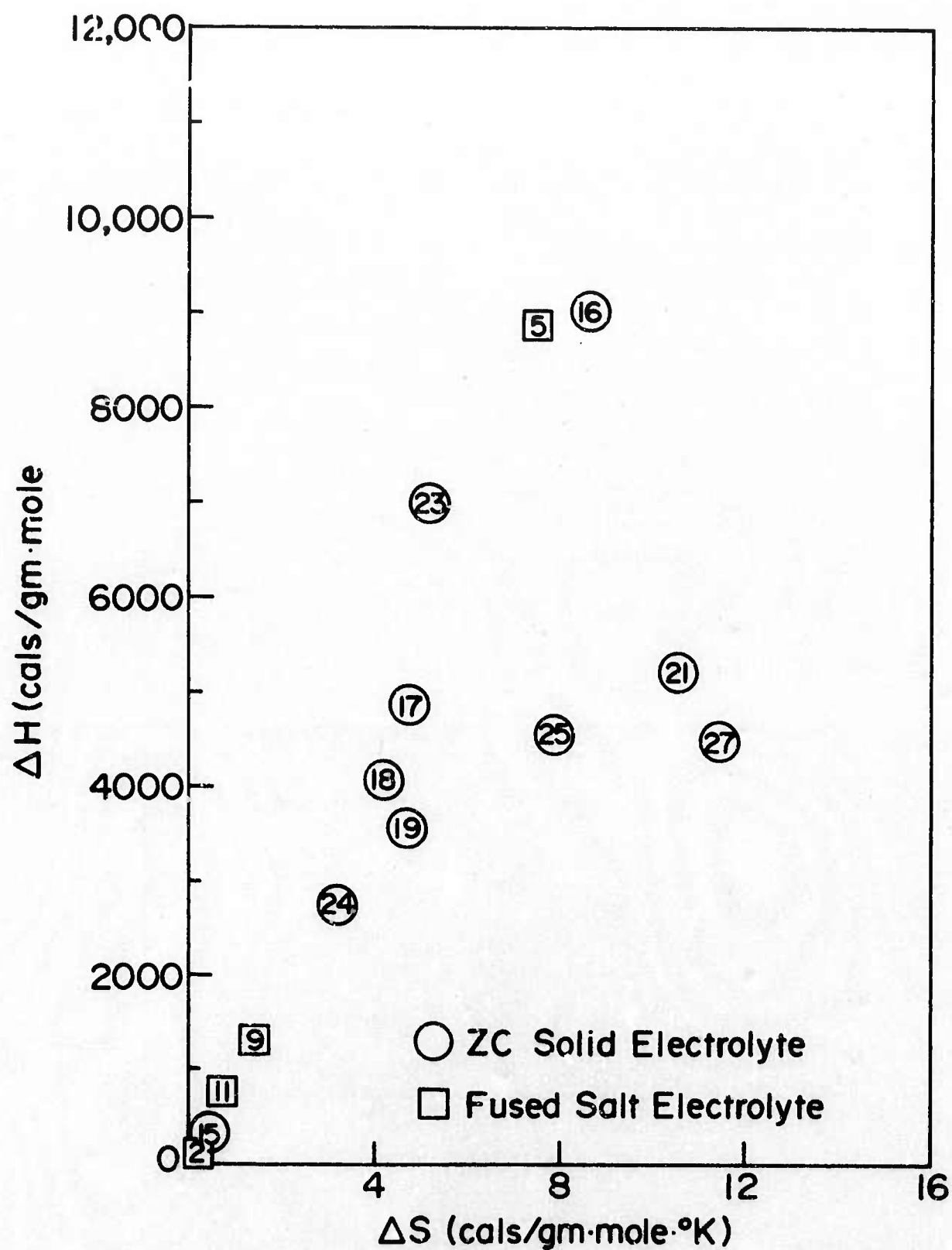
marginal[10] for the calcia-doped zirconia electrolytes and there-
fore yttria-doped thoria and other oxygen sensors are under study
at present to extend the measurement range. The lower range is
set by time required to reach equilibrium and the conductivity
of the solid electrolyte. It appears that 650°C is about the
lower practical limit even with crushed samples.

Thus far, one series has been completed where only one
major variable was changed. The results are shown in Fig. 3,
together with a number of other properties measured on the same
samples. The entropy and enthalpy show the expected trend,
however, it is apparent that not much change occurs from 1250°C
to 1800°C. The enthalpy shows a somewhat larger change in the
same range. Both entropy and enthalpy are quite large, but are
neither the largest nor smallest of all the samples now measured.
Values of ~1500 cal/mole and 5 cal/mole-°K for enthalpies and
entropy have been reported from other types of measurements on
related systems[11].

The X-ray data correlate roughly in this series with the
thermodynamic measurements. However, d(002) shows a significant
change while the atomic configuration is almost constant. This
may well be due to strain relaxation which is confirmed by the
lowering of ΔH. These findings are consistant with the formation
of closed pores as indicated by the steady drop in xylene density.
This is confirmed by the drop in surface area open to nitrogen
(Table 7) and the trend of intrusion pore volume as measured
by Hg porosimetry (Table 8). Unfortunately, no reliable void

FIGURE 3

-18-
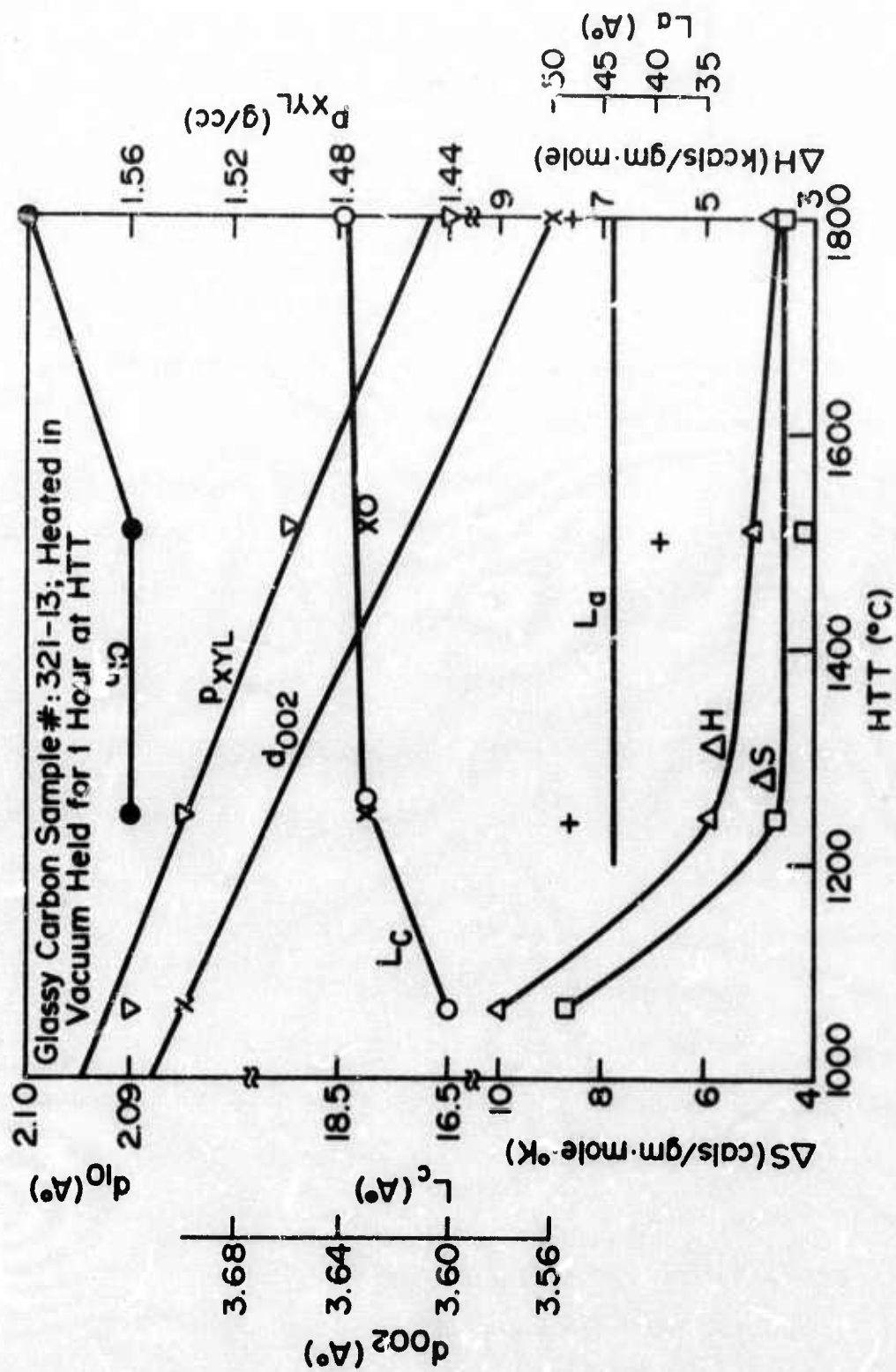
measurements from small angle X-ray scattering are yet available for these samples.

It is also worthwhile to note that a given value of d(002) does not necessarily correspond to a given disorder. For example, the Beckwith-2000°C sample shows X-ray parameters roughly equal (Table 4) to those of 321-13-1900°C, but it has far higher disorder, i.e., 10.5 versus 4.23 cal/mole-°K.

There is also some indication that the atmosphere of high temperature treatment is important. Sample 321-13 shows a higher disorder after treatment to 2000°C in N_2 than 1800°C in vacuum.

It is also worth noting from Fig. 2 that the highest values of disorder do not necessarily indicate a high value of enthalpy.

The cell measurements also yield useful information about the fraction of sites occupied by oxygen by using an independently measured value for the oxygen exchange equilibrium:

$$CO_2(g) + C_f = CO(g) + C_o \qquad\qquad I$$
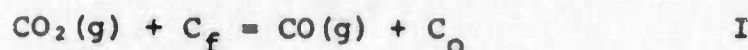
$$K_I = \frac{P_{CO} \cdot C_o}{P_{CO_2} \cdot C_f}$$

$$C_o + C_f = C_t$$

In this formulation C refers to the number of sites for surface oxygen per unit weight and the subscript designates the total number (C_t), the number of occupied (C_o), and the number free, (C_f).

The value for K_I determined in the range $800°$-$1400°C$ is

$$\ln K_I = -\frac{11,575}{T} + 8.50$$

The same value of K_I applies for activated graphite, activated charcoal, and Ceylon graphite and it is therefore presumed to be independent of type of carbon[12].

Simultaneous exchange of oxygen and carbon can occur according to the reaction

$$C_O = CO(g) + n \, C_f \tag{1}$$

where n is either $0, 1$, or 2, depending on the type of surface oxygen complex.

If one considers the bulk reactions,

$$C(s) + CO_2(g) = 2CO(g) \tag{II}$$

$$CO(g) + \tfrac{1}{2}O_2(g) = CO_2(g) \tag{2}$$

$$C_{Graphite} = C_{Glassy} \tag{III}$$
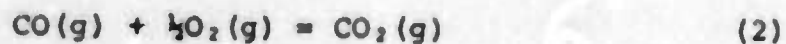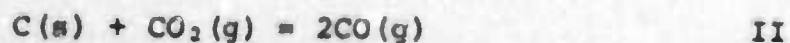
together with reaction I, it is possible to derive an expression for C_O/C_f as a function of the experimentally measured quantities,

$$\frac{C_O}{C_f} = \frac{X_O}{X_f} = \frac{K_I}{2}\left(-1 + \sqrt{1 + \frac{4Pe^{-\Delta G_{III}/RT}}{K_{II}}}\right)$$

In this expression P is the total pressure and is well approximated by

$$P = P_{CO} + P_{CO_2}$$

-20-

while X_o and X_f are the fraction of occupied and free sites, respectively. Of course,

$$X_o + X_f = 1$$

and

$$\ln K_{II} = -\frac{20,503}{T} + 21.0$$

Figure 4 shows the results for 1 atmosphere for graphite and for sample 321-13 with HTT of 1060°C and 1800°C. On the same plot the measured ΔG_{III} are shown for comparison.

An interesting observation is that for 321-13 (1800°C) the fraction of occupied sites is significantly higher than for graphite. This may well account for the well-known lower reactivity of glassy carbon relative to graphite.

Various attempts to calculate the thermodynamic properties from assumed models of structure are being made. While it may, of course, be possible to find models that yield agreement with the ΔS and ΔH measurement, it will of course never be possible to establish the existence of the particular model in this manner. It is, however, possible to show that some structural models are not consistent and can therefore be ruled out.

First, it may be asserted that the relatively large configurational entropies already measured can not be rationalized with a purely microcrystalline model. If the material were perfectly crystalline, there would be no configurational entropy associated with the solid. Introduction of large numbers of

-21-
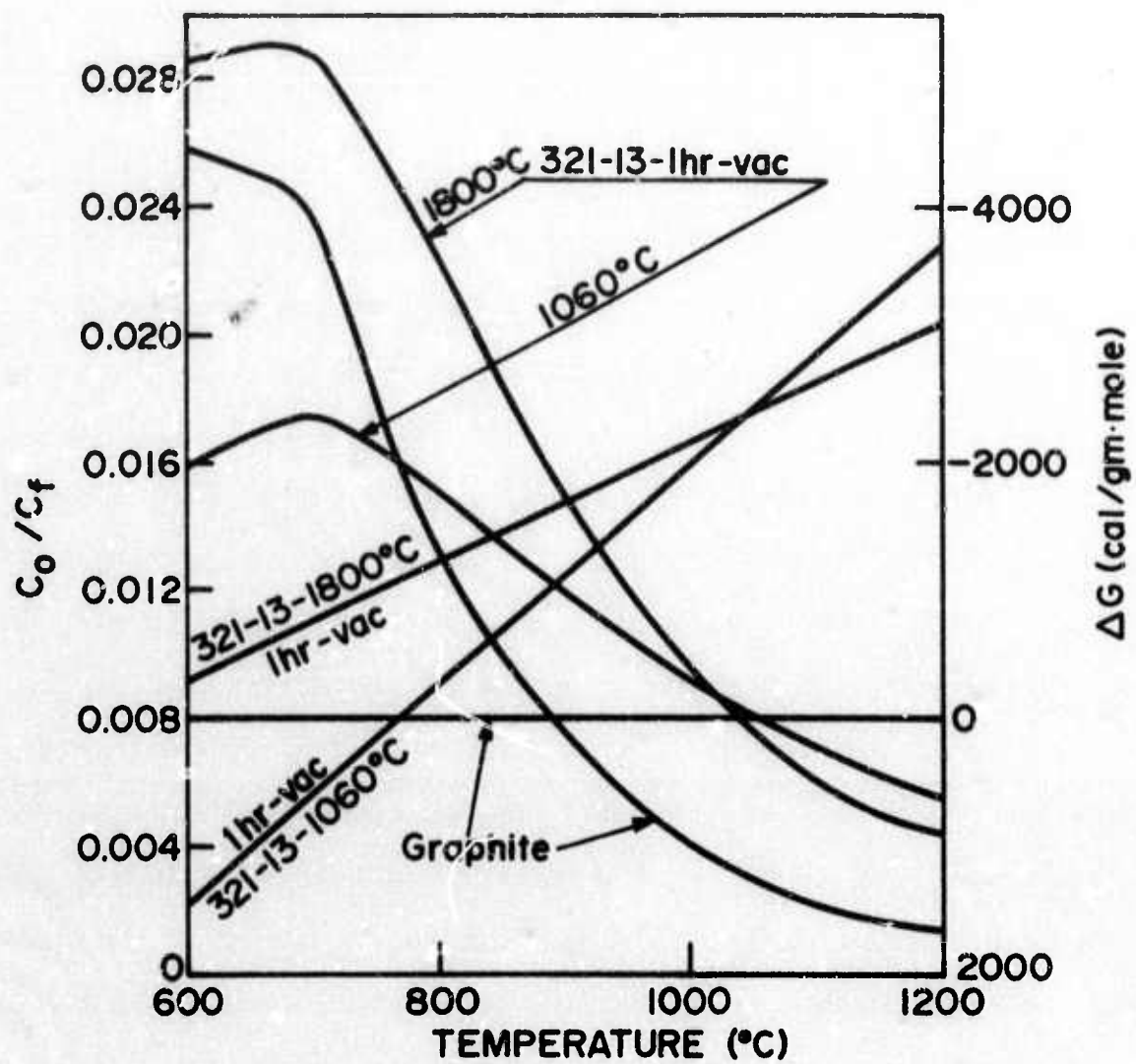
FIGURE 4

atomic defects within layer planes is unlikely and still would not yield entropy values of the magnitude observed.

If one uses the estimate of surface area (500 m^2/gm) derived from small angle X-ray scattering measurements[13] together with reasonable values for surface entropy (1 erg/cm^2-°K) and energy (2000 ergs/cm^2) for carbon, it would be possible to account for only 1.5 cal/mole-°K in entropy and 3000 cal/mole-°K enthalpy.

Assuming a crystal size approximated by ℓ_c and ℓ_a from X-ray data would yield as an upper bound interfacial entropy and enthalpy of 1.2 cal/mole-°K and 2500 cal/mole, respectively.

Since many of the carbons studied have yielded entropies substantially in excess of any of the estimates, it is concluded that there must be substantial disorder on a scale of atomic dimensions within the solid phase.

A first approximation calculation of the entropy introduced by introducing stacking faults through random mixing of rhombohedral stacked sequences and hexagonal sequences can be made as follows:

Consider an ensemble of N carbon atoms stacked ideally in n_ℓ layers of equidistant and parallel planes. Let the fraction of carbon atoms participating in rhombohedral and hexagonal stacking be x and y, respectively, then

No. of atoms in rhombohedral sequences = Nx

No. of planes in rhombohedral sequences = Nx $\cdot$ $\dfrac{n_\ell}{N}$ = $n_\ell \cdot x$

No. of planes in hexagonal sequences = $n_\ell y$

No. of sequences of planes stacked ABC = $\dfrac{n_\ell \cdot x}{3}$

No. of sequences of planes stacked AB = $\dfrac{n_\ell \cdot y}{2}$

Total No. of sequences = $n_\ell(x/3 + y/2)$

The number of ways Ω of arranging the n_ℓ planes in the above sequences is

$$\Omega = \frac{[n_\ell(\frac{x}{3} + \frac{y}{2})]!}{(n_\ell \frac{x}{3})!\,(n_\ell \frac{y}{2})!}$$

The usual Sterling's approximation yields

$$\ln\Omega = n_\ell(\frac{x}{3} + \frac{y}{2})\ \ln[n_\ell(\frac{x}{3} + \frac{y}{2})] - \frac{n_\ell x}{3}\ \ln\frac{n_\ell x}{3} - \frac{n_\ell y}{2}\ \ln\frac{n_\ell y}{2}$$

The entropy can then be calculated using $\dfrac{n_\ell}{N} = \dfrac{2}{4} = \dfrac{1}{2}$ for perfect graphite layers.

X(%)	S, cal/mole-°K
1	.020
5	.078
10	.120
25	.216
50	.296

where X is the percent of carbon atoms participating in rhombohedral stacking.

If it were assumed that the planes were not made up of hexagons as is usually thought, but were instead quinoidal as suggested by Ergun[14], each plane would have three angular

rotational positions. In this case the total entropy would be increased, but still not to the values observed.

X(%)	S, cal/mole-°K
1	1.11
5	1.17
10	1.21
25	1.30
50	1.39

Another model has been assumed using mixed tetrahedral and trigonal bonding. While there is inadequate direct evidence to substantiate the contentions of Ergun and Tiensuu[18], Noda and Inagaki[17], Kakinoki[15] and Kakinoki et al.[16] that glassy carbon contains some tetrahedral bonding, there is inadequate precision in the radial distribution functions[19],[20] to rule out this possibility.

Of many crystalline forms in which carbon exists, only four, i.e., hexagonal and rhombohedral graphite and cubic and hexagonal diamonds, can be completely characterized, and these are true allotropes, all occuring naturally.

The following coherency relationships have been found[21] in hexagonal graphite and hexagonal diamond:

(100) Hexagonal diamond//(001) Hexagonal graphite

[001] Hexagonal diamond//[210] Hexagonal graphite

[010] Hexagonal diamond//[010] Hexagonal graphite

The planar and linear atomic densities along the above planes and directions match within 10%. In the proposed structural model

various crystalline forms of carbon are considered. It has been assumed that the structure is basically layer type, and the vacant sites and different kinds of carbon-carbon bonds do not interact with each other.

A statistical method has been used to calculate the configurational entropy by Boltzman's equation and a first nearest neighbor quasi-chemical approach has been used to compute the configurational enthalpy. The presence of other types of bonds is assumed not to change the energetics of the existing bonds. Configurational enthalpy, entropy, and the corresponding vibrational contributions have been combined to obtain the total Gibb's free energy of the defective crystal. Then, the equilibrium structural properties have been predicted by minimizing the total Gibb's free energy.

Consider an ensemble composed of $(N+n)$ atom sites, out of which there are n vacant sites and N occupied by carbon atoms. Let the percentage of tetragonal bonded atoms be X and the real density be d_2 gm./cm^3. Every trigonal and tetragonal atom $[N(1-X/100)$ and $X/100$, respectively] has 3/2 c-c bonds in the plane and $\frac{1}{2}$ c-c bond out of the plane. The number of bonds of all kinds considered in this model along with their bond lengths and energies are listed below. The number of bonds have been calculated using first nearest neighbor interaction and the bond energy has been computed using the bond length-bond energy relationship as proposed by Feilchenfeld[22].

Quasi-Chemical Parameters

Kind of Bond	No. of Bonds (Pij)	Bond Length $\overset{\circ}{A}$	Bond Energy Kcal/g-mole bonds (Eij)
AA	$3/2N(1-X/100)^2$	1.415	$-$ 109
BB	$3/2N(X/100)^2$	1.555	$-$ 82
AB	$3N(X/100)(1-X/100)$	Variable	Variable
A'A'	$\frac{1}{2}N(1-X/100)^2$	3.35	$-$ 8
B'B'	$\frac{1}{2}N(X/100)^2$	1.555	$-$ 82
A'B'	$N(X/100)(1-X/100)$	Variable	Variable

A and B refer to the trigonal and tetragonal atoms, and the dash refers to the bonds out of the plane. The configurational enthalpy of the disordered crystal is:

$$-H_c \text{ (Kcal/g-mole)} = \sum_{ij} P_{ij}E_{ij} = 167.5 - 7(X/100)(1-X/100)$$

The configurational entropy of glassy carbon of density d_2 and having X% of tetragonal atoms is:

$$S_c = -\frac{R}{d_1}\left[d_2 \ell n\left(\frac{d_2}{d_1}\right) + (d_1-d_2)\ell n\left(\frac{d_1-d_2}{d_1}\right)\right]$$

$$- 4R\left[\frac{X}{100}\left(1-\frac{X}{100}\right)\ell n\ 2 + \left(1-\frac{X}{100}\right)\ell n\left(1-\frac{X}{100}\right)\right.$$

$$\left. + \left(\frac{X}{100}\right)\ell n\left(\frac{X}{100}\right)\right]$$

The density of the glassy carbon without missing atoms (d_1) can be calculated based on the unit cells of hexagonal graphite and hexagonal diamond. Both the structures have four carbon atoms per unit cell, and hence the volume of the unit cell composed

of X percent of diamond type of atoms would be

$$V_X = [35.17 - 12.51(X/100)] \times 10^{-24} cm^3$$

The density would therefore be:

$$d_1 = 2.27 \ (1-0.003557X)^{-1}$$

It is evident from the papers of Takahashi and Westrum[23] and Takahaski et al.[24] that the heat capacity, and hence both vibrational enthalpy and entropy of glassy carbon approach the value of graphite at higher temperatures. Hence, in formulating the total Gibb's free energy at higher temperatures, the vibrational enthalpy and entropy of graphite have been used. This implicity but unfortunately assumes that the heat capacity of glassy carbon is not a function of its density, d_2, and the degree of disorderness, X.

In the proposed model the appropriate values of energy are reasonably well-known for graphite-graphite and for diamond-diamond bonding. However, recent work[25] on vaporization indicates that a significant amount of the carbon that vaporizes is in molecular groups. This would affect the value used somewhat. The most serious uncertainties lie in selecting the values to be used for the mixed bonding of the type A'B' and AB.

It is reasonable to assume that these energies are bounded by the values for graphite-graphite and diamond-diamond and therefore the calculation has been carried out using three sets of values. Probably the best guess is that the in plane
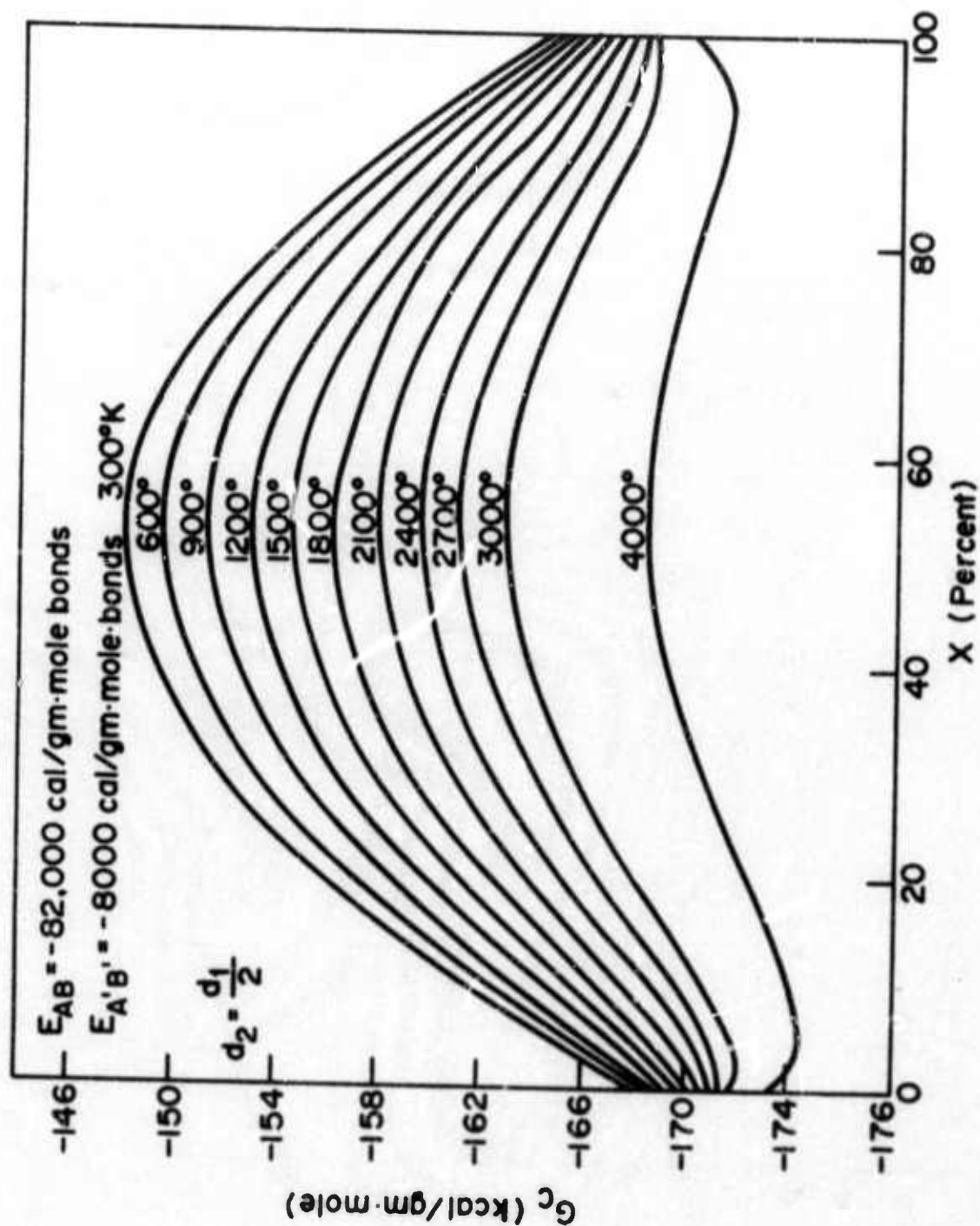
FIGURE 5
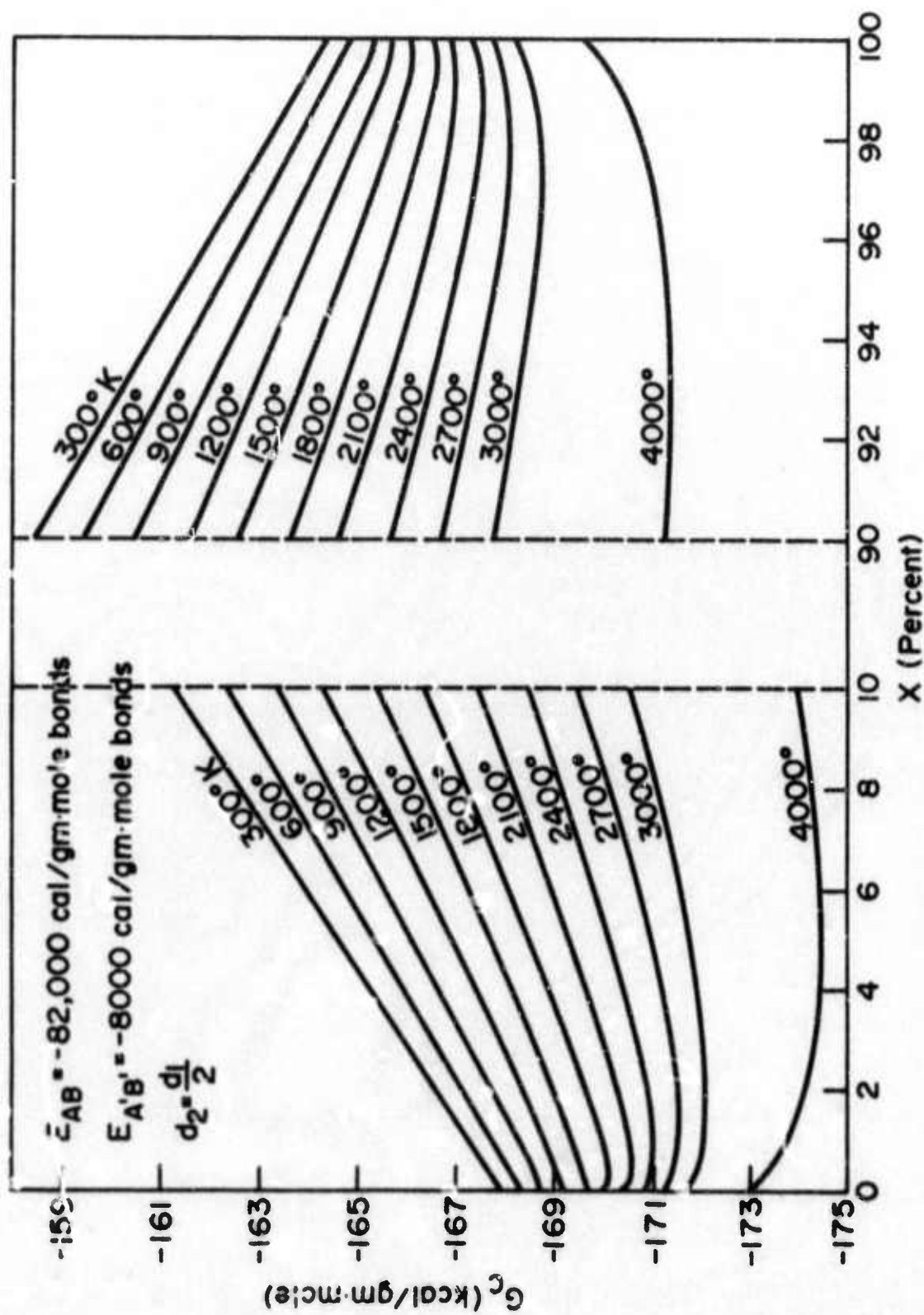
FIGURE 6

bonding approaches diamond and the between plane bonding
approaches graphite. The results of the free energy minimization
for this case are shown in Fig. 5 and 6. The minima always occur
at $d_2 = \frac{d_1}{2}$, but the shapes and locations of the curves are not
very much affected by density. This model yields several inter-
esting features. The system displays the characteristics of
phase separation except that it should be noted that in this case
the overall X of a material may change since it is not subject to
conservation of mass considerations. The results clearly show
that at low temperatures, phases of nearly perfect graphite-
graphite and diamond-diamond are most stable. The graphite phase
is, of course, slightly more stable. As the temperature increases
the minima shift away from the end points. It should be pointed
out that the minima are very "shallow", i.e., very small free
energy differences are involved with shifting of the fraction
diamond bonding near the end points, and there is a significant
free energy barrier to jump between the "pure" phases. In this
case any local regions that by way of early structural arrange-
ment in the precursor polymers involved substantial mixed bonds
would tend to move toward the closest pure phase, but could
not easily jump the free energy barrier between. Any regions
starting with pure bonding would at high temperature develop a
modest amount of mixed bonding, but the free energy changes are
very small as can be seen in Fig. 6 which shows an expanded
scale view of the end point regions.

If the mixed bonding energies are changed to assume the interplane and intra-plane mixed bonding of graphite, the diagram assumes a different character. In this case shown in Fig. 7, a minimum exists in the mid-region of the diagram. The minimum is very shallow at low temperatures. These parameters would predict a substantial amount (~50%) of diamond bonding should exist at high temperature.

The same general features are shown in the model where interplane mixed bonding is that of graphite while intra-plane mixed bonding is that of diamond (Fig. 8). This is the case of the fabled diamond cross-link. In this case a minima occurs in the center region of the diagram, but the free energy of this minimum is substantially lower than the other cases. Such a model would predict that glassy carbons would have substantial diamond bonding. The predicted density of 1.37 gm/cm^3 is not far from the experimental values.

From the foregoing results, it is clear that mixed bonding could very well be present in glassy carbons, but that the form of the free energy curves is quite sensitively affected by the exact energy of the mixed type bond.

Further work in refinement and extension of model calculations is continuing.

B. Pore Structure

The details of pore structure are being investigated with a variety of techniques, including small angle X-ray
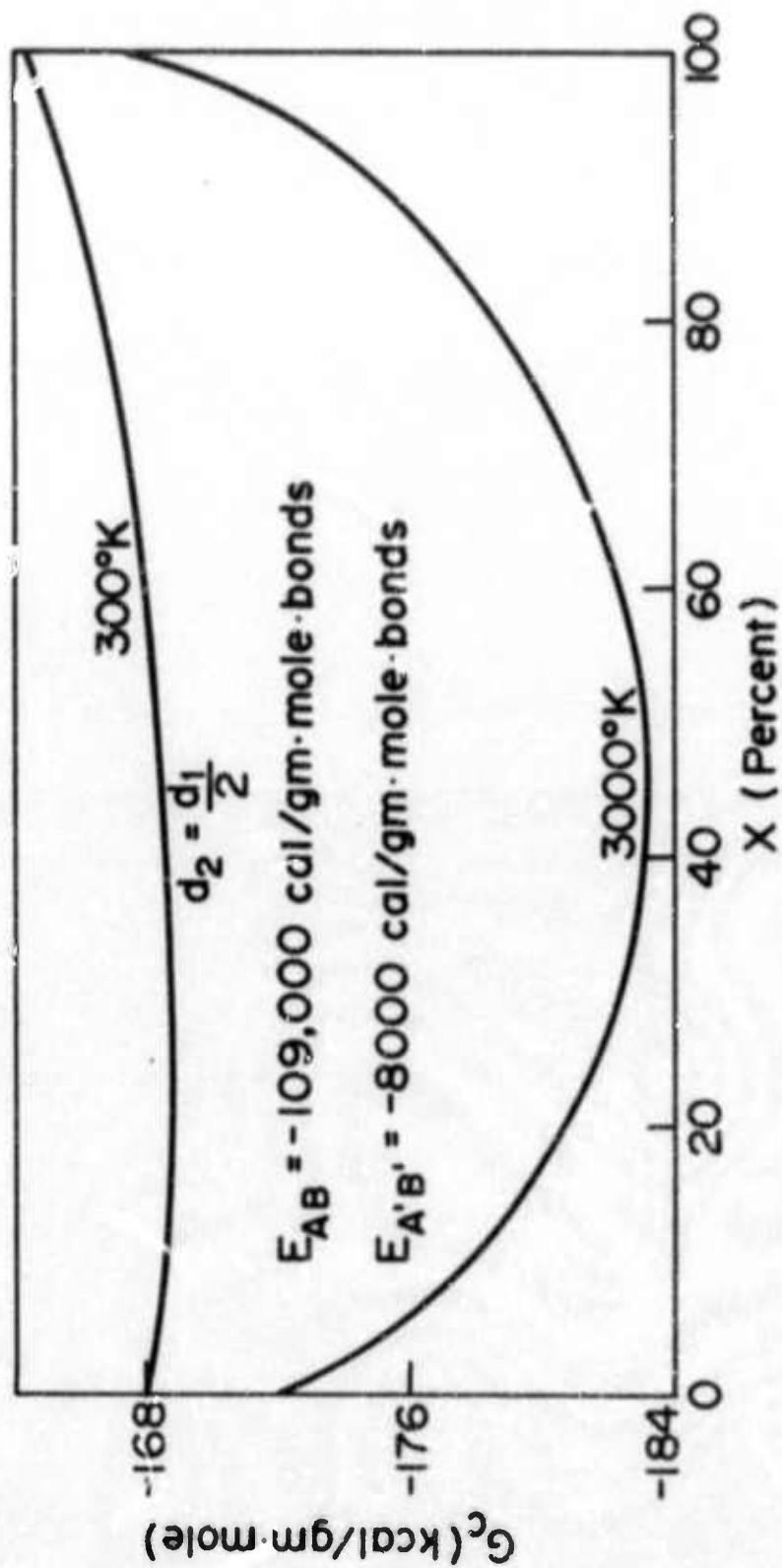
FIGURE 7
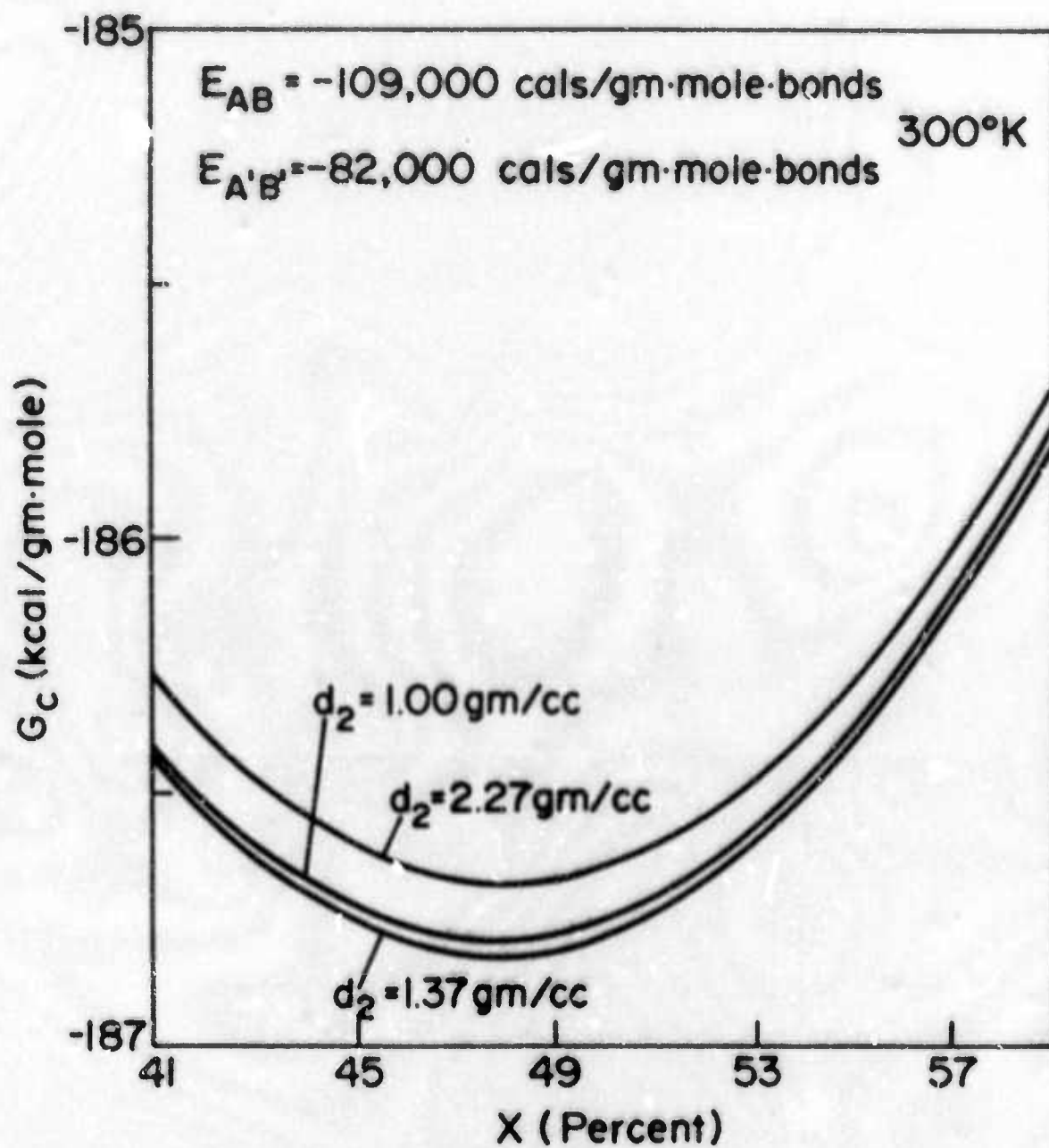
FIGURE 8

scattering, scanning electron microscopy, pycnometry, surface
adsorption, and Hg porosimetry.

Small Angle X-ray Scattering

Small angle X-ray scattering is being used to study
microporosity of selected glassy carbon samples. Recent theo-
retical developments[26-28] in small angle X-ray analysis allow
the determination of general structural parameters of both the
solid and pore phases. Determination of pore size, pore shape,
distribution of pore sizes, internal surface area, length of
coherence, range of inhomogeneity and X-ray density can be done
when a detailed analysis is made. In addition to these parameters,
a knowledge of the helium density permits the determination of
closed and open porosity.

Thus far, only preliminary investigations on a few
selected samples has been accomplished due to experimental
difficulties. Guinier's analysis is used to determine the pore
size. The analysis also indicates whether a sample is monodisperse
or polydisperse. Porod's plot is used to obtain a preliminary
idea of the variation of electron density in the samples.

For the evaluation of Guinier's radius, R_G, of pores
the approximation

$$I(s) = n^2 \exp[- \frac{4}{3} \pi^2 R_G^2 s^2]$$

is considered valid at sufficiently small angles. Here I(s)
is the scattered intensity, n^2 is a constant for a particular

sample and s is $2\theta/\lambda$ (2θ = scattering angle, λ = wavelength of radiation). The plot of log I(s) - s^2 should be a straight line if the sample is monodisperse, i.e., pore size distribution is very narrow. The size of the pores may be calculated from the R_G if shape of the pores is known.

Porod's plot (log I(s) versus s) has been shown to be linear over a wide range of s values if the density transitions between the phases are sharp.

A Rigaku-Denki small angle unit equipped with a proportional counter, automatic step-scanner and digital print-out is being used to measure the scattered intensity. As reported earlier[3], the slot collimation is being utilized because pinhole collimation gives a very small intensity requiring very long experiments. As expected, slit collimation has reduced the experimental time considerably.

Ni-filtered Cu $K\alpha$ radiation is used with a pulse height discriminator to insure that the proportional counter registers counts from a narrow wavelength range. A graphite crystal monochromator will be employed to provide a more perfectly monochromatic wavelength for accurate analysis.

Figures 9-11 show the Guinier's plots for some of the samples studied. In these plots I(s), the observed scattering intensity measured using slit collimation, requires correction for slit smearing. A computer program for making the collimation correction is in progress. The present results have been drawn using the smeared intensity and should be interpreted cautiously.
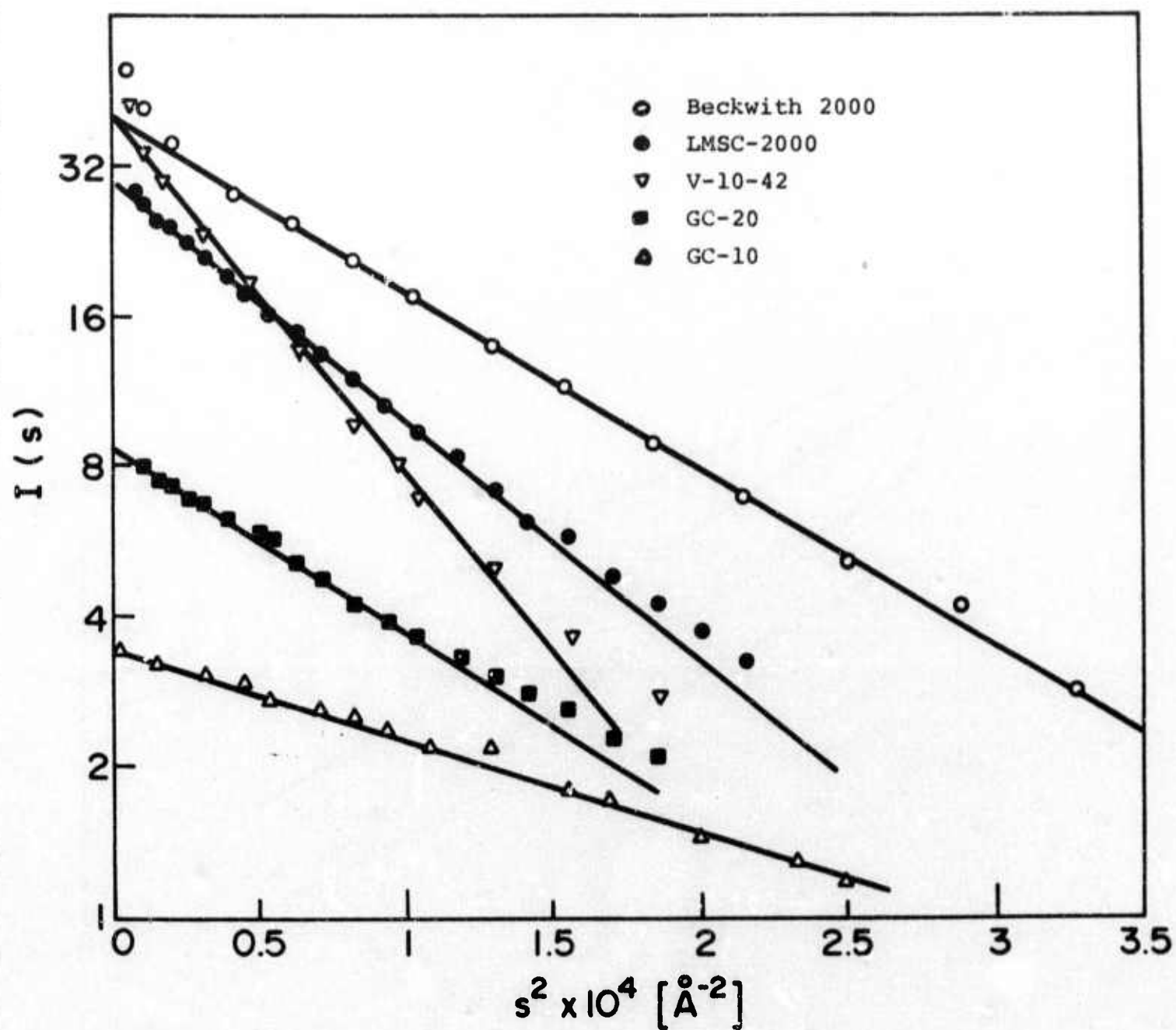
FIGURE 9.   Guinier's plots for various commercial samples
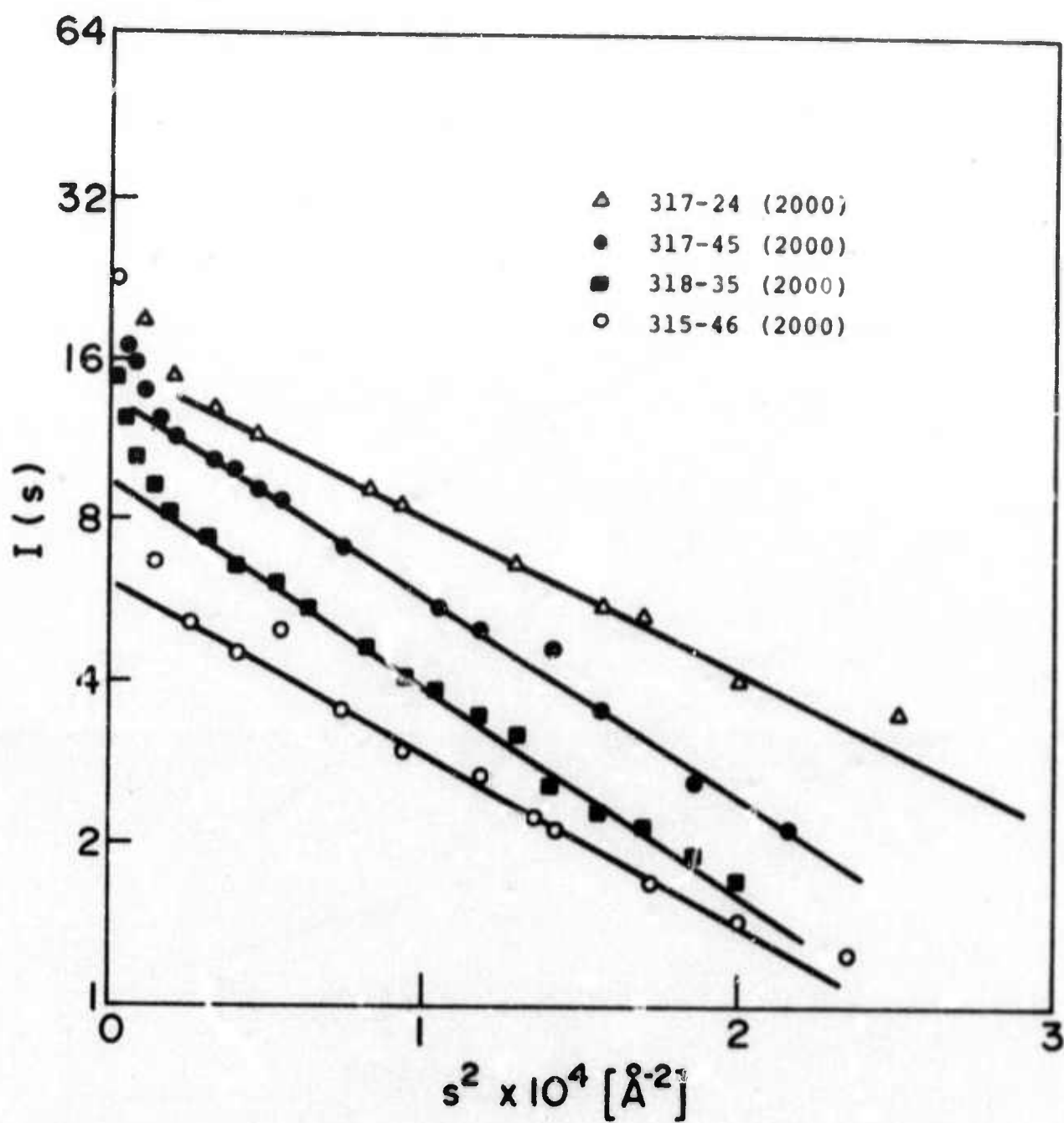
FIGURE 10. Guinier's plots for four of our samples which obey Guinier's law well.
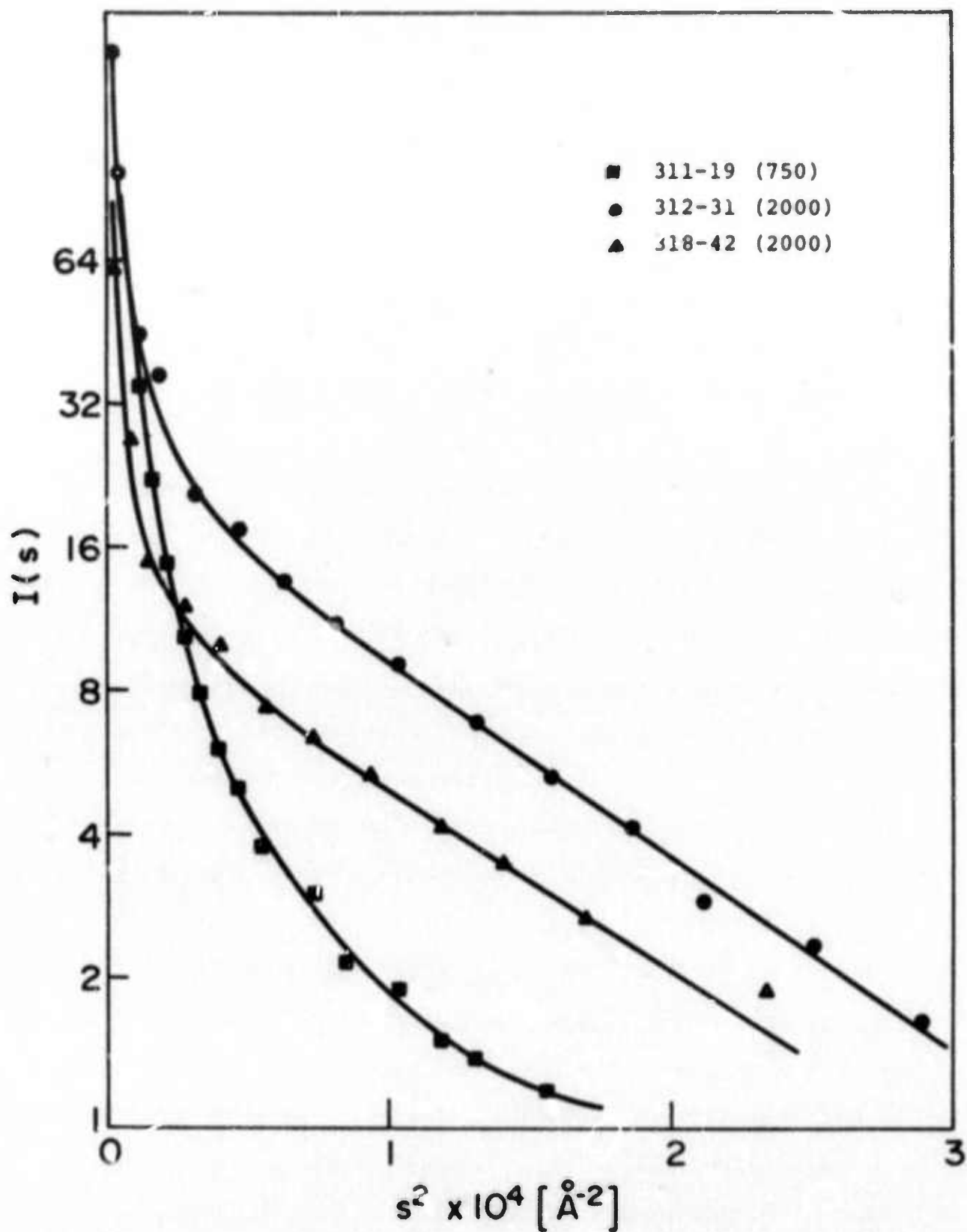
FIGURE 11. Guinier's plots for samples showing polydispersity.

In most of the cases the log $I(s) - s^2$ plot is found to
obey Guinier's law; i.e., a linear relationship from very low
s^2 to about $s^2 = 2 \times 10^{-4}$ $\overset{o}{A}{}^{-2}$. Figure 9 shows the plots for five
commercial samples which obey Guinier's law very well. The R_G
values for these samples along with the reported values are
given in Table 5. As can be seen, our values are much higher
than values reported in the literature. One possible reason for
this discrepancy may be the collimation corrections yet to be
made.

Guinier's plot for several samples which obey the law
well are shown in Figure 10. One can, however, see that in all
of these cases the intensity tends to rise at very low s^2 values,
whereas this was not observed in any commercial samples. This
indicates that in the samples shown in Figure 10, pores larger
than given by R_G are present though probably in small percentages.

Figure 11 shows Guinier's plots for samples 311-19 (750°),
312-31 (2000°) and 318-42 (2000°), none of which obey Guinier's
law well. In 312-31 (2000°) and 318-42 (2000°) a straight line
portion at higher s^2 values may be imagined. However, 311-19
(750°) does not follow a linear relationship at all. It may be
inferred for 312-31 (2000°) and 318-42 (2000°) that most of the
pores are of a size given by the respective R_G values, however a
substantial fraction is of larger size. The sample 311-19 (750°)
is completely polydisperse. Table 6 gives R_G values for samples
made at the University of Michigan.

-40-

The wide range of pore size sometimes encountered is contrary to the notion that glassy carbons have a very narrow pore size range.

Figures 12-14 show Porod's plots for various samples studied. Figure 12 shows equivalent plots for commercial samples. All the plots have two regions. First, a very flat region at lower s values. The second at higher s values is a straight line. The slopes of the straight line portion varies from sample to sample between 2.8 and 3.5. The straight line portion indicates sharp density transition from one phase to another as pointed out by Porod.

Figure 13 shows that the regions at lower s values are not as flat as observed for commercial samples, however, a straight line portion is present in all cases. Figure 14 plots for polydisperse samples show the absense of flat regions. One can see that 311-19 (750°) which is completely polydisperse obeys Porod's law very well from very low to very high s values. Further conclusions must await suitable corrections for collimation.

Electron Scanning Microscopy

At least one fracture surface of each sample has been photographed by SEM. The pictures have proved valuable in checking the uniformity and size of solids and voids in all but the finest material having pore sizes below 100Å. The pore size values obtained agree reasonably with the pore size determined by Hg porosimetry, while the particle size agrees reasonably

-41-
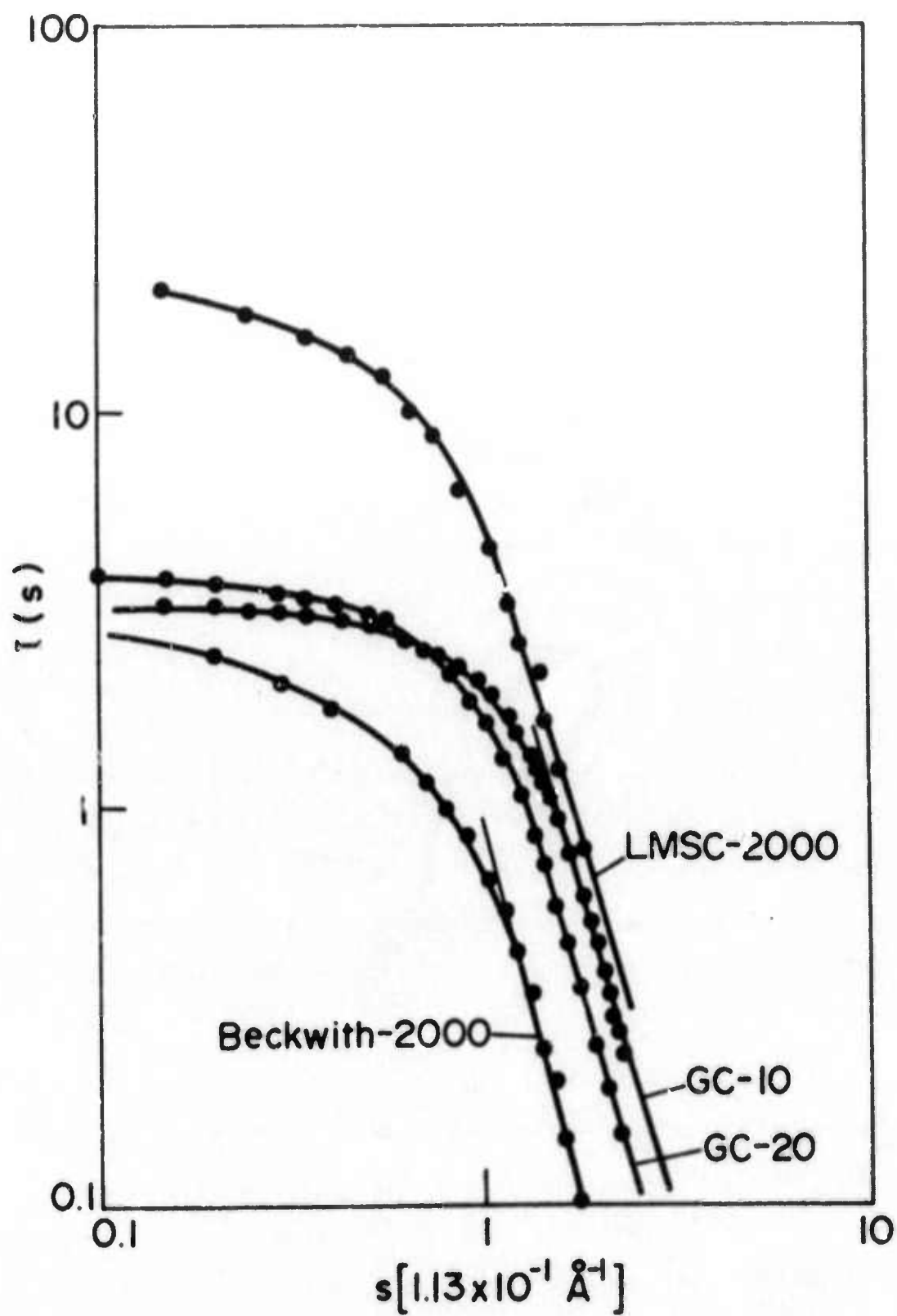
FIGURE 12. Porod's plots for various commercial samples.

-42-
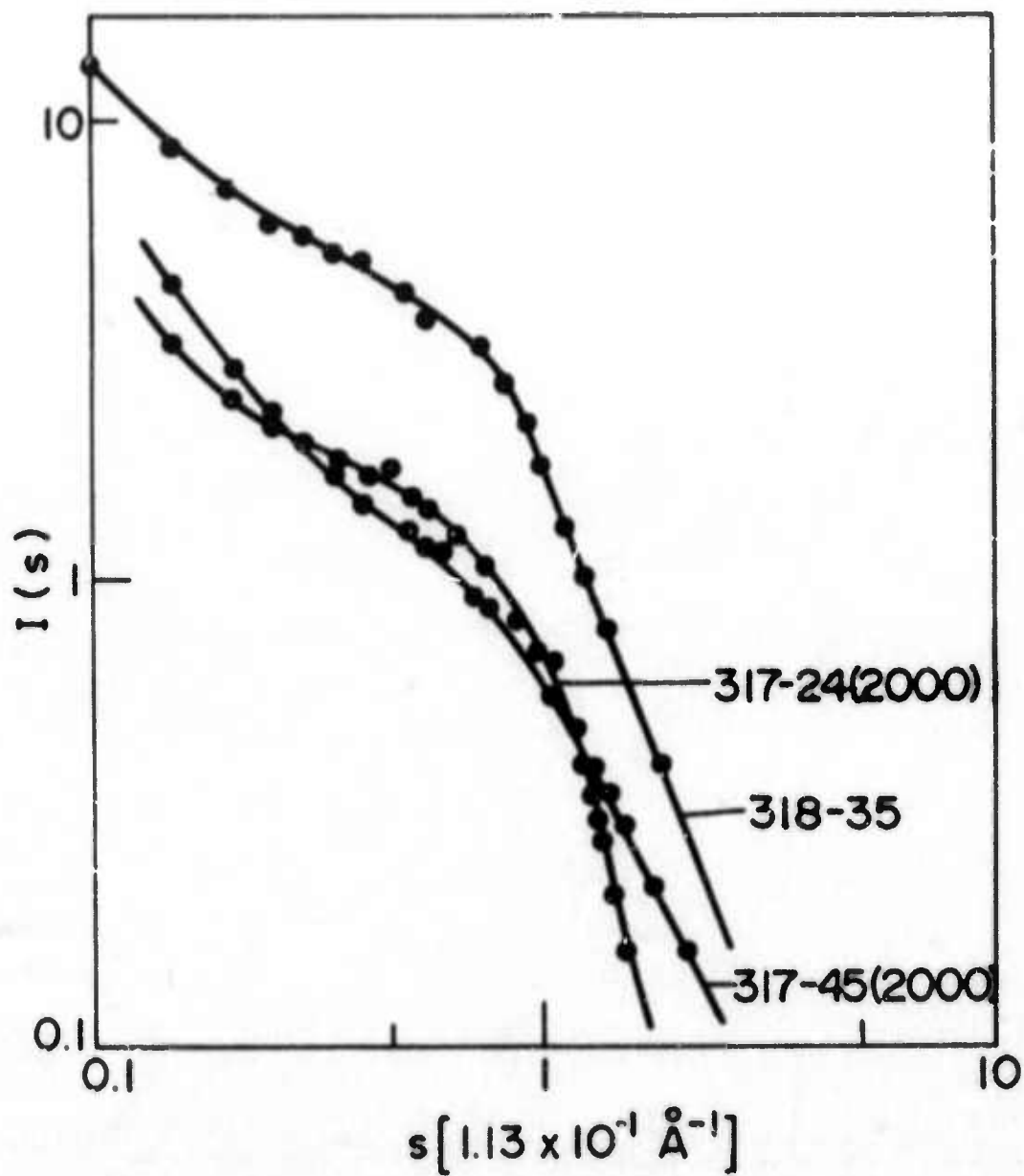
FIGURE 13. Porod's plots for some of our samples obeying
Guinier's law well.

-43-
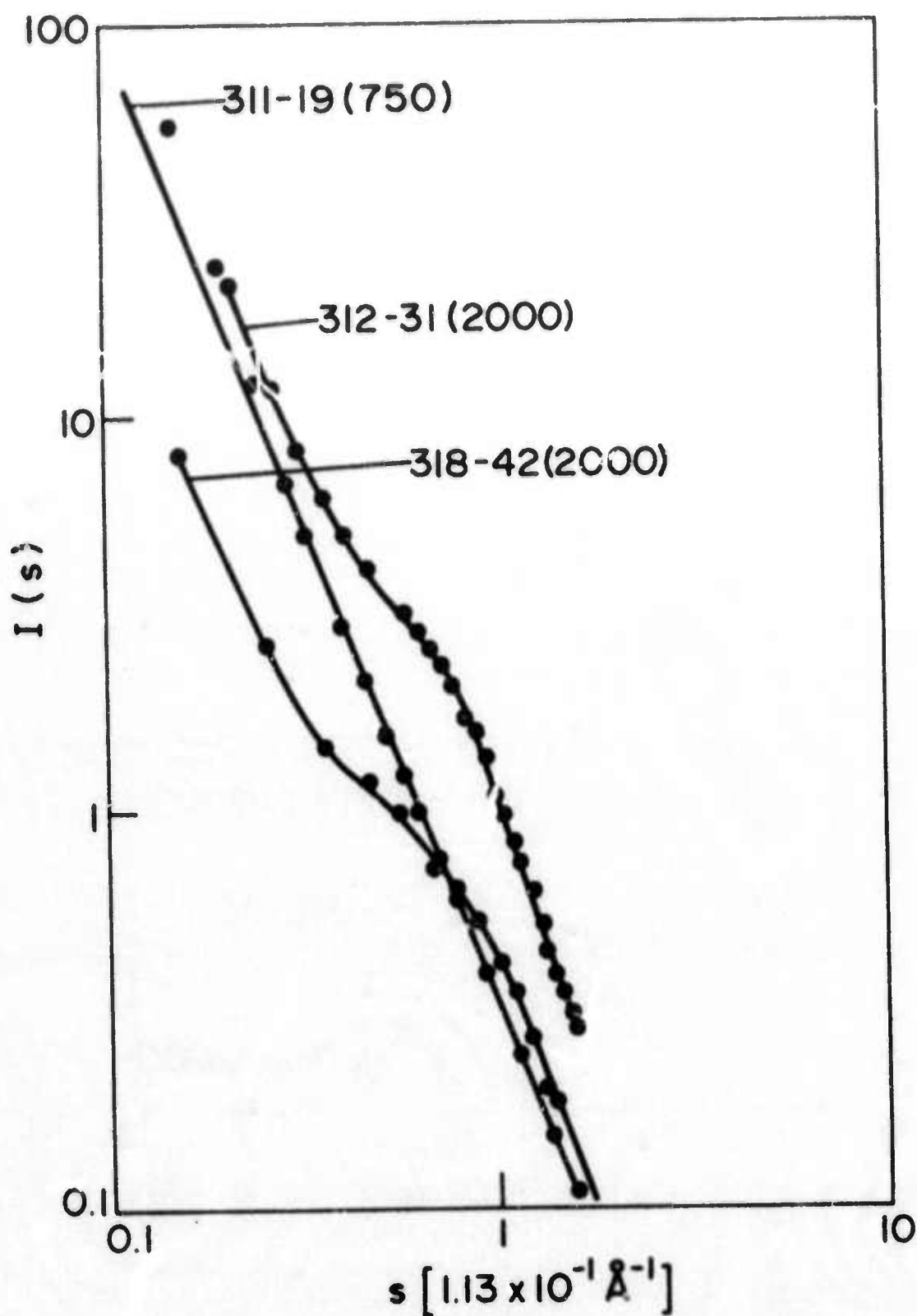
FIGURE 14. Porod's plots for samples showing polydispersity.

with impregnated polished sections obtained with the light microscope. No structural features in addition to those previously reported[1,2,3] have been encountered.

Pycnometry

Xylene immersion density measurements have been substituted for He density due to the inability to achieve accurate, reproducible results. The xylene densities are quite reproducible and show much less sample to sample variation. It was found that the grinding of samples in either alumina or tungsten carbide lined ball mills introduced enough wear material from the liner and/or balls to cause a measurable difference in density. The presence of Al_2O_3 or WC was confirmed by X-ray analysis of the powder. This is a remarkable result in view of the high hardness of the liner materials. At present, samples are pulverized by a small steel hand hammer mill. If prolonged crushing is avoided, no significant iron is picked up.

Data for samples thus far measured, together with the geometrically determined apparent densities, are given in Table 9. Figure 3 shows one example of the variation of xylene density with HTT.

Surface Area

Additional surface area data have been gathered since those in Table 7 reported previously[3]. One series (321-13) was run to establish the change in surface area with HTT. In this case a sample heated only to 367°C was included. It showed a relatively large surface area (257 m^2/gm) but smaller than that

-45-

found for many 700°C samples. At higher temperatures the surface area falls continuously in line with expectation. However, comparing the Hg pore volume and pore size distribution (Table 8) indicates that this drop in surface must be associated with a pore size smaller than 30Å, the approximate lower limit for Hg intrusion.

Mercury Porosimetry

Mercury porosimetry was used to determine pore size distribution, interconnected pore volume, density and median pore diameter values. A summary of data obtained to date is shown in Table 8. In most cases, a rather sharp pore size distribution was observed, however, a few samples yielded a wide distribution. Results to date indicate the possibility of tailoring a pore spectrum at all size levels.

Higher processing temperature (HTT) closes the very fine pores and causes them to grow according to surface area and X-ray scattering results. The macropore system, even though it is very fine (∿30Å) in some cases, changes relatively little up to 2000°C.

IV.   Property Evaluation

Because the glassy carbons under investigation were produced under a wide range of processing variables, a large degree of variation in structure and physical properties was observed. The mechanical properties investigated thus far include hardness (DPH), compressive strength, ultimate tensile strength (Dimetral

compression) and sonic modulus of elasticity. In addition, internal friction and electrical resistivity were measured on selected samples.

Hardness

Hardness testing has been temporarily suspended, since it has thus far been impossible to find a technique that yields meaningful data.

Compressive and Ultimate Tensile Strength

Further results are reported in Table 9 and presented on "reduced" basis in Table 10. Values were revised where additional data warranted change.

Various correlations have been attempted between strength properties and processing variables, apparent density, real density and pore size without great success. The raw data show a broad correlation with apparent density; with higher strength occurring at higher density. Also, a fair correlation exists with intrusion pore diameter, higher strengths with smaller pores. An additional correlation between strength and mean carbon path determined microscopically was attempted, but the results were not encouraging.

The reduced data shown in Table 10 show less range than the raw data. As one method of data reduction, the various mechanical properties are divided by density to yield value of specific strength. On a specific basis these carbon materials compare very favorably with the best available structural materials. Considering the high temperature capability of

-47-

carbon, the comparison becomes even more favorable.

In addition, the area dependent properties have been normalized by either multiplying or dividing by the area fraction carbon, which is proportional to the volume fraction unavailable to He (i.e., ρ_a/ρ_{He}), assuming all pores open to He. It can be seen that this normalization considerably reduces the range of values exhibited by the various carbons. However, since the compressive and tensile strengths are certainly dependent upon macro-structure as well as fine scale binding of carbon atoms, some range of reduced properties is to be expected.

Sonic Modulus and Internal Friction

Additional sonic modulus data have been included in Tables 9 and 10. No new conclusions can be drawn. However, the previous conclusion that glassy carbons have a wide range of modulus is again confirmed. This conclusion is warranted even when made on an area reduced basis.

Internal friction measurements have been discontinued for the present. While remarkable differences in behavior of the various samples have been noted, no straightforward method of correlating these changes to structure has been developed.

Resistivity

Refinements of the measuring set-up have allowed more accurate measurements, particularly at low resistivity. Cumulative data is presented in Tables 9 and 10.

It is interesting to note that the resistivity of nearly all samples on a reduced basis falls between 10^{-3}–10^{-4}

Ω-cm which is the same as for other glassy carbon materials pyrolyzed to 2000°C.

References

1. E. E. Hucke, "Glassy Carbons", Semi-Annual Report, January 1972, Contract No. DAHC15-71-C-0283.

2. Ibid, June 1972.

3. Ibid, January 1973.

4. K. Antonowicz, A. Jesmanowicz, and J. Wieczorek, Carbon 10, 81 (1972).

5. Joseph Lawrence Schmitt, Jr., "Carbon Molecular Sieves as Selective Catalyst Supports", Ph.D. Thesis, The Pennsylvania State University, December 1970.

6. A. G. Whittaker and P. L. Kinter, Science 165, 589 (1969).

7. A. G. Whittaker and B. Tooper, 11th Biennial Conference on Carbon, Extended Abstracts and Program, Gatlinburg, Tennessee, June 4-8, 184 (1973).

8. S. Ergun, 11th Biennial Conference on Carbon, Extended Abstracts and Program, Gatlinburg, Tennessee, June 4-8, 189 (1973).

9. C. R. Houska and B. E. Warren, J. Appl. Phys. 25, 1503 (1954).

10. E. E. Hucke and S. K. Das "A Proposed Method for the Evaluation of the Thermodynamic Properties of the Glassy Carbon-Graphite Equilibrium," Preliminary Reports, Memoranda, and Technical Notes of the ARPA Materials Summer Conference, July 1971, Contract No. DAHC15-71-C-0253.

11. M. C. Shen and A. Eisenberg, Rubber Chemistry and Technology 43, 95 (1970).

12. S. Ergun and M. Mentser, *Chemistry and Physics of Carbon*, Vol. 1, p. 203, Marcel Dekker, Inc., New York, 1965.

13. R. Perret and W. Ruland, J. Appl. Crystallography 5, Part 3, 183 (1972).

14. S. Ergun and R. R. Schehl, Carbon 11, 127 (1973).

15. J. Kakinoki, Acta Cryst. 18, 578 (1965).

16. J. Kakinoki, K. Katada, T. Hanawa and T. Ino, Acta Cryst. 13, 171 (1960).

17. T. Noda and M. Inagaki, Bull. Chem. Soc. Japan 37, 1534 (1964).

Preceding page blank

18. S. Ergun and V. H. Tiensuu, Acta Cryst. $\underline{12}$, 1050 (1959).

19. R. W. Lindberg, "Radial Distribution Analysis of Glassy Carbon, Masters Thesis, Stanford University, October, 1969.

20. S. Ergun, to be published in Phys. Rev.

21. J. S. Kasper, Abstracts, papers presented at the Eighth Conference on Carbon, Abstract No. 179, Carbon $\underline{6}$, 237 (1968).

22. H. Feilchenfeld, J. Phys. Chem. $\underline{61}$, 1133 (1957).

23. Y. Takahashi and E. F. Westrum, Jr., J. Chem. Thermo. $\underline{2}$, 847 (1970).

24. J. Yokoyama, M. Murabayashi, Y. Takahashi and T. Mukaibo, TANSO $\underline{65}$, 44 (1971) (in Japanese).

25. R. T. Meyer, 11th Biennial Conference on Carbon, Extended Abstracts and Program, Gatlinburg, Tennessee, June 4-8, 55 (1973).

26. G. Porod, Z. Kolloid $\underline{124}$, 83 (1951).

27. G. Porod, Z. Kolloid 125, 51 (1952).

28. W. Ruland, J. Appl. Cryst. $\underline{1}$, 308 (1968).

APPENDIX

TABLE 1   SUMMARY OF X-RAY DATA

                    (All values in Angstroms)

                    Symbols Used in the Tables

Experimental Condition

        All the samples were run in a Phillips-Norelco Diffrac-

tometer using CuKα radiation under the following conditions:

        Tube Voltage: 45KV
        Tube Current: 14mA
        Proportional Counter Voltage: 1.622KV
        Proportional Counter Time Constant: 4 sec.
        Chart Speed: 1/2 inch/min.
        Scan Speed: 1.2 degree (2θ)/min.
        Slits: 1°/006"/1° at Primary/Scattering/Secondary

        Sample used of thickness of 3mm in all cases except

where otherwise designated. The value of d(10) refers to the

unresolved (100) and (101) peak.

(002) Peak Type

        S: "Smooth" (or single phase) Peak
        NVS: "Not Very Smooth" Peak
        2P: "2 Phase" Peak
        3P: "3 Phase" Peak

Sample Designation	Temp. (°C)	(002) Peak Type	d(002)	Lc	d(10)	La
Graphite, solid 3mm & 1mm thick		S	3.37	Very High	2.13	Very High
Graphite		S	3.37	Very High	2.13	Very High
Graphite, natural (Reported)		S	3.35	Very High	2.13	Very High
Graphite, synthetic (Reported)		S	3.37	Very High	2.13	Very High

Sample Designation	Temp. (°C)	(002) Peak Type	d(002)	Lc	d(10)	La
Commercial Samples						
Lockheed, solid	2000	S	3.53	21.2	2.09	98.0
Lockheed, reported	2000		3.56	19.0	--	--
Beckwith, solid	2000	S	3.55	23.2	2.09	112.0
Beckwith, reported	2000		3.54	15.0	--	50.0
Tokai, solid	1000	S	3.70	14.2	2.07	43.7
Tokai, reported	2000		--	--	--	--
Atomergic Chemicals Co., V-25, solid	2500	S	3.40	38.4	2.09	69.0
Atomergic Chemicals Co., V-25, reported	2500					
Atomergic Chemicals Co., V-10	1000	NVS	3.44	42.0	2.10	71.0
Atomergic Chemicals Co., V-10, reported	1000		--	--	--	--
Hercules H-54	1795	S	3.49	28.0	2.09	51.0
311-9	2000	S	3.54	28.0	2.10	57.0
311-19	700	S	3.63	18.0	--	--
311-20	2000	S	3.53	27.2	2.10	46.0
311-21	2000	S	3.52	27.2	2.10	54.0
311-22	2000	2P	2.49 3.45	29.0	2.12	>125.0
311-25	700	S	3.70	21.0	--	--
311-30A	2000	S	3.51	23.4	2.10	54.0
311-31	2000	S	3.50	25.0	2.10	51.0
312-8	2000	S	3.52	27.0	2.10	42.0
312-9	2000	2P	3.52 3.45	27.0	2.10	57.0
312-10	700	S	3.65	16.2	--	--
312-10	2000	S	3.49	35.0	2.11	53.0
312-14	2000	S	3.51	29.0	2.09	61.0
312-14A	2000	3P	3.46 3.43 3.36	32.0	2.12	>150.0
312-15	2000	S	3.52	27.1	2.11	51.0
312-16	2000	3P	3.47 3.43 3.36	32.1	2.11	51.0
312-21	2000	S	3.51	30.8	2.10	57.0
312-26	2000	S	3.51	27.8	2.09	48.0
312-28	2000	S	3.51	27.2	2.10	51.0
312-29	2000	S	3.51	34.0	2.10	57.0
312-31, solid	2000	S	3.57	27.6	2.10	56.0
312-32	2000	S	3.51	30.8	2.10	54.0
312-33	2000	NVS	3.48	30.8	2.10	52.8

Sample Designation	Temp. (°C)	(002) Peak Type	d(002)	Lc	d(10)	La
312-34	2000	2P	3.46 3.44	33.0	2.11	46.2
312-39	2000	S	3.49	29.8	2.10	53.0
312-40	2000	2P	3.48 3.45	30.1	2.09	54.0
312-43	2000	2P	3.48 3.43	33.2	2.11	51.0
312-44	2000	2P	3.48 3.44	42.0	2.11	51.0
312-48	2000	3P	3.46 3.43 3.37	30.4	2.10	37.0
312-49	2000	S	3.52	31.1	2.11	61.0
315-1	2000	S	3.53	27.2	2.10	48.0
315-2	2000	2P	3.49 3.43	29.0	2.10	54.0
315-3	700	S	3.71	16.2	--	--
315-5	2000	2P	3.49 3.44	29.0	2.11	54.0
315-8	2000	2P	3.49 3.44	28.2	2.10	56.0
315-9	2000	2P	3.47 3.44	33.0	2.11	47.0
315-14	2000	S	3.53	26.3	2.10	54.0
315-18	2000	3P	3.40 3.382 3.351	45.0	--	--
315-20	680	S	3.70	16.3	--	--
315-20A	2000	2P	3.53 3.43	28.0	2.10	57.0
315-21C	2000	2P	3.52 3.43	27.8	2.10	57.0
315-22	665	S	3.67	16.4	--	--
315-22	2000	S	3.52	28.0	2.10	51.0
315-24A	2000	2P	3.47 3.38	20.0	--	--
315-25A	2000	S	3.52	26.5	2.09	48.0
315-26B	2000	3P	3.50 3.41 3.37	26.5	2.10	46.0
315-26C	680	S	3.69	17.1	--	--
315-28	2000	2P	3.52 3.43	26.0	2.10	46.0
315-28B	600	S	3.70	16.8	--	--
315-30	2000	2P	3.56 3.43	24.0	2.09	48.0
315-31	680	S	3.70	18.2	--	--
315-34	680	S	3.69	15.4	--	--

Sample Designation	Temp. (°C)	(002) Peak Type	d(002)	Lc	d(10)	La
315-36	2000	3P	3.52	24.3	2.10	48.5
			3.43			
			3.37			
315-37	680	S	3.63	17.5	--	--
315-37	2000	S	3.50	26.3	2.098	42.0
315-38	680	S	3.63	18.8	--	--
315-38	2000	2P	3.49	27.1	2.097	46.0
			3.43			
315-39	2000	2P	3.53	27.2	2.098	57.0
			3.43			
315-39	680	S	3.63	20.0	--	--
315-40	2000	S	3.54	25.6	2.097	51.0
315-41	2000	NVS	3.49	23.6	2.098	51.0
315-42	2000	S	3.56	27.2	2.098	46.0
315-43	2000	NVS	3.52	24.3	2.098	51.0
315-43	700	S	3.67	17.4	--	--
315-44	2000	2P	3.55	23.1	2.10	40.2
			3.45			
315-45	2000	S	3.49	27.2	2.10	46.6
315-46A	2000	2P	3.55	23.1	2.098	57.0
			3.43			
316-6	2000	NVS	3.50	27.0	2.11	57.0
316-7, Run 1	2000	S	3.49	28.0	2.10	45.0
316-7, Run 2	2000	S	3.52	27.0	2.10	53.0
316-15	2000	2P	3.40	32.0	--	--
316-28	2000	S	3.50	27.2	2.10	51.0
316-32	2000	2P	3.42	53.0	--	--
			3.40			
317-1	700	S	3.71	20.0	--	--
317-1	2000	S	3.46	45.0	2.11	63.0
317-2	700	S	3.68	15.7	--	--
317-2	2000	NVS	3.48	24.6	2.09	47.0
317-6	700	S	3.71	13.0	--	--
317-6	2000	NVS	3.55	22.0	2.10	55.0
317-7	700	S	3.68	16.0	--	--
317-7	2000	NVS	3.46	27.5	2.10	50.0
317-8	700	S	3.71	11.5	--	--
317-8	2000	2P	3.56	20.0	2.10	44.0
			3.46			
317-10	2000	NVS	3.48	26.0	2.10	68.0
317-11	700	S	3.71	16.3	--	--
317-13	700	S	3.72	15.0	--	--
317-13	2000	NVS	3.47	24.0	2.08	66.0
317-14	700	S	3.71	15.7	--	--
317-14	2000	NVS	3.45	27.0	2.09	46.0
317-15	700	S	3.71	15.3	--	--
317-15	2000	NVS	3.47	26.0	2.09	54.0
317-16	2000	S	3.54	24.0	2.09	53.0

Sample Designation	Temp. (°C)	(002) Peak Type	d(002)	Lc	d(10)	La
317-18	2000	S	3.59	21.0	2.09	58.0
317-19	700	S	3.68	16.5	--	--
317-19	2000	NVS	3.49	30.0	2.09	52.0
317-20	700	S	3.66	17.5	--	--
317-20	2000	S	3.50	25.6	2.09	48.0
317-24, Run 1	2000	NVS	3.52	24.0	2.09	45.0
317-24, Run 2, solid	2000	NVS	3.49	21.0	2.09	50.0
317-25	2000	S	3.53	20.0	2.09	50.0
317-26, Run 1	2000	NVS	3.48	26.0	2.09	48.0
317-26, Run 2, solid	2000	2P	3.46 3.43	24.2	2.10	51.0
317-28	2000	NVS	3.46	25.0	2.09	52.0
317-29	700	2P	3.43 3.42	21.5	--	--
317-29, Run 1	2000	NVS	3.43	65.0	--	--
317-29, Run 2	2000	NVS	3.426	75.0	--	--
317-30	2000	2P	3.44 3.40	29.5	--	--
317-31A	2000	S	3.58	22.0	2.10	46.0
317-32	700	S	--	--	--	--
317-32	2000	2P	3.51 3.48	23.6	2.08	49.0
317-33	700	S	3.68	17.0	--	--
317-33	2000	S	3.414	92.0	2.10	49.0
317-34	700	S	3.68	17.0	--	--
317-34	2000	3P	3.44 3.42 3.36	30.0	2.09	50.0
317-35	700	S	3.71	16.0	--	--
317-35	2000	3P	3.50 3.43 3.36	26.5	2.10	62.0
317-37	700	S	3.68	15.6	--	--
317-37	2000	NVS	3.43	43.0	2.10	63.0
317-38	700	S	3.68	15.6	--	--
317-38	2000	3P	3.54 3.43 3.37	25.0	2.09	51.0
317-39, Run 1	2000	3P	3.45 3.43 3.36	28.0	2.10	52.0
317-39, Run 2, solid, 1mm thick	2000	3P	3.52 3.42 3.37	24.2	2.09	45.0
317-39, Run 3, solid, 1mm thick	2000	3P	3.52 3.41 3.37	23.5	2.09	49.0

Sample Designation	Temp. (°C)	(002) Peak Type	d(002)	Lc	d(10)	La
317-40	2000	3P	3.49	24.8	2.10	48.0
			3.42			
			3.36			
317-41A	2000	S	3.53	26.5	2.10	48.0
317-41B	2000	S	3.53	28.0	2.10	54.0
317-42	2000	3P	3.49	26.0	2.10	42.6
			3.42			
			3.36			
317-43	2000	3P	3.45	26.0	2.09	56.0
			3.42			
			3.35			
317-44	2000	3P	3.48	30.0	2.09	55.0
			3.42			
			3.35			
317-45, solid, 1mm thick	700	S	3.75	12.9	--	--
317-45, Run 1	2000	3P	3.48	25.0	2.09	60.0
			3.40			
			3.35			
317-45, Run 2	2000	3P	3.46	24.0	2.09	42.0
			3.42			
			3.35			
317-46	2000	3P	3.43	31.5	2.10	75.0
			3.42			
			3.36			
317-47	2000	3P	3.50	27.0	2.10	60.0
			3.42			
			3.36			
317-48, Run 1	700	S	3.71	16.2	--	--
317-48, Run 2	700	S	3.87	17.4	--	--
317-48, Run 1	2000	3P	3.45	40.0	2.10	60.0
			3.43			
			3.37			
317-48, Run 2 solid, 1mm thick	2000	3P	3.46	34.0	2.10	59.0
			3.43			
			3.37			
317-49	700	S	3.71	15.7	--	--
317-49, Run 1	2000	3P	3.49	29.0	2.09	62.0
			3.41			
			3.35			
317-49, Run 2 solid, 1mm thick	2000	3P	3.46	33.0	2.09	60.0
			3.44			
			3.37			
317-50	700	S	3.67	15.6	--	--
318-1	2000	S	3.55	28.0	2.10	54.0
318-2	2000	S	3.51	27.0	2.10	55.0
318-3, Run 1	700	S	3.70	16.7	--	--
318-3, Run 2	700	S	3.69	16.7	--	--

Sample Designation	Temp. (°C)	(002) Peak Type	d(002)	Lc	d(10)	La
318-3	2000	2P	3.46 3.41	26.0	2.11	51.0
318-4	700	S	3.66	16.8	--	--
318-6A	2000	S	3.50	31.0	2.09	59.0
318-7, Run 1	2000	S	3.50	28.0	2.10	65.0
318-7, Run 2, solid	2000	S	3.49	28.0	2.10	45.0
318-8, Run 1	2000	S	3.45	39.0	2.10	63.0
318-8, Run 2 solid, 2mm thick	2000	S	3.45	43.5	2.10	77.0
318-9	2000	2P	3.48 3.46	32.5	2.11	57.0
318-10	520	S	3.74	15.2	--	--
318-10	2000	S	3.49	33.8	2.12	50.0
318-11, Run 1	2000	NVS	3.42	77.0	2.10	38.0
318-11, Run 2	2000	NVS	3.43	78.0	2.11	40.0
318-12	2000	3P	3.49 3.43 3.36	31.4	2.09	59.0
318-13	2000	NVS	3.42	44.0	2.10	58.0
318-14	700	S	3.65	16.0	--	--
318-14	2000	3P	3.48 3.43 3.36	30.5	2.10	60.0
318-15, Run 1	700	S	3.75	16.0	--	--
318-15, Run 2	700	S	3.75	15.1	--	--
318-15	2000	3P	3.45 3.42 3.37	30.2	2.10	60.0
318-16	700	S	3.72	15.7	--	--
318-16	2000	2P	3.43 3.41	39.0	2.09	49.0
318-17	700	S	3.68	16.7	--	--
318-17	2000	NVS	3.45	42.0	2.11	59.0
318-18, Run 1	700	S	3.68	16.4	--	--
318-18, Run 2	700	S	3.71	16.3	--	--
318-18	2000	S	3.55	25.6	2.10	44.0
318-19	2000	S	3.52	26.0	2.09	59.0
318-20	700	S	3.67	16.0	--	--
318-20	2000	S	3.53	21.0	2.09	48.0
318-21, Run 1	700	S	3.78	14.0	--	--
318-21, Run 2	700	S	3.75	15.4	--	--
318-21	2000	S	3.55	23.6	2.10	55.0
318-22	700	S	3.70	15.4	--	--
318-22, Run 1	2000	NVS	3.44	65.0	2.10	55.0
318-22, Run 2	2000	NVS	3.44	64.0	2.11	54.0
319-23	700	S	3.74	16.0	--	--
318-23	2000	S	3.63	63.0	2.10	73.0
318-24	700	S	3.64	16.7	--	--

Sample Designation	Temp. (°C)	(002) Peak Type	d(002)	Lc	d(10)	La
318-24	2000	S	3.44	45.0	2.10	68.0
318-26, Run 1	700	S	3.69	15.7	--	--
318-26, Run 2	700	S	3.75	16.1	--	--
318-26, Run 3	700	S	3.69	16.7	--	--
318-27	2000	2P	3.45 3.41	35.4	2.10	47.0
318-28	700	S	3.75	18.0	--	--
318-28	2000	2P	3.47 3.42	27.0	--	--
318-29, Run 1	2000	NVS	3.45	30.0	2.08	62.0
318-29, Run 2, solid, 1mm thick	2000	2P	3.50 3.44	30.5	2.10	65.0
318-29, Run 3	2000	2P	3.52 3.42	31.0	2.10	60.0
318-30	700	S	3.64	15.2	--	--
318-30, Run 1	2000	2P	3.48 3.43	34.1	2.11	69.0
318-30, Run 2	2000	3P	3.45 3.41 3.36	31.0	2.11	63.0
318-31, Run 1	2000	2P	3.45 3.43	35.5	2.10	64.0
318-31, Run 2	2000	3P	3.47 3.41 3.36	31.0	2.11	63.0
318-32, Run 1	700	S	3.64	15.7	--	--
318-32, Run 2	700	S	3.63	16.0	--	--
318-32	2000	S	3.44	47.0	2.10	65.0
318-33	700	S	3.66	16.7	--	--
318-33	2000	NVS	3.46	28.0	2.11	64.0
318-34	700	S	3.63	16.5	--	--
318-34	2000	3P	3.49 3.43 3.36	37.0	2.10	59.0
318-35	700	S	3.71	15.3	--	--
318-35	2000	3P	3.50 3.44 3.37	34.0	2.11	67.0
318-36	700	S	3.68	17.0	--	--
318-36	2000	2P	3.51 3.44	28.0	2.10	49.0
318-37	700	S	3.71	16.1	--	--
318-37	2000	3P	3.46 3.43 3.376	33.6	2.10	52.0
318-38	700	S	3.71	15.6	--	--
318-38	2000	3P	3.47 3.43 3.37	28.0	2.10	49.0

Sample Designation	Temp. (°C)	(002) Peak Type	d(002)	Lc	d(10)	La
318-39, Run 1	700	S	3.71	17.0	--	--
318-39, Run 2	700	S	3.65	17.2	--	--
solid, 1mm thick						
318-39	2000	S	3.51	26.1	2.09	60.0
318-40	700	S	3.71	15.0	--	--
318-40	2000	2P	3.52	28.0	2.11	54.0
			3.45			
318-41	700	S	3.71	14.8	--	--
318-41	2000	S	3.50	28.0	2.09	57.0
318-43, Run 1	700	S	3.69	17.0	--	--
318-43, Run 2	700	S	3.71	17.8	--	--
solid, 1mm thick						
318-43, solid	2000	S	3.44	31.0	2.12	58.0
318-44	700	S	3.72	15.6	--	--
318-44	2000	S	3.55	27.2	2.10	44.0
318-45	700	S	3.71	15.7	--	--
318-45	2000	S	3.56	25.4	2.10	46.0
318-46	700	S	3.71	15.9	--	--
318-46, solid	2000	S	3.53	26.2	2.11	51.0
1mm thick						
318-47	700	S	3.71	15.0	--	--
318-47	2000	NVS	3.49	29.0	2.10	48.0
318-48, Run 1	2000	S	3.53	26.8	2.10	54.0
318-48, Run 2	2000	S	3.52	29.2	2.10	42.0
318-50, Run 1	700	S	3.71	14.3	--	--
318-50, Run 2	700	S	3.71	15.5	--	--
318-50	2000	S	3.53	26.0	2.10	46.0
318-51	2000	S	3.56	27.2	2.10	56.0
318-52	2000	S	3.53	26.5	2.10	54.0
318-53, Run 1	2000	S	3.52	26.5	2.10	54.0
318-53, Run 2	2000	S	3.54	30.0	2.10	60.0
318-54	700	S	3.66	17.0	--	--
318-55	700	S	3.71	15.2	--	--
318-56	2000	S	3.54	27.0	2.10	54.0
318-58	700	S	3.71	18.0	--	--
318-58	2000	NVS	3.51	28.2	2.10	51.0
318-59	700	S	3.68	16.7	--	--
318-59	2000	S	3.51	26.0	--	--
318-60	700	S	3.70	15.7	--	--
318-60	2000	2P	3.47	32.0	--	--
			3.44			
318-61	700	S	3.71	18.6	--	--
318-61	2000	S	3.52	23.3	2.09	55.0
318-62	700	S	3.70	15.3	--	--
318-62	2000	S	3.56	22.5	2.10	51.0
321-1	700	S	3.66	5.0	--	--
321-2	700	2P	3.63	17.4	--	--
			3.57			

Sample Designation	Temp. (°C)	(002) Peak Type	d(002)	Lc	d(10)	La
321-2	2000	3P	3.54 3.43 3.38	22.8	2.10	51.5
321-3	700	S	3.64	17.4	--	--
321-3	2000	S	3.53	24.3	2.10	51.0
321-4	700	S	3.64	17.2	--	--
321-4	2000	-	--	--	--	--
321-5	700	S	3.63	15.4	--	--
321-5	2000	S	3.49	26.4	2.09	53.7
321-6	700	S	3.64	17.0	--	--
321-6	2000	S	3.54	27.7	2.10	48.0
321-7	700	S	3.69	18.0	--	--
321-7	2000	-	--	--	--	--
321-8	700	S	3.69	17.5	--	--
321-8	2000	-	--	--	--	--
321-9	700	S	3.67	17.4	--	--
321-9	2000	-	--	--	--	--
321-10	700	S	3.67	17.0	--	--
321-10	2000	-	--	--	--	--
321-11	700	S	3.71	17.0	--	--
321-11	2000	2P	3.54 3.46	27.2	2.10	65.0
321-12	700	S	3.63	16.8	--	--
321-12	2000	S	3.53	26.4	2.094	56.0
321-13	700	S	3.66	17.0	--	--
321-13	2000	2P	3.49 3.42	33.2	2.09	61.0
321-16A	2000	3P	3.50 3.43 3.36	30.8	2.10	57.0
321-16B	2000	S	3.50	28.8	2.10	44.0
321-16C	700	S	3.63	15.2	--	--
321-17	700	S	3.60	18.7	--	--
321-17B	2000	S	3.49	28.8	2.10	44.0
321-18A	2000	3P	3.50 3.43 3.37	29.8	2.10	49.0
321-18B	700	S	3.63	15.2	--	--
321-19A	2000	2P	3.54 3.426	25.0	2.09	46.0
321-19A	700	S	3.63	17.1	--	--
321-19B	2000	NVS	3.43	39.2	2.10	53.8
321-20A	700	S	3.63	17.5	--	--
321-20A	2000	3P	3.52 3.42 3.36	28.0	2.10	61.0
321-20B	2000	3P	3.53 3.426 3.37	37.0	2.10	46.0
321-21A	700	S	3.63	18.0	--	--

Sample Designation	Temp. (°C)	(002) Peak Type	d(002)	Lc	d(10)	La
321-21A	2000	NVS	3.43	41.6	2.10	51.0
321-21B	700	S	3.64	18.4	--	--
321-21B	2000	S	3.52	27.0	2.10	57.0
321-22A	2000	2P	3.52	27.6	2.10	53.0
			3.43			
321-22B	700	S	3.70	16.1	--	--
321-23	2000	S	3.49	33.0	2.10	54.0
321-23A	700	S	3.63	18.4	--	--
321-23B	700	S	3.36	16.5	--	--
321-23B	2000	3P	3.52	29.6	2.10	51.0
			3.43			
			3.36			
321-24	700	S	3.70	15.8	--	--
321-24A	700	S	3.63	16.2	--	--
321-24B	700	S	3.63	16.5	--	--
321-24B	2000	S	3.43	35.4	2.09	57.0
321-25	700	S	3.63	18.4	--	--
321-25	2000	NVS	3.47	30.8	2.10	60.8
321-25A	700	S	3.60	21.0	--	--
321-25A	2000	NVS	3.43	40.2	2.10	60.5
321-26	700	S	3.67	15.0	--	--
321-26	2000	S	3.52	27.2	2.094	48.5
321-26A	700	S	3.63	18.1	--	--
321-26A	2000	S	3.52	27.2	2.094	54.0
321-27	2000	S	3.52	29.8	2.10	51.0
321-29	700	S	3.63	16.8	--	--
321-29	2000	3P	3.49	24.8	2.094	58.0
			3.40			
			3.35			
321-30	700	S	3.63	19.6	--	--
321-31	2300	3P	3.44	49.0	2.10	60.5
			3.41			
			3.37			
321-31A	2300	NVS	3.40	90.0	2.11	58.0
321-31B	2300	3P	3.49	37.0	2.11	69.0
			3.43			
			3.37			
321-31C	700	S	3.60	18.8	--	--
321-31C	2300	3P	3.49	34.5	2.11	69.0
			3.426			
			3.37			
321-31D	700	S	3.63	17.4	--	--
321-31D	2300	S	3.47	37.2	2.11	69.0
321-31E	700	S	3.63	17.4	--	--
321-31E	2300	NVS	3.426	61.6	2.11	69.0
321-31F	700	S	3.60	18.5	--	--
321-31F	2300	S	3.45	44.0	2.10	69.0
321-31G	2300	2P	3.47	35.0	2.10	56.0
			3.43			

Sample Designation	Temp. (°C)	(002) Peak Type	d(002)	Lc	d(10)	La
321-31I	2300	2P	3.49 3.38	40.0	2.11	69.0
321-32	700	S	3.60	18.9	--	--
321-34	2300	S	3.42	57.5	2.10	78.5
321-34A	2300	S	3.426	51.4	2.10	42.0
321-36A	2300	S	3.47	53.6	2.11	64.5
321-36B	700	S	3.63	18.2	--	--
321-36C	2300	S	3.43	70.0	2.10	46.0
321-37	2000	S	3.52	30.8	2.10	54.0
321-37A	700	S	3.60	18.1	--	--
321-37B	2000	3P	3.53 3.44 3.36	27.2	2.10	54.0
321-38B	700	S	3.63	17.7	--	--
321-39	2000	2P	3.48 3.426	34.1	2.10	57.0
321-39B	700	S	3.63	16.4	--	--
321-41C	2000	3P	3.49 3.43 3.36	32.6	2.10	62.5
321-42A	700	S	3.63	18.8	--	--
321-42A	2000	2P	3.49 3.43	35.5	2.10	60.5
321-42B	700	S	3.63	16.7	--	--
321-42B	2000	2P	3.50 3.43	25.3	2.10	64.4
321-43B	700	S	3.63	19.3	--	--
321-43B	2000	2P	3.49 3.42	35.0	2.098	59.4
321-43B$_1$	2000	2P	3.50 3.426	36.8	2.11	59.5
321-43B$_2$	2000	2P	3.50 3.43	33.0	2.10	57.0
321-44A	2000	3P	3.50 3.43 3.36	30.8	2.10	51.0
321-44B	2000	3P	3.50 3.43 3.36	29.0	2.10	54.0
321-45A	2200	S	3.49	33.0	2.10	57.0
321-45B	2200	S	3.47	45.5	2.10	40.5
321-46A	2000	2P	3.49 3.43	31.7	2.10	60.4
321-46B	2000	3P	3.46 3.43 3.36	30.8	2.10	51.0
321-46C	2000	3P	3.47 3.43 3.36	35.6	2.10	51.0

Sample Designation	Temp. (°C)	(002) Peak Type	d(002)	Lc	d(10)	La
321-46D	2000	3P	3.50	31.7	2.10	64.4
			3.43			
			3.36			
321-48A	2000	S	3.50	31.8	2.10	57.0
321-48B	2000	S	3.50	33.0	2.10	64.4
321-48C	2000	S	3.50	33.0	2.10	60.4
321-49A	2000	S	3.49	33.0	2.10	60.4
321-49B	2000	NVS	3.426	51.2	2.10	54.0
321-51	2000	NVS	3.43	91.5	2.11	69.0
321-51A	2000	NVS	3.43	107.5	2.11	68.0
321-52	2000	NVS	3.43	91.2	2.11	60.5
322-1A	2000	3P	3.44	26.4	2.085	57.3
			3.37			
			3.33			
322-1B	2000	S	3.40	41.5	2.085	--
322-2B	1600	S	3.50	23.0	2.085	37.3
322-3B	1600	S	3.53	22.0	2.085	61.0
322-9A	2000	S	3.37	105.0	2.10	49.6
322-9B	2000	S	3.38	117.0	2.09	51.0
322-10A	2000	2P	3.43	33.0	2.085	--
			3.38			
322-10B	2000	2P	3.50	30.8	2.10	69.0
			3.43			
322-10C	2000	2P	3.49	33.4	2.085	--
			3.43			
322-10D	2000	2P	3.50	28.6	2.10	60.0
			3.43			
322-11A	1670	S	3.55	22.0	2.085	51.2
322-11B	1670	S	3.49	23.0	2.085	47.0
322-11B	2000	2P	3.47	33.0	2.085	48.5
322-12A	1600	S	3.56	23.0	2.085	40.5
322-12B	1670	S	3.56	22.0	2.10	57.0
322-13B	1670	S	3.53	31.8	2.085	50.2
322-14A	1670	S	3.50	23.0	2.085	--
322-14B	1670	S	3.56	21.0	2.09	46.0
322-15B	1670	S	3.56	25.0	2.085	48.4
322-16A	1670	S	3.56	23.5	2.085	--
322-16B	1670	S	3.56	22.0	2.085	41.0
322-17A	1670	S	3.56	22.2	2.085	68.0
322-17B	1670	S	3.56	22.0	2.085	51.4
322-18B	1670	S	3.50	28.8	2.085	61.5
322-19B	1670	S	3.56	20.6	2.085	48.5
322-20	1670	S	3.50	21.4	2.085	30.2
322-21B	1670	S	3.56	17.0	2.085	69.5
322-23A	1300	S	3.56	17.4	2.085	--
322-25A	1410	S	3.56	18.5	2.085	46.1
322-25B	1410	S	3.56	19.2	2.07	121.0
322-26A	1410	S	3.50	25.6	2.085	51.0
322-26B	1410	S	3.50	19.2	2.085	40.2

Sample Designation	Temp. (°C)	(002) Peak Type	d(002)	Lc	d(10)	La
322-27A	1410	S	3.59	20.0	2.085	57.3
322-27B	1410	S	3.56	19.3	2.085	--
322-28A	1410	S	3.56	19.4	2.08	40.2
322-28B	1410	S	3.56	17.8	2.085	53.2
322-29	1410	S	3.56	20.1	2.085	40.2
322-29B	1410	S	3.56	21.0	2.085	53.2
322-31A	1410	S	3.56	23.0	2.085	40.4
322-31B	1410	S	3.56	18.8	2.085	54.0
322-32	1350	S	3.56	18.2	2.085	48.5
322-34	1350	S	3.56	19.2	2.085	46.0
322-35	1350	S	3.56	20.6	2.075	54.0
322-36	1543	S	3.56	19.2	2.085	53.0
322-37	1543	S	3.56	23.0	2.085	--
322-40	1440	S	3.53	23.6	2.085	66.0
322-41	1440	S	3.56	20.4	2.085	61.0
322-42A	1440	S	3.56	21.4	2.085	37.1
322-42B	1440	S	3.56	21.4	2.085	65.0
322-46	1440	S	3.53	19.6	2.08	--
322-47A	1440	S	3.50	21.5	2.085	74.0
322-47B	1440	S	3.56	20.0	2.085	51.6
322-48A	1600	S	3.49	21.5	2.085	51.0
322-49	1460	S	3.53	24.4	2.10	49.0
322-49	1600	S	3.52	23.0	2.085	--
322-53A	1460	S	3.56	20.0	2.09	54.2
322-53B	1460	S	3.56	20.0	2.10	--
322-53C	1460	S	3.56	18.4	2.085	49.0
322-54A	1460	S	3.56	18.7	2.085	48.2
322-58	1500	NVS	3.50	21.0	2.085	53.0
322-58A	1500	S	3.49	21.0	2.085	51.0
322-59	1500	S	3.56	24.4	2.085	53.8
322-61	1500	NVS	3.47	37.0	2.09	60.0
322-62	1500	S	3.47	30.8	2.085	97.0
322-62A	700	S	3.56	18.3	--	--
322-63A	1500	S	3.46	35.6	2.10	72.5
322-63	1500	NVS	3.42	31.6	2.10	51.0
322-64	1370	S	3.56	18.5	2.085	54.0
322-66	1370	S	3.56	19.8	2.085	46.0
322-67A	1370	S	3.53	23.0	2.085	53.0
322-67B	1370	S	3.56	20.8	2.085	49.0
322-68A	1370	S	3.56	19.5	2.085	48.0
322-68B	1370	S	3.56	19.6	2.09	51.0
322-69	1370	S	3.56	18.5	2.085	54.0
323-1	1370	S	3.60	18.4	2.08	40.5
323-2	1370	S	3.60	18.4	2.07	44.0
323-2A	1370	S	3.60	18.4	2.07	48.0
323-3	1370	S	3.49	23.0	2.07	51.0
323-3A	1370	S	3.56	19.4	2.08	46.0
323-4	1370	S	3.58	18.9	2.07	54.0
323-4A	1370	S	3.58	20.0	2.07	51.0

Sample Designation	Temp. (°C)	(002) Peak Type	d(002)	Lc	d(10)	La
323-5	1000	S	3.63	16.4	2.07	42.0
323-5A	1000	S	3.63	15.4	2.07	46.0
323-6A	1000	S	3.63	16.8	2.07	42.0
323-6	1000	S	3.63	16.0	2.07	51.0
323-7	1000	S	3.63	18.1	2.07	46.0
323-8	1000	S	3.63	18.4	2.07	44.0
323-8A	1000	S	3.63	17.2	2.07	36.0
323-9	1000	S	3.63	15.6	2.07	44.5
323-9A	1000	S	3.63	16.4	2.07	37.0
323-11A	1000	S	3.63	16.2	2.07	35.0
323-11B	1000	S	3.63	17.7	2.07	37.2
323-11C	1000	S	3.63	17.4	2.07	32.0
323-11D	1000	S	3.63	16.4	2.08	37.2
323-11E	1000	S	3.63	16.7	2.07	39.0
323-11F	1000	S	3.63	16.4	2.07	49.0
323-11G	1000	S	3.63	17.7	2.07	46.0
323-12	1000	S	3.63	17.7	2.07	44.0
323-12A	1000	S	3.63	17.7	2.07	37.0
323-13	1000	S	3.63	18.8	2.07	40.5
323-13A	1000	S	3.63	17.0	2.07	51.0
323-14	1000	S	3.62	16.7	2.08	48.5
323-19	1000	S	3.63	17.7	2.07	37.2
323-20	1000	S	3.63	17.1	2.07	40.5
323-20A	1000	S	3.63	16.8	2.07	51.0
323-21	1000	S	3.63	15.6	2.07	42.0
323-22	1000	S	3.63	16.2	2.07	40.5
323-24	1000	S	3.63	19.1	2.07	38.6
323-25	1000	S	3.63	16.2	2.07	39.0
323-25A	1000	S	3.63	16.0	2.07	39.0
323-27	1000	S	3.63	15.5	2.07	42.0

TABLE 2   Sizes of the Structural Features Observed in Bright and Dark Field Electron Micrographs Compared to Crystallite Sizes Obtained from X-ray Analysis

Sample #	Platelet Dia. Å	Granulation* Dia. Å	Dark Field Dia. Å** (002)	(100)	X-ray Lc	(Å) La	(002) Peak Type
311-19(2000)	150-500	30-40	20-40	--	--	--	--
311-19(750)×	150-350	20-30	--	--	14	19	S
312-31(2000)	200-500	20-45	20-45	--	27.6	56	S
312-31(2000)	150	35	30	>100	28	56	S
317-24(2000)	250	42	60†	--	24	45	NVS
317-29(2000)	>250	60	30-70†	--	65-75	--	NVS
317-35(2000)	250-500	35	--	--	92	49	S
317-45(2000)	>500	30	--	--	25	60	3P
317-48(2000)×	250	55	--	--	34	59	3P
317-49(2000)×	250-500	45	40†	--	33	60	3P
318-12(2000)	250-500	60	50	110†	31	59	3P
318-22(2000)	>500	40-60	35	--	65	55	NVS
318-22(700)	250	--	--	--	15.7	--	S
318-23(2000)	250	50	50	--	63	73	S
318-23(700)	--	--	--	--	16	--	S
318-29(2000)×	>500	30-40	60	--	31	63	2P
321-31C(2000)×	250	35	60	80	35	69	3P
321-31D(2300)	250	40	35	80	37	69	S

*Diameter corresponds to distances between nearest neighbor.
**Diameter of diffracting regions obtained from (002) or (100) diffraction halos.
†Some of the crystallites giving rise to halos or spots are very large in size, i.e., up to 500Å.
×A second structural feature was observed in the bright field micrographs of these samples. This new feature appeared to be long regular cylinders 500Å in diameter by about 1µ long. Regular striations along the length were spaced 45Å apart.

TABLE 3   Electron Diffraction Results Compared to X-ray Diffraction Results for d(002) and d(10) Spacings ($\mathring{A}$)

Sample #	X-ray		Electron Diffraction		(002)
	d(002)	d(10)	d(002)	d(10)	Peak Type
Graphite	3.35	2.13	3.37	2.12	--
311-19(2000)	3.56	2.17	3.45	2.09	--
311-19(750)	3.70	2.19	--	2.07	S
312-31(2000)	3.54	2.12	3.53	2.16	S
	3.57	2.10	3.53†	2.12	S
317-24(2000)	3.50	2.10	3.53†	2.10†	NVS
317-29(2000)	3.43	--	3.35†	2.12	NVS
			3.45		
317-33(2000)	3.414	2.10	3.35†	2.10	S
317-45(2000)	3.35	2.09	3.50	2.10	3P
	3.48				
317-48(2000)	3.46	2.10	3.48†	2.12	3P
317-49(2000)	3.48	2.09	3.48†	2.10	3P
318-12(2000)	3.49	.09	3.47†	2.11	3P
318-22(2000)	3.44	2.10	3.37†	2.07	NVS
318-22(700)	3.70	--	3.50	2.11	S
			3.42†		
318-23(2000)	3.43	2.10	3.50†	2.10	S
318-23(700)	3.74	--	--	2.07	S
318-29(2000)	3.45	2.08	3.45	2.12	2P
321-31C(2300)	3.43	2.11	3.56†	2.12	3P
321-31D(2300)	3.47	2.11	3.50*	2.125	S

*In this sample no spots were seen on any diffraction halo.
†In addition to Debye-Scherrer rings, a number of sharp diffracting spots were observed on or close to the ring.

TABLE 4   THERMODYNAMIC MEASUREMENTS ON GLASSY CARBON SAMPLES

Run #	Electrolyte	Sample No.	HTT (°C)	HTt (hr)	HTT Atmosphere	ΔH (cal/gr-mole)	ΔS (cal/gr-mole-°K)
FS-2	Fused Salt	321-10	1600	∿1	Nitrogen	180	0.17
FS-5	Fused Salt	321-7	1412	∿1	Nitrogen	8,909	7.45
FS-9	Fused Salt	321-9	1543	∿1	Nitrogen	1,330	1.38
FS-11	Fused Salt	321-7	1600	∿1	Nitrogen	752	0.65
ZC-15	Zirconia/calcia	UCAR-2BY Oriented Graphite Plates	--	-	--	280	0.20
ZC-16	Zirconia/calcia	321-13	1060	1	Vacuum	9,029	8.66
ZC-17	Zirconia/calcia	321-13	1243	1	Vacuum	4,934	4.70
ZC-18	Zirconia/calcia	321-13	1510	1	Vacuum	4,160	4.23
ZC-19	Zirconia/calcia	321-13	1800	1	Vacuum	3,689	4.60
ZC-21	Zirconia/calcia	Beckwith D-82-2	2000	-	--	5,193	10.5
ZC-23	Zirconia/calcia	321-13	2000	∿1	Nitrogen	7,002	5.1
ZC-24	Zirconia/calcia	321-7	1002	1	Vacuum	2,745	3.12
ZC-25	Zirconia/calcia	321-7	2000	∿1	Nitrogen	4,530	7.72
ZC-27	Zirconia/calcia	Hercules H-54	1795	1	Vacuum	4,510	11.28

TABLE 5 R$_G$ for Various Commercial Samples

| | R$_G$ (Å) | | | |
Sample	Pinhole Collimation*	Slit Collimation†	Reported	Dispersity
LMSC-2000	32.9	29.0	15.1	Monodisperse
LMSC-2600	--	40.5	--	"
GC-10	10.8	18.0	7.9	"
GC-20	10.0	23.0	10.0	"
V-25	--	29.5	10.0	"
V-10-42	--	34.0	14.8	"
Beckwith-2000	--	25.0	--	"

TABLE 6 R$_G$ for Samples Made at University of Michigan*

| | R$_G$ (Å) | | |
Sample	Pinhole Collimation	Slit Collimation	Dispersity
311-19 (750)	--	**	Polydisperse
312-31 (2000)	31.6	26.6	"
315-46 (2000)	--	23.0	Monodisperse
317-24 (2000)	--	21.5	"
317-39 (2000)	--	25.8	"
317-45 (2000)	16.4	25.3	"
317-68 (2000)	--	33.5	"
317-49 (2000)	--	23.6	"
318-11 (2000)	20.4 & 44.4	--	Bidisperse
318-14 (2000)	--	35.2	Monodisperse
318-35 (2000)	--	26.5	"
318-41B (700)	14.5	21.2	"
318-42 (2000)	31.7	25.7	Polydisperse
318-44 (2000)	23.5	--	Monodisperse
318-45 (700)	21.7	--	"
318-45 (2000)	27.3	--	"
318-46 (2000)	15.8	--	"
318-48 (700)	7.7	--	"
318-48 (2000)	19.7	--	"

*Results using pinhole collimation reported earlier.
**Very wide distribution of pores did not permit determination of average pore size.
†R$_G$ value is average of 2 or 3 runs made under slit collimation. Widths of slits vary in different runs but heights always the same and very much more than widths.

TABLE 7

Sample #	Temp.°C	He Density (gm/cm^3)	Surface Area Knudsen Flow (m^2/gm)	Specific Surface Area (m^2/gm)
311-32	2000	1.41	3.0	26.4
317-9	700	1.83	--	506.0
317-9	2000	1.70	12.5	59.9
317-12	700	1.80	9.1	510.0
317-12	2000	1.72	--	109.0
318-22	700	1.79	--	459.0
318-22	2000	1.51	--	49.6
321-9	700	1.46	--	541.2
321-9	2000	1.28X*	--	12.7
321-13	367	--	--	257.0
321-13	700	--	--	--
321-13	1066	1.56X	--	72.4
321-13	1227	1.54X	--	56.6
321-13	1504	1.50X	--	51.3
321-13	1795	1.44X	--	47.9
321-24B	2000	1.48X	--	61.3
321-25A	2000	1.45X	--	36.9
323-8	1000	1.51X	--	--
323-26A	1038	1.46X	--	--
323-50	1000	1.51X	--	203.0

*X indicated Xylene

TABLE 8

Sample #	Temp.°C	ρ_{He} real[1] (g/cc)	ρ_{Hg} real[2] (g/cc)	ρ_{Hg} app. (g/cc)	MPD (μ)	IPV (cc/g)
GC No.1		1.47	1.482	1.424	.003	.0273
302-5	2320	--	1.509	.647	2.97	.8828
302-12	2320	--	1.501	.559	3.62	1.1224
305-6 6.62 Mo	2000	1.94	1.802	.636	2.54	1.0151
305-12	2000	1.55	1.562	.557	4.19	1.1560
305-18 .4 Mo	2000	1.77	1.718	.606	2.49	1.0678
308P-2 #2		1.586	1.505	1.034	.009	.3030
308P-3 #3		1.611	1.486	1.077	.008	.2559
310-1	1000	1.27	1.446	.814	.023	.5411
310-3	1000	--	1.424	.805	.020	.5454
310-17A	2000	1.50	1.175	.639	.119	.7130
310-18	1000	1.48	1.452	.687	.039	.7666
310-18	2000	1.15	1.366	.648	.044	.8110
310-20	2000	1.09	1.458	1.029	.009	.2855
310-29	2000	1.89	1.533	.944	.014	.3959
311-21	2000	1.59	1.339	.731	.038	.6221
311-22	2000	1.00	.847	.484	.154	.8809
312-19A	730	1.20	1.481	.879	.629	.4626
312-29	728	1.52	1.441	1.038	.014	.2709
312-31	2000	1.41	1.490	.923	.025	.4118
312-45	2000	1.26	1.302	1.214	.005	.0540
312-48	2000	1.53	1.392	.861	.121	.4425
312-49	2000	1.34	1.404	1.031	.011	.2579
315-1	2000	1.50	1.431	.962	47.0	.3412
317-5	2000	1.42	1.313	.873	.071	.4039
317-18	2000	1.50	1.255	.953	39.1	.281
318-22	700	1.79	1.426	.771	.057	.5958
318-22	2000	1.51	1.576	.937	.054	.4334
318-45	2000	1.37X	1.20	.78	.0078	.021
321-7	2000	1.54	1.04	.76	.028	.34714
321-9	700	1.46	1.24	.98	.0073	.205
321-9	2000	1.36	1.4	1.2	.0057	.016
321-13	700	--	2.00	.96	.042	.49883
321-13	1504	1.50X[3]	1.09	.51	.046	.48293
321-13	1795	1.44X	1.24	.77	.044	.47032
321-17	2000	1.43	1.17	.59	2.15	.299
321-18	2000	1.67	1.16	.87	.175	.247

---

*Glassy Carbon No. 1 - Le Carbone, p. 6927.
[1] Real density as determined by He pycnometry
[2] Real density as determined by Hg
[3] X indicates Xylene

Sample #	Temp.°C	ρ_{He} real[1] (g/cc)	ρ_{Hg} real[2] (g/cc)	ρ_{Hg} app. (g/cc)	MPD (μ)	IPV (cc/g)
321-19	2000	1.80	1.56	.98	.049	.379
321-20	2000	1.60	1.63	.70	.088	.345
321-21	2000	1.79	1.30	.85	.041	.377
321-25	2000	--	2.20	1.14	.011	.088
321-31	2000	1.41	1.49	1.34	.0195	.075
322-14A	1300	--	--	--	2.2	.826
322-14A	1412	1.74	--	--	1.7	.494
322-14B	1300	--	--	--	2.3	.501
322-14B	1412	--	--	--	1.5	.496
322-17A	1300	--	--	--	4.5	.604
322-17A	1412	--	--	--	4.4	.271
322-17B	1300	--	--	--	2.5	.382
322-17B	1412	--	--	--	2.0	.534
322-19A	1300	--	--	--	1.0	.461
322-19A	1412	1.9	--	--	.08	.472
322-19B	1300	--	--	--	.65	.466
322-19B	1412	--	--	--	.95	.468
322-20	1300	--	--	--	1.8	.432
322-20	1412	1.57X	--	--	1.5	.666
322-21A	1300	1.50X	--	--	18.0	.503
322-21A	1412	--	--	--	3.5	.420
322-21B	1412	1.52X	--	--	10.0	.400
322-21D	1300	--	--	--	8.0	.780
322-22A	1300	--	--	--	1.1	.308
322-22A	1412	1.48X	--	--	1.2	.443
322-22B	1300	--	--	--	1.4	.457
322-22B	1412	1.49X	--	--	1.2	.440
322-23A	1300	1.55X	--	--	1.5	.443
322-23A	1412	1.47X	--	--	1.2	.458
322-23B	1300	2.08X	--	--	.32	.453
322-23B	1412	1.61X	--	--	.35	.458
322-24A	1300	1.54X	--	--	1.3	.395
322-24A	1412	--	--	--	1.3	.563
322-24B	1300	--	--	--	1.9	.620
322-24B	1412	1.59X	--	--	1.4	.888
322-32	1350	1.60X	--	--	1.4	.571
322-35	1350	1.43X	--	--	6.0	.472
322-41	1440	1.59X	--	--	.07	.669
322-45	1500	1.72X	--	--	4.2	.421
322-46	1500	1.48X	--	--	1.4	.550
322-47A	1500	1.47X	--	--	1.3	.652
322-48	1605	1.53X	--	--	6.0	.634
322-49	1400	--	--	--	7.0	.841
322-49	1400	--	--	--	7.0	.607
322-49	1600	1.51X	--	--	7.0	.595
322-50	1600	1.52X	--	--	6.0	.545
322-50	1400	1.48X	--	--	6.0	.679
323-26A	1038	1.46X	1.37	.53	1.27	.497

Physical Properties

TABLE 9

Sample #	Temp.°C	ρapp. (g/cc)	ρreal (g/cc) He	ρreal (g/cc) Xyl	Resistivity Ω-cm (×10)	Hardness (DPH)	Int. Frict. (×10³)	Sonic Mod. psi (×10⁻⁶)	Compr. Str. psi (×10⁻³)	Ult. Str. psi (×10⁻³)
310-35	2000	(0.57)*	--	2.07	--	--	--	--	5.18	1.01
311-34	2000	(0.60)	--	--	--	--	--	--	7.2	7.04
311-35	2000	0.51	--	--	.294	--	1.43	0.35	6.85	1.23
312-13	2000	(1.07)	--	--	--	--	--	--	50.0	4.85
312-14	2000	(1.00)	1.44	--	--	--	--	--	36.0	--
312-16	2000	(0.77)	1.27	1.45	--	--	--	--	1.73	2.83
312-27	2000	(1.15)	--	--	--	--	--	--	--	7.78
312-29	2000	(1.07)	1.52	--	--	--	--	--	39.7	--
312-32	2000	(0.90)	1.47	--	--	--	--	--	29.2	5.13
312-33	2000	--	1.59	--	--	90	--	--	--	--
312-34	2000	(0.92)	1.38	--	--	--	--	--	--	1.11
312-44	2000	--	1.18	1.22	--	98	--	--	27.3	--
312-45	680	--	--	--	--	135	--	--	--	--
312-45A	2000	--	1.26	1.29	--	176	--	--	--	--
312-46	680	--	--	--	--	107	--	--	--	--
312-46	2000	--	--	--	--	105	--	--	--	--
312-49	2000	(1.10)	1.3	1.45	--	--	--	--	--	5.96
315-1	2000	(0.89)	1.49	--	--	--	--	--	--	--
315-2	2000	0.70	1.52	--	.349	--	--	1.27	1.47	0.36
315-3	2000	--	1.38	1.49	--	--	--	--	--	--
315-4	2000	--	1.55	--	--	--	--	--	--	--
315-14	2000	(0.96)	1.6	--	--	--	--	--	47.7	4.7
315-17	2000	(0.79)	--	1.45	--	--	--	--	29.3	2.51
315-20	2000	(0.84)	1.6	--	--	--	--	--	--	--
315-20A	2000	0.84	1.6	--	.180	--	0.93	1.48	--	--
315-20B	2000	0.77	1.60	--	.275	--	1.63	1.37	--	--

*Data in parenthesis obtained from unmachined cylinders. All other densities from machined cylinders.

-76-

Sample #	Temp.°C	ρapp. (g/cc)	ρreal (g/cc) He	ρreal (g/cc) Xyl	Resistivity Ω-cm (×10)	Hardness (DPH)	Int. Frict. (×10³)	Sonic Mod. psi (×10⁻⁶)	Compr. Str. psi (×10⁻³)	Ult. Str. psi (×10⁻³)
315-20C	2000	0.88	1.60	--	.203	--	0.54	1.52	--	--
315-21B	2000	(0.96)	--	1.37	--	--	--	--	--	6.60
315-21C	2000	0.91	1.52	1.47	.147	--	0.26	1.54	46.8	7.12
315-21D	2000	(1.01)	--	1.16	--	--	--	--	27.0	7.64
315-22	2000	(0.90)	1.63	1.16	--	--	--	--	--	--
315-24	2000	(1.15)	1.78	--	--	--	--	--	--	--
315-25A	2000	(0.88)	--	1.43	--	--	--	--	24.3	4.61
315-25B	2000	(0.87)	--	1.58	--	--	--	--	--	4.78
315-25C	2000	0.88	1.41	--	.317	--	2.38	1.55	35.5	7.38
315-26B	2000	(0.88)	--	1.45	--	--	--	--	30.5	6.63
315-26C	2000	0.80	1.45	--	.057	--	--	1.20	25.5	4.24
315-26D	2000	0.83	1.45	--	.149	--	--	1.38	36.6	--
315-28	2000	(0.96)	1.46	--	--	--	--	--	37.3	4.39
315-30	2000	(0.91)	1.49	--	--	--	--	--	--	--
315-31	2000	(0.85)	1.48	--	--	--	--	--	--	--
315-31B	2000	0.80	1.46	--	.119	--	0.37	1.44	35.1	5.15
315-31C	2000	0.93	1.48	--	.237	--	0.47	1.65	--	--
315-31D	2000	0.91	1.46	--	.220	--	0.42	1.60	36.2	6.6
315-32	2000	(0.99)	1.43	--	--	--	--	--	45.0	6.35
315-33	2000	0.78	1.50	--	.195	--	1.50	1.26	--	--
315-34C	2000	0.60	1.58	--	.294	--	0.31	0.87	21.0	2.95
315-34D	2000	0.66	1.57	--	.137	--	2.01	1.22	16.4	2.73
315-35B	2000	(0.87)	1.89	1.75	--	--	--	--	--	--
315-37	2000	0.53	1.61	1.48	.262	--	0.31	0.61	14.2	2.51
315-38	2000	(0.72)	1.51	--	--	--	--	--	--	--
315-38A	2000	0.72	1.51	--	.237	--	--	0.93	2.40	2.97
315-39A	2000	0.96	1.64	1.43	.188	--	0.47	1.78	35.9	5.59
315-39B	2000	0.96	1.64	1.43	.029	--	1.28	1.76	28.5	4.41
315-40	2000	(0.87)	1.33	1.41	--	--	--	--	--	--
315-41	2000	0.63	1.67	1.41	.220	--	--	--	15.0	--
315-41A	2000	0.77	1.67	--	.038	--	1.18	1.35	18.6	2.0
315-41B	2000	0.79	1.67	--	.157	--	0.98	1.28	16.0	2.02
315-42	2000	0.87	1.83	1.47	.249	--	0.35	1.65	--	--

Sample #	Temp. °C	ρ app. (g/cc)	ρ real (g/cc) He	ρ real (g/cc) Xyl	Resistivity Ω-cm (×10)	Hardness (DPH)	Int. Frict. (×10³)	Sonic Mod. psi (×10⁻⁶)	Compr. Str. psi (×10⁻³)	Ult. Str. psi (×10⁻¹)
315-43	2000	(1.04)	--	1.48	--	--	--	--	50.0	--
315-44	2000	0.76	1.78	1.43	.214	--	0.32	1.43	--	--
315-45	2000	(0.88)	1.39	1.49	--	--	--	--	--	--
315-45B	2000	0.76	--	1.67	.039	--	0.28	5.8	--	--
315-46	2000	(1.094)	--	1.51	--	240	--	--	--	--
315-46	2000	(1.094)	--	1.51	--	105	--	--	--	--
315-46A	2000	(.899)	1.55	--	--	58	--	--	2.5	2.23
317-1	2000	(1.21)	1.67	1.21	--	--	--	--	56.5	7.5
317-2	2000	0.71	1.74	1.45	.088	--	--	0.91	23.7	2.97
317-5	2000	(0.78)	1.42	1.31	--	58	--	--	33.1	7.50
317-6	2000	(0.78)	1.88	1.45	--	--	--	--	--	--
317-7	2000	(0.79)	1.82	1.43	--	--	--	--	--	--
317-8	2000	1.00	1.64	1.44	--	--	--	1.82	40.5	2.29
317-9	2000	(0.93)	1.76	--	--	--	--	--	32.3	5.77
317-10	2000	0.79	1.42	--	.009	--	0.75	1.45	43.7	6.00
317-12	2000	(0.89)	1.60	--	--	--	--	--	--	5.82
317-13	2000	(0.88)	1.88	1.45	--	--	--	--	--	--
317-14	2000	(0.87)	1.49	--	--	--	--	--	27.4	4.69
317-15	2000	(0.91)	1.46	--	--	--	--	--	33.6	4.09
317-18	2000	0.72	1.50	1.26	.088	--	--	0.86	5.1	3.30
317-19	2000	(1.13)	1.68	--	--	--	--	--	28.2	8.75
317-20	2000	(1.05)	1.51	--	--	--	0.39	--	--	--
317-23	2000	(0.83)	--	1.46	--	--	--	--	7.6	1.90
317-24	2000	0.76	1.57	--	.187	--	0.76	1.45	49.1	4.37
317-25	2000	(0.88)	1.69	1.41	--	--	--	1.51	34.1	2.85
317-26	2000	0.78	1.48	--	.195	14	0.66	--	4.7	0.92
317-27	2000	--	--	--	--	--	--	--	37.3	--
317-28	2000	(0.93)	1.7	1.45	--	--	--	--	--	--
317-29	2000	0.74	1.65	1.49	.122	--	--	0.86	16.4	2.48
317-30	2000	(0.77)	1.68	1.51	--	--	--	--	--	--
317-31	2000	(0.70)	1.45	--	--	--	--	--	--	--
317-32	2000	0.89	1.72	1.43	.224	--	--	1.64	44.2	5.05
317-33	2000	(1.02)	1.46	--	--	73	--	--	40.2	5.60

Sample #	Temp. °C	ρ app. (g/cc)	ρ real (g/cc) He	ρ real (g/cc) Xyl	Resistivity Ω-cm ($\times10$)	Hardness (DPH)	Int. Frict. ($\times10^3$)	Sonic Mod. psi ($\times10^{-6}$)	Compr. Str. psi ($\times10^{-3}$)	Ult. Str. psi ($\times10^{-3}$)
317-34	2000	0.65	1.56	1.50	.321	--	--	2.07	24.0	4.61
317-35	2000	(0.98)	1.40	--	--	--	--	--	--	--
317-37	2000	0.90	1.34	1.43	.225	80	0.31	1.61	40.6	6.90
317-38	2000	0.90	1.34	1.43	.268	62	1.27	1.01	37.6	4.20
317-39	2000	0.77	1.27	--	.032	49	0.19	1.20	26.7	3.58
317-40	2000	0.85	1.47	--	.184	--	--	1.25	22.8	3.44
317-41	2000	(0.93)	--	1.59	--	--	--	--	10.0	2.35
317-41A	2000	(0.90)	--	1.37	--	--	--	--	7.4	1.91
317-41B	2000	(1.12)	1.48	--	--	--	--	--	27.0	3.90
317-42	2000	0.87	1.45	--	.135	53	--	1.54	39.8	5.30
317-43	2000	(0.90)	1.40	--	--	--	--	--	15.0	2.47
317-44	2000	0.84	1.51	--	.007	52	1.68	1.35	27.3	2.13
317-45	2000	(0.88)	1.40	--	--	--	--	--	32.3	5.2
317-46	2000	0.81	1.48	--	.112	71	--	1.27	34.6	4.95
317-47	2000	(0.97)	1.39	--	--	49	--	--	27.5	5.62
317-48	2000	1.16	1.46	--	--	--	--	1.23	--	--
317-49	2000	0.80	1.51	--	.34	--	1.31	0.89	11.1	3.0
318-1	2000	0.79	1.51	--	.169	--	--	0.71	--	2.56
318-2	2000	(0.95)	1.45	--	--	--	--	--	--	--
318-2C	680	0.69	--	--	907.0	--	--	0.80	34.5	4.77
318-3	2000	--	1.37	1.51	--	--	--	--	--	--
318-6A	2000	(1.17)	1.45	1.34	.165	--	--	0.65	.82	--
318-7	2000	0.78	1.49	--	--	60	--	--	18.2	1.67
318-8	2000	(0.96)	--	1.49	--	--	--	--	32.7	5.62
318-8A	2000	(0.97)	1.50	--	--	56	--	--	27.4	--
318-9	2000	(0.96)	1.48	--	--	--	--	--	--	5.19
318-10	2000	(0.99)	1.58	--	--	--	--	1.48	--	--
318-11	2000	0.91	1.50	--	--	51	--	--	--	5.09
318-12	2000	(0.93)	--	--	--	61	--	--	--	--
318-13	2000	(1.03)	1.47	1.23	--	71	--	--	--	--
318-14	2000	0.77	1.51	--	.285	31	0.41	0.41	4.74	0.83
318-15	2000	(0.95)	1.48	--	--	40	--	--	--	--
318-16	2000	0.94	1.48	--	.270	47	--	1.43	28.2	4.02

Sample #	Temp.°C	ρapp. (g/cc)	ρreal (g/cc) He	ρreal (g/cc) Xvl	Resistivity Ω-cm (×10)	Hardness (DPH)	Int. Frict. (×10³)	Sonic Mod. psi (×10⁻⁶)	Compr. Str. psi (×10⁻³)	Ult. Str. psi (×10⁻³)
318-17	2000	0.74	1.46	--	.189	53	0.18	1.18	33.2	4.35
318-18	2000	--	1.48	--	--	46	--	--	--	--
318-18B	2000	--	--	--	--	--	--	--	--	5.28
318-19	2000	(0.77)	1.41	--	--	65	--	--	--	--
318-20	2000	--	1.50	--	--	56	--	--	--	--
318-21	2000	--	1.37	1.49	--	--	--	--	--	--
316-22	2000	0.83	1.45	--	.237	44	--	1.29	29.5	4.37
316-22	700	(0.78)	1.48	--	--	39	--	--	--	--
316-23	2000	(0.91)	1.49	--	--	54	--	--	--	--
318-24	2000	0.97	1.29	1.52	--	61	--	1.49	--	4.47
318-24C	2000	0.92	1.29	1.53	--	--	--	--	25.0	--
318-26	2000	(0.99)	1.59	--	--	70	--	--	--	--
318-27	2000	(0.87)	1.38	--	.177	--	--	1.33	--	--
318-28	2000	0.84	1.45	--	.194	26	--	1.52	0.23	0.73
318-29	2000	0.63	1.45	--	--	60	--	1.52	21.9	5.82
318-30	2000	1.08	1.49	--	--	21	--	0.1	1.6	0.19
318-31	2000	0.55	1.31	1.36	.215	53	2.41	--	19.7	--
318-32	2000	(0.84)	1.57	--	--	57	--	1.3	32.2	4.75
318-33	2000	0.80	--	1.53	.101	--	0.73	1.48	28.7	4.85
318-34	2000	1.07	1.45	--	.118	67	--	1.35	26.4*	4.57
318-35	2000	0.88	1.43	--	.107	--	--	2.17	18.6*	3.34
318-36	2000	1.02	1.41	--	.112	--	--	--	25.7*	3.90
318-37	2000	0.92	1.48	--	--	--	--	--	--	--
318-38	2000	--	1.52	--	.085	--	--	2.99	34.9*	7.95
318-39	2000	1.23	1.57	--	--	106	--	--	--	--
318-41	2000	(1.05)	1.44	--	--	103	--	--	--	--
318-43	2000	(1.03)	--	1.42	--	--	--	3.1	--	--
318-44	2000	(1.09)	--	1.46	.070	56	--	2.34	42.3*	7.35
318-45	2000	1.27	--	1.37	.41	--	--	--	3.5	8.27
318-46	2000	1.02	--	1.46	--	--	--	--	--	--
318-48	2000	1.08	1.43	--	--	--	--	--	--	--

*Head speed .05 in/min., all others .02 in/min.

-80-

Sample #	Temp.°C	ρ app. (g/cc)	ρ real (g/cc) He	ρ real (g/cc) Xyl	Resistivity Ω-cm (×10)	Hardness (DPH)	Int. Frict. (×10³)	Sonic Mod. psi (×10⁻⁶)	Compr. Str. psi (×10⁻³)	Ult. Str. psi (×10⁻³)
318-50	2000	--	--	--	--	--	--	--	--	5.73
318-51	2000	(0.88)	1.43	--	--	--	--	0.83	17.3	1.44
318-52	2000	1.01	1.41	--	.130	--	--	1.66	17.7	2.54
318-53	2000	(0.87)	1.42	1.43	--	--	--	--	4.73	1.60
318-56	2000	(0.85)	1.34	1.51	--	--	--	0.10	--	--
318-58	2000	0.98	--	1.38	.237	--	--	2.15	--	6.02
318-59	2000	0.95	1.38	1.42	--	--	--	1.78	31.7	4.20
318-60	2000	0.95	1.71	1.38	.150	54	--	1.47	36.2*	7.63
318-61	2000	1.01	1.75	--	.403	--	--	--	22.6*	3.96
318-62	2000	0.90	1.39	--	--	69	--	--	41.4	6.98
321-1B	2000	--	--	--	--	--	--	--	4.36	.87
321-3	2000	0.98	1.57	--	.340	78	--	--	40.0*	7.18
321-5	2000	(0.99)	1.52	--	--	--	--	--	--	--
321-6	2000	1.09	1.60	--	.31	81	--	2.33	41.7*	8.27
321-7	2000	(0.91)	1.54	--	--	--	--	--	--	--
321-8	2000	0.90	1.46	--	.546	105	--	1.48	38.9*	7.00
321-9	2000	1.17	1.36	1.28	--	120	--	--	54.2	9.75
321-10	2000	1.26	1.34	--	.100	99	--	2.99	54.9*	10.85
321-11	2000	0.95	1.43	--	.114	95	--	1.54	40.5	5.16
321-11C	2000	--	--	--	--	132	--	--	37.0	6.08
321-12	2000	0.97	1.32	--	.121	--	--	1.22	14.9	2.52
321-13	2000	0.95	1.48	1.50	.115	131	--	1.67	36.2	6.04
321-15	2000	(0.96)	1.56	--	--	--	--	--	34.5	5.98
321-16A	2000	(0.85)	1.84	--	--	--	0.21	1.55	24.3	4.52
321-16B	2000	(C.93)	1.75	1.39	--	--	--	--	--	--
321-17B	2000	(0.94)	1.41	--	--	--	0.22	1.81	36.7	5.26
321-18A	2000	(0.95)	1.67	1.42	--	--	--	--	--	--
321-18B	2000	(0.64)	--	1.49	--	--	0.2	--	--	--
321-19A	2000	(0.87)	1.65	1.42	--	115	0.15	1.73	39.6	5.67
321-19B	2000	(0.83)	1.80	1.46	--	87	0.11	1.83	31.5	6.04
321-20A	2000	(0.99)	1.72	1.41	--	--	--	1.49	31.4	5.76

*Head speed .05 in/min., all others .02 in/min.

Sample #	Temp.°C	$\rho_{app.}$ (g/cc)	ρ_{real} (g/cc) He	ρ_{real} (g/cc) Xyl	Resistivity Ω-cm (×10)	Hardness (DPH)	Int. Frict. (×10³)	Sonic Mod. psi (×10⁻⁶)	Compr. Str. psi (×10⁻³)	Ult. Str. psi (×10⁻³)
321-20B	2000	(0.70)	1.50	--	--	--	--	--	34.8	6.21
321-21A	2000	0.94	1.74	1.45	.2	--	--	1.65	45.5	6.35
321-21B	2000	1.00	--	1.47	.2	--	--	1.93	46.4	6.16
321-22A	2000	0.94	1.79	1.44	.28	--	--	1.44	31.9	6.14
321-22B	2000	(0.98)	--	1.54	--	--	--	--	34.8	4.58
321-22C	2000	0.93	--	1.50	.17	--	--	1.43	36.1	4.35
321-22D	2000	0.92	--	1.47	.19	--	--	1.42	33.7	5.15
321-23	2000	1.04	1.74	--	.12	--	--	2.05	58.6	7.28
321-23A	2000	0.96	--	1.53	.27	--	--	1.64	40.9	6.36
321-23B	2000	0.97	1.77	1.44	.18	--	--	1.69	42.7	5.98
321-24	2000	1.02	--	1.60	.19	--	--	1.95	47.8	6.39
321-24A	2000	0.95	--	1.46	.14	--	--	1.05	49.1	7.04
321-24B	2000	1.07	--	1.48	.15	--	--	2.22	45.1	6.76
321-25A	2000	0.70	--	1.45	.13	--	--	0.08	27.9	5.14
321-26	2000	(0.50)	1.43	1.56	--	--	--	--	26.4	0.77
321-26A	2000	(0.45)	1.54	--	--	--	--	--	--	--
321-27	2000	0.86	1.52	--	.11	--	--	0.62	9.7	1.34
321-29	2000	0.96	1.64	1.42	.18	--	--	1.59	40.0	5.94
321-31	2300	(0.81)	1.41	--	--	--	--	--	--	--
321-31A	2300	(0.97)	1.40	--	--	--	--	--	--	--
321-31B	2300	(0.91)	1.56	--	--	--	--	--	--	--
321-31C	2300	(0.88)	1.41	--	--	--	--	--	--	--
321-31D	2300	--	--	1.53	--	--	--	--	33.3	4.08
321-31F	2300	0.75	--	1.68	.23	--	--	0.70	13.6	2.23
321-31G	2300	1.03	1.66	--	.18	--	--	--	22.2	3.53
321-31I	2300	(1.02)	1.48	--	--	--	--	--	--	--
321-31J	2000	0.91	--	1.48	.16	--	--	1.15	22.6	3.99
321-31P	2000	0.89	--	1.25	.24	--	--	1.16	25.0	3.60
321-31Q	2000	0.98	--	1.53	.17	--	--	1.64	40.5	6.23
321-31R	2000	0.87	--	1.48	.18	--	--	0.85	22.2	1.85
321-31S	2000	0.9?	--	1.39	.17	--	--	1.53	36.9	5.58
321-32A	2000	0.94	1.36	1.50	.18	--	--	0.91	35.5	3.78
321-32B	2000	0.93	1.30	1.52	.20	--	--	0.92	36.9	5.76

Sample #	Temp.°C	ρapp. (g/cc)	ρreal (g/cc) He	ρreal (g/cc) Xyl	Resistivity Ω-cm (×10)	Hardness (DPH)	Int. Frict. (×10³)	Sonic Mod. psi (×10⁻⁶)	Compr. Str. psi (×10⁻³)	Ult. Str. psi (×10⁻³)
321-32C	2000	0.92	1.25	1.50	.21	--	--	0.93	41.4	6.11
321-32D	2000	0.92	--	1.47	.25	--	--	1.49	--	--
321-32D₁	2000	0.84	--	1.47	.29	--	--	0.2	--	--
321-32E	2000	0.94	1.33	--	.24	--	--	1.56	41.9	5.89
321-32F	2000	(0.96)	--	1.54	--	--	--	.91	33.3	4.28
321-32G	2000	0.95	--	--	.22	--	--	1.56	31.8	4.52
321-33A	2000	0.94	1.41	--	.16	--	--	1.49	39.8	5.96
321-33B	2000	0.89	--	1.47	.33	--	--	--	53.6	6.69
321-34	2300	(0.95)	1.6	--	--	--	--	1.49	31.3	7.55
321-34A	2300	0.96	1.59	--	.27	--	--	2.94	33.3	2.92
321-34B	2300	0.94	--	1.59	.18	--	--	1.46	--	--
321-34D	2300	0.95	--	1.49	--	--	--	0.92	40.9	5.43
321-34E	2300	0.95	1.21	--	.38	--	--	1.15	--	2.46
321-36A	2300	(1.11)	1.80	1.44	--	--	--	--	50.4	7.23
321-36B	2300	1.07	1.66	1.35	.29	--	--	--	--	--
321-36C	2300	(1.11)	1.43	--	--	--	--	--	--	--
321-37	2300	(1.07)	1.41	--	.24	--	--	0.42	--	1.09
321-37B	2300	.66	1.50	--	--	--	--	--	5.53	0.45
321-37D₁	2300	--	--	1.76	.44	--	--	0.94	2.51	0.36
321-37E	2300	0.79	--	1.56	--	--	--	0.08	1.39	0.22
321-37F	2300	0.65	--	1.62	.31	--	--	0.2	1.05	0.40
321-37Q	2300	0.71	--	--	.22	--	--	0.72	1.67	1.31
321-39	2300	0.84	1.60	--	.30	--	--	--	6.80	.06
321-40	2300	(0.60)	1.42	--	--	--	--	--	0.50	--
321-41B	2300	(0.77)	1.51	--	.29	--	--	0.35	--	--
321-42A	2000	0.77	--	1.44	.28	--	--	0.20	2.05	0.57
321-42B	2000	0.65	1.48	--	.36	--	--	0.60	1.14	0.42
321-43A	2200	0.73	1.55	--	.46	--	--	0.10	1.31	0.37
321-43B	2200	0.61	1.44	--	--	--	--	--	0.73	0.22
321-44A	2200	(0.96)	1.81	1.46	--	--	--	--	--	--
321-44B	2200	(0.98)	1.56	--	--	--	--	--	--	--
321-45A	2200	(1.17)	1.78	1.42	--	--	--	--	--	--
321-45B	2200	(1.04)	1.84	1.50	--	--	--	--	--	--

Sample #	Temp. °C	ρapp. (g/cc)	ρreal (g/cc) He	ρreal (g/cc) Xyl	Resistivity Ω-cm (×10)	Hardness (DPH)	Int. Frict. (×10³)	Sonic Mod. psi (×10⁻⁶)	Compr. Str. psi (×10⁻³)	Ult. Str. psi (×10⁻³)
321-46A	2200	(0.83)	1.40	--	--	--	--	--	--	--
321-46B	2200	0.82	1.43	--	.26	--	--	0.16	2.04	0.49
321-46C	2200	(0.87)	1.6C	--	--	--	--	--	--	--
321-47A	1600	(1.13)	2.0?	1.48	--	--	--	--	--	--
321-47B	1600	(1.18)	1.6?	--	--	--	--	--	--	--
321-47C	1600	(0.91)	1.84	1.45	--	--	--	--	--	--
321-48A	1600	(0.79)	1.40	--	--	--	--	--	--	--
321-48B	1600	0.83	1.43	--	.24	--	--	0.34	2.65	0.60
321-48C	2000	(0.78)	1.58	--	--	--	--	--	--	--
321-49A	1600	(0.91)	1.51	--	--	--	--	--	--	--
321-49B	1600	(0.80)	1.44	--	--	--	--	--	--	--
321-49C	1600	(0.91)	1.51	--	--	--	--	--	--	--
321-50	1600	(1.00)	1.69	--	--	--	--	--	--	--
321-50B	1600	1.02	1.43	--	.15	--	--	1.5	28.2	4.52
321-50C	1600	(1.03)	1.45	--	--	--	--	--	--	--
321-51	2350	(0.99)	1.50	--	.21	--	--	0.73	9.1	1.36
321-51A	2350	0.96	1.53	--	--	--	--	--	--	--
321-52	2000	--	1.3	1.52	--	--	--	--	--	--
321-53	2000	(1.12)	2.07	1.47	--	--	--	--	--	--
322-1A	1600	0.82	--	1.59	.24	--	--	0.27	4.00	0.78
322-1B	1600	0.73	1.98	--	.39	--	--	0.26	--	--
322-2A	1600	(0.87)	2.02	1.59	--	--	--	--	--	--
322-3A	1600	0.71	--	1.59	.18	--	--	0.73	6.80	0.69
322-3B	1600	(0.78)	2.0	1.52	--	--	--	--	--	--
322-5	2000	(0.86)	1.55	--	--	--	--	--	--	--
322-6	2000	(0.86)	1.41	--	--	--	--	--	--	--
322-10C	2100	(0.84)	1.8	1.49	.207	--	--	0.25	--	0.17
322-11A	1670	0.74	--	--	.26	--	--	0.24	0.791	0.24
322-11B	1670	C.72	1.9	--	.26	--	--	0.24	2.23	0.24
322-12A	1600	0.55	--	1.43	.28	--	--	0.24	2.04	--
322-12B	1600	0.73	--	1.50	.23	--	--	0.35	4.06	--
322-13A	1670	0.78	--	1.45	.17	--	--	0.59	--	--
322-14A	1670	(0.76)	1.74	--	--	--	--	--	--	--

Sample #	Temp °C	ρapp. (g/cc)	ρreal (g/cc) He	Xyl	Resistivity Ω-cm (×10)	Hardness (DPH)	Int. Frict. (×10³)	Sonic Mod. psi (×10⁻⁶)	Compr. Str. psi (×10⁻³)	Ult. Str. psi (×10⁻³)
322-15B	1670	0.79	--	1.48	.19	--	--	0.57	6.82	--
322-16A	1670	(0.81)	1.89	--	--	--	--	--	--	--
322-16B	1670	0.78	--	1.54	.22	--	--	0.35	3.97	0.82
322-17B	1670	0.71	--	1.48	.37	--	--	0.2	--	0.37
322-18A	1670	1.07	1.98	1.49	.09	--	--	2.17	37.3	6.29
322-19A	1670	(0.85)	--	--	--	--	--	--	--	--
322-19B	1670	0.79	--	1.55	.28	--	--	0.33	4.16	0.41
322-20	1400	0.78	--	1.57	.17	--	--	0.77	8.97	1.43
322-21	1400	0.74	--	1.45	.22	--	--	0.53	3.34	0.74
322-22A	1400	(0.88)	--	1.48	--	--	--	--	4.1	1.19
322-22B	1400	(0.89)	--	1.49	--	--	--	--	5.2	1.19
322-22B	1400	(0.54)	--	1.47	--	--	--	--	--	--
322-23B	1300	(0.83)	--	1.C1	--	--	--	--	--	4.07
322-24A	1300	(0.87)	--	1.51	--	--	--	--	--	1.28
322-24B	1400	(0.82)	--	1.59	--	--	--	--	--	1.28
322-25A	1410	0.82	--	1.48	.11	--	--	1.56	23.17	3.24
322-25A	1670	0.88	--	1.64	.13	--	--	1.48	19.68	2.17
322-26	1400	0.98	--	--	.11	--	--	2.04	27.15	3.6
322-27A	1400	0.83	--	1.42	.08	--	--	1.58	24.94	2.63
322-28A	1400	(0.93)	--	1.44	.10	--	--	--	18.4	3.16
322-29A	1400	0.66	--	1.46	.19	--	--	0.68	10.62	1.63
322-30	1410	0.85	1.64	1.42	.18	--	--	0.79	2.68	0.773
322-31B	1410	0.69	--	1.58	.34	--	--	0.24	1.85	0.363
322-32	1350	0.74	--	1.60	.24	--	--	0.36	3.06	0.465
322-33	1350	0.71	--	1.62	.22	--	--	0.60	2.775	1.32
322-34	1350	0.75	--	1.34	.13	--	--	1.07	13.43	3.85
322-35	1350	0.77	--	1.43	.22	--	--	0.68	11.8	1.33
322-36	1543	0.88	--	1.45	.10	--	--	1.29	23.0	3.74
322-37	1543	0.78	--	1.44	.20	--	--	0.47	3.697	1.178
322-38	1543	0.73	--	1.68	.17	--	--	0.93	11.16	2.47
322-39	1440	0.59	--	1.55	.18	--	--	0.72	10.1	2.94
322-40	1440	0.79	--	1.59	.11	--	--	1.14	13.95	3.45
322-41	1440	0.73	--	1.59	.17	--	--	0.84	9.83	2.597

Sample #	Temp.°C	ρapp. (g/cc)	ρreal (g/cc) He	ρreal (g/cc) Xyl	Resistivity Ω-cm (×10)	Hardness (DPH)	Int. Frict. (×10³)	Sonic Mod. psi (×10⁻⁶)	Compr. Str. psi (×10⁻³)	Ult. Str. psi (×10⁻³)
322-42A₃	1440	0.72	--	--	.14	--	--	0.88	10.77	2.97
322-42A₄	1440	0.64	--	--	.23	--	--	0.68	13.9	1.00
322-42B₁	1440	0.66	--	1.44	.20	--	--	0.69	9.89	1.96
322-42B₂	1440	0.75	--	1.46	.18	--	--	0.87	13.19	2.22
322-42B₃	1440	0.73	--	1.46	.27	--	--	0.89	19.4	3.11
322-42B₄	1440	0.66	--	1.51	.17	--	--	0.70	12.2	1.07
322-42B₅	1440	.68	--	--	.19	--	--	0.76	--	--
322-12B₆	1440	0.75	--	1.49	.19	--	--	0.97	16.85	1.26
322-45	1440	0.82	--	1.72	.20	--	--	0.68	6.76	2.04
322-48	1605	0.68	--	1.48	.29	--	--	0.43	2.16	0.992
322-49A	1605	0.79	--	1.46	.15	--	--	0.79	--	--
322-50	160u	0.73	--	1.52	.15	--	--	0.56	--	--
322-51	14.0	(0.78)	--	1.56	--	--	--	--	--	--
322-56	1500	(1.00)	--	1.53	--	--	--	--	--	--
322-56A	1500	(0.96)	--	1.33	--	--	--	--	--	--
322-57	1500	(1.06)	--	1.63	--	--	--	--	--	--
322-57A	1500	(1.03)	--	1.62	--	--	--	0.4	--	--
322-61	1500	0.74	--	1.46	.189	--	--	1.21	--	--
322-62	1500	0.96	--	1.49	.095	--	--	1.69	--	--
322-63	1500	1.00	--	1.56	.074	--	--	2.47	--	--
322-63A	1500	1.19	--	1.49	.057	--	--	1.92	--	--
322-64	1370	0.98	--	1.60	.076	--	--	--	--	--
322-64A	1370	(1.10)	--	1.51	--	--	--	1.89	--	--
322-64B	1370	0.93	--	1.61	.085	--	--	--	--	--
322-65	1370	(1.28)	--	1.43	--	--	--	--	--	--
322-66	1370	(1.09)	--	1.37	--	--	--	1.32	--	--
322-67	1350	0.85	--	1.64	.099	--	--	--	--	--
322-67A	1370	(0.84)	--	1.52	--	--	--	1.33	--	--
322-67B	1370	0.82	--	1.41	.101	--	--	0.53	--	--
322-68	1370	0.74	--	1.52	.180	--	--	--	--	--
322-68A	1370	(0.79)	--	1.25	.150	--	--	--	--	--
322-68B	1370	(0.77)	--	1.48	--	--	--	--	--	--
322-69	1370	0.69	--	1.50	.189	--	--	0.42	--	--

Sample #	Temp.°C	$\rho_{app.}$ (g/cc)	ρ_{real} (g/cc) He	ρ_{real} (g/cc) Xyl	Resistivity Ω-cm (×10)	Hardness (DPH)	Int. Frict. (×10³)	Sonic Mod. psi (×10⁻⁶)	Compr. Str. psi (×10⁻³)	Ult. Str. psi (×10⁻³)
322-69A	1370	0.72	--	1.47	.198	--	--	0.42	--	--
322-70	1370	0.69	--	1.44	.224	--	--	0.38	--	--
323-1	1370	(1.01)	--	1.46	--	--	--	--	--	--
323-2	1370	0.78	--	1.45	.112	--	--	1.15	--	--
323-2A	1370	0.80	--	1.44	.111	--	--	1.30	--	--
323-3	1370	(0.98)	--	1.51	--	--	--	--	--	--
323-3A	1370	1.13	--	1.53	.061	--	--	2.48	--	--
323-4	1370	0.78	--	1.47	.176	--	--	0.55	--	--
323-4A	1370	0.78	--	1.47	.179	--	--	0.55	--	--

TABLE 10 Physical Properties Correlated with Density

Sample #	$E_s/\rho_{app.}$ in($\times 10^{-6}$)	$\sigma_{cs}/\rho_{app.}$ in($\times 10^{-3}$)	$\sigma_{UTS}/\rho_{app.}$ in($\times 10^{-3}$)	$E_s\left(\dfrac{\rho_{real}}{\rho_{app.}}\right)$ psi($\times 10^{-6}$)	$\sigma_{cs}\left(\dfrac{\rho_{real}}{\rho_{app.}}\right)$ psi($\times 10^{-3}$)	$\sigma_{UTS}\left(\dfrac{\rho_{real}}{\rho_{app.}}\right)$ psi($\times 10^{-3}$)	$\rho\left(\dfrac{\rho_a}{\rho_{He}}\right)$ Ω-cm($\times 10$)
310-35	--	252.4	49.2	--	18.8	3.67	--
311-34	--	332.3	325.9	--	--	--	--
311-35	19.2	37.2	66.9	--	--	--	--
312-13	--	1298.0	125.9	--	--	--	--
312-14	--	1000.0	--	--	51.8*	--	--
312-16	--	62.2	102.1	--	3.26	5.33	--
312-27	--	--	188.0	--	--	--	--
312-29	--	1030.6	--	--	56.4*	8.38*	--
312-32	--	901.2	158.3	--	47.7*	1.09*	--
312-34	--	824.2	33.5	--	40.9*	7.86	--
312-49	--	--	150.5	--	--	0.78*	--
315-2	50.3	58.5	14.3	2.76*	3.2*	1.04*	.016*
315-14	--	1235.5	136.0	--	71.2*	--	--
315-17	--	1030.0	88.3	--	--	--	--
315-20A	48.8	--	--	2.82*	--	--	--
315-20B	49.3	--	--	2.85*	--	--	.013*
315-20C	48.1	--	--	2.76*	--	--	.009*
315-21B	--	--	191.0	--	78.2*	10.45	--
315-21C	45.8	1428.6	217.6	2.51*	40.6	11.9*	.009*
315-21D	--	743.0	209.5	--	38.9	11.47	--
315-25A	--	767.0	145.5	--	--	7.39	--
315-25B	--	--	152.6	--	56.9*	7.75	--
315-25C	48.8	1120.5	232.9	2.41*	50.3	11.8*	.020*
315-26B	--	962.8	209.3	--	46.4*	10.92	--
315-26C	41.7	888.9	147.2	2.18*	63.9*	7.7*	.003*
315-26D	46.2	1224.9	--	2.34*	56.7*	--	.009*
315-28	--	1079.3	127.0	--	63.4*	6.68*	--
315-31B	50.0	1218.8	178.8	2.63*	--	9.4*	.007*
315-31C	49.3	--	--	2.63*	58.1*	--	.015*
315-31D	48.8	1105.0	201.5	2.56*	65.0*	10.6*	.014*
315-32	--	1262.6	178.2	--	--	9.2*	--

*Calculated with helium (otherwise with xylene).

Sample #	$E_s/\sigma_{app.}$ in($\times 10^{-6}$)	$\sigma_{cs}/\rho_{app.}$ in($\times 10^{-3}$)	$\sigma_{UTS}/\rho_{app.}$ in,$\times 10^{-3}$	$E_s\left(\dfrac{\rho_{real}}{\rho_{app.}}\right)$ psi($\times 10^{-6}$)	$\sigma_{cs}\left(\dfrac{\rho_{real}}{\rho_{app.}}\right)$ psi($\times 10^{-3}$)	$\sigma_{UTS}\left(\dfrac{\rho_{real}}{\rho_{app.}}\right)$ psi($\times 10^{-3}$)	$\rho\left(\dfrac{\rho_a}{\rho_{He}}\right)$ Ω-cm($\times 10$)
315-33	44.9	--	--	2.42*	--	--	.010*
315-34C	40.3	972.2	136.6	2.29*	55.3*	7.7*	.011*
315-34D	51.5	690.2	114.9	2.91*	39.0*	6.5*	.006*
315-37	31.9	744.2	131.6	1.70	39.7	7.01	.009
315-38A	35.9	925.9	114.6	1.95*	50.3*	6.2*	.011*
315-39A	51.5	1036.8	161.7	2.65	53.5	8.33	.013
315-39B	51.0	824.7	127.6	2.62	42.5	6.57	.002
315-41	--	612.8	--	--	31.1	--	.001
315-41A	48.7	671.0	72.2	2.93*	40.3*	4.3*	.002*
315-41B	45.9	563.0	69.9	2.69	33.8*	4.3*	.007*
315-42	52.7	--	--	2.79	--	--	.015
315-43	--	1335.5	--	--	71.1	--	--
315-44	52.1	--	--	2.69	--	--	.011
315-45B	211.9	--	2.48	12.74	--	--	.002
315-46A	--	2.78	--	--	4.4*	3.9*	--
317-1	--	1297.1	172.2	--	56.1	7.5	--
317-2	35.6	922.0	116.2	1.85	48.4	6.07	.009
317-5	--	1175.0	266.0	--	55.6	12.6	--
317-8	50.4	1120.9	63.4	2.62	57.6	3.30	--
317-9	--	964.8	172.3	--	61.1*	10.9*	--
317-10	50.9	1536.6	210.9	2.61*	78.5*	10.8*	.001*
317-12	--	--	181.6	--	--	10.5*	--
317-14	--	874.8	149.7	--	46.9*	8.03*	--
317-15	--	1025.6	124.8	--	53.9*	6.6*	--
317-18	33.0	126.0	104.0	1.51	8.93	5.78	.005
317-19	--	693.2	215.1	--	41.9*	13.0*	--
317-23	--	254.0	63.4	--	13.4	3.34	--
317-24	52.9	1794.6	159.7	2.99*	101.4*	9.0*	.009*
317-25	--	1076.4	89.9	--	54.6	4.57	--
317-26	53.7	167.4	32.8	2.86*	8.9*	1.7*	.010*
317-29	32.3	615.0	92.8	1.73	33.0	4.99	.006
317-32	51.3	1380.0	113.0	2.63	71.0	8.11	.014
217-33	--	1092.0	152.0	--	57.5*	8.0*	--

Sample #	$E_s/\rho_{app.}$ in(×10⁻⁶)	$\sigma_{cs}/\rho_{app.}$ in(×10⁻³)	$\sigma_{UTS}/\rho_{app.}$ in(×10⁻³)	$E_s\left(\frac{\rho_{real}}{\rho_{app.}}\right)$ psi(×10⁻⁶)	$\sigma_{cs}\left(\frac{\rho_{real}}{\rho_{app.}}\right)$ psi(×10⁻³)	$\sigma_{UTS}\left(\frac{\rho_{real}}{\rho_{app.}}\right)$ psi(×10⁻³)	$\rho\left(\frac{\rho_a}{\rho_{He}}\right)$ Ω-cm(×10)
317-34	88.4	1025.6	197.0	4.78	55.4	10.6	.014
317-37	49.8	1049.0	212.0	2.56	64.5	10.9	.011
317-38	31.1	1156.0	129.0	1.60	59.7	6.67	.017
317-39	43.3	963.0	129.0	1.98*	44.0*	5.9*	.002*
317-40	40.7	742.0	112.0	2.16*	39.4*	5.95*	.011*
317-41	--	298.0	70.0	--	17.1	4.0	--
317-41A	--	228.0	58.8	--	11.3	2.9	--
317-41B	--	668.0	96.5	--	35.7*	5.15*	.008*
317-42	49.1	1266.0	169.0	2.63*	66.3*	6.8*	--
317-43	--	462.0	76.0	--	23.4*	3.84*	.0004*
317-44	44.6	903.0	70.4	2.43*	4.91*	3.83*	--
317-45	--	1017.0	164.0	--	51.4*	8.3*	.006*
317-46	43.5	1183.0	215.0	2.32*	63.2*	9.7*	--
317-47	--	785.0	160.0	--	39.3*	8.05*	.018*
317-48	29.9	--	--	1.57*	--	--	.009*
317-49	30.8	385.4	104.2	1.67*	20.9*	5.7*	.011
318-1	24.8	--	89.8	1.35*	--	4.9*	--
318-2C	25.0	1076.8	148.9	1.12	--	--	--
318-7	23.2	29.2	28.0	--	1.41	2.87	--
318-8	--	526.6	162.6	--	28.2*	8.7*	--
318-8A	--	936.4	--	--	50.23	--	--
318-9	--	92.8	150.2	--	42.8*	8.1*	--
318-11	45.3	--	155.0	2.58	--	9.8*	.015*
318-14	14.6	170.9	29.9	.76*	9.0*	1.6*	.017*
318-16	42.3	831.0	118.0	2.26*	44.4*	2.3*	.019*
318-17	44.2	1246.2	163.0	2.66*	65.5*	8.51*	.014*
318-22	43.2	987.0	146.0	2.25*	51.5*	7.63*	--
318-24	42.5	--	--	2.35	--	--	--
318-24C	--	752.0	134.0	--	33.6	6.01	.010*
318-28	43.9	--	--	2.30*	--	--	.008*
318-29	--	10.1	32.2	--	.5*	1.7*	--
318-30	39.2	563.3	149.62	2.10*	30.2*	8.03*	--
318-21	6.8	80.3	9.6	0.33	3.96	0.47	.009

Sample #	$E_s/\rho_{app.}$ in(×10⁻⁶)	$\sigma_{cs}/\rho_{app.}$ in(×10⁻³)	$\sigma_{UTS}/\rho_{app.}$ in(×10⁻³)	$E_s\left(\dfrac{\rho_{real}}{\rho_{app.}}\right)$ psi(×10⁻⁶)	$\sigma_{cs}\left(\dfrac{\rho_{real}}{\rho_{app.}}\right)$ psi(×10⁻³)	$\sigma_{UTS}\left(\dfrac{\rho_{real}}{\rho_{app.}}\right)$ psi(×10⁻³)	$\rho\left(\dfrac{\rho_a}{\rho_{He}}\right)$ Ω-cm(×10)
318-32	--	650.0	--	--	36.5*	--	--
318-33	46.9	1118.1	164.9	2.62	61.6	9.1	.053
318-34	--	742.0	125.0	--	38.9*	6.57*	--
318-35	46.9	831.0	144.0	2.41*	42.9*	7.4*	.070*
318-36	36.6	505.0	90.6	1.87*	25.7*	4.62*	.008*
318-37	65.7	773.0	117.0	3.50*	41.3*	6.3*	.007*
318-39	67.3	785.0	179.0	3.82*	44.5*	10.1*	.007*
318-45	67.6	--	--	3.34	--	--	.006
318-46	62.7	1149.0	200.0	3.35	60.5	10.5	.029
318-48	--	89.7	212.0	--	4.63*	10.95*	--
318-51	26.0	546.0	45.3	4.23*	23.2*	2.3*	.093*
318-52	46.2	486.8	69.9	2.35*	24.7*	3.55*	--
318-53	--	151.0	51.1	--	7.9*	2.7*	.154
318-58	2.8	--	165.0	.15	--	9.3	--
318-59	60.1	886.0	117.0	3.00	44.2	5.9	.010
318-60	52.0	1055.0	222.0	2.7	54.1	11.4	.029
318-61	40.4	620.0	109.0	2.00	30.9	5.4	--
318-62	--	1195.0	201.0	--	60.2*	10.1*	.021*
321-3	--	1130.0	203.0	--	64.1*	11.5*	.021*
312-6	59.5	1061.0	210.0	3.43*	61.3*	12.1*	.034*
321-8	45.6	1197.0	215.0	2.39*	63.1*	11.4*	--
321-9	--	1283.0	231.0	--	59.3	10.7	.009*
321-10	66.0	1207.0	238.0	3.18*	58.4*	11.5*	.076*
321-11	44.9	1184.0	151.0	2.36*	60.9*	7.77*	.089*
321-12	35.0	427.0	72.0	1.67*	20.3*	3.4*	.007
321-13	48.7	1032.0	176.0	2.64	57.2	9.54	--
321-15	--	994.00	173.0	--	56.1*	9.7*	--
321-16A	50.7	792.0	148.0	3.36*	52.6*	9.8*	--
321-17B	53.5	1089.0	155.0	2.71*	55.1*	7.9*	--
321-18B	80.1	1726.0	246.0	4.02	92.2	13.2	--
321-19A	58.4	1006.0	193.0	2.99	51.4	9.9	--
321-19B	49.9	1055.0	192.0	2.62	55.2	10.1	--
321-20B	--	1381.0	246.4	--	74.6*	13.3*	--

Sample #	$E_s/\rho_{app.}$ in($\times10^{-6}$)	$\sigma_{cs}/\rho_{app.}$ in($\times10^{-3}$)	$\sigma_{UTS}/\rho_{app.}$ in($\times10^{-3}$)	$E_s\left(\dfrac{\rho_{real}}{\rho_{app.}}\right)$ psi($\times10^{-6}$)	$\sigma_{cs}\left(\dfrac{\rho_{real}}{\rho_{app.}}\right)$ psi($\times10^{-3}$)	$\sigma_{UTS}\left(\dfrac{\rho_{real}}{\rho_{app.}}\right)$ psi($\times10^{-3}$)	$\rho\left(\dfrac{\rho_a}{\rho_{He}}\right)(\times10)$ Ω-cm($\times10$)
321-21A	48.8	1344.6	187.6	2.54	70.2	9.8	.013
321-21B	53.6	1288.9	171.1	2.83	68.2	9.1	.014
321-22A	42.6	543.0	181.0	2.21	48.9	9.4	.018
321-22B	--	986.4	129.8	--	54.7	7.19	--
321-22C	42.6	1074.4	129.5	2.31	58.2	7.02	.011
321-22D₄	42.7	1013.9	154.9	2.27	53.8	8.23	.012
321-23	54.8	1565.0	194.0	3.4*	98.0*	12.2*	.008*
321-23A	47.5	1183.4	184.0	2.61	65.2	10.1	.017
321-23B	48.4	1222.8	171.0	2.51	63.4	8.88	.012
321-24	52.9	1297.1	173.0	3.06	74.9	10.0	.012
321-24A	30.6	1430.5	205.1	1.6	75.5	10.8	.009
321-24B	57.6	1170.8	175.5	3.1	62.4	9.4	.011
321-25A	26.9	1103.0	213.5	1.41	58.2	11.2	.006
321-26	--	1466.7	42.8	--	82.4	2.4	--
321-27	20.0	313.3	43.3	1.2*	17.1*	2.4*	.006*
321-29	46.0	1157.0	172.0	2.81	59.2	8.79	.012
321-31F	26.0	503.8	82.6	1.6	30.5	5.0	.052
321-31G	--	599.0	95.2	--	36.0*	5.7*	.011*
321-31J	34.9	687.0	121.0	1.87	36.8	6.5	.010
321-31P	36.1	777.0	111.9	1.63	35.1	5.1	.017
321-31Q	46.3	1143.8	175.9	2.56	63.2	9.73	.011
321-31R	27.0	388.0	58.9	1.45	20.8	3.15	.011
321-31S	44.1	1063.9	160.9	2.22	53.4	8.08	.012
321-32A	26.9	1049.0	111.7	1.45	56.6	6.03	.011
321-32B	27.4	1098.2	171.4	1.50	60.3	9.41	.012
321-32C	27.98	1245.5	183.8	1.52	67.5	9.96	.013
321-32D	44.8	--	--	2.38	--	--	.016
321-32D₁	6.59	--	--	0.35	--	--	.017
321-32E	45.9	1233.7	173.4	2.21*	59.28*	8.33*	.017*
321-32F	26.3	963.5	123.8	1.46	53.4	6.87	--
321-32G	45.45	926.5	131.98	--	--	--	--
321-33A	--	1171.9	175.5	--	59.7*	8.94*	.011*
321-33B	46.3	1666.9	208.0	2.46	88.53	11.05	.02

Sample #	$E_s/\rho_{app.}$ in($\times10^{-6}$)	$\sigma_{cs}/\rho_{app.}$ in($\times10^{-3}$)	$\sigma_{UTS}/\rho_{app.}$ in($\times10^{-3}$)	$E_s\left(\dfrac{\rho_{real}}{\rho_{app.}}\right)$ psi($\times10^{-6}$)	$\sigma_{cs}\left(\dfrac{\rho_{real}}{\rho_{app.}}\right)$ psi($\times10^{-3}$)	$\sigma_{UTS}\left(\dfrac{\rho_{real}}{\rho_{app.}}\right)$ psi($\times10^{-3}$)	$\rho\left(\dfrac{\rho_a}{\rho_{He}}\right)$ Ω-cm($\times10$)
321-34A	42.96	902.4	217.7	2.47*	51.8*	12.5*	.016*
321-34B	86.56	980.5	85.98	4.97	56.3	4.94	.011
321-34D	42.54	--	--	2.29	--	--	--
321-34E	26.8	1191.6	158.2	1.17*	52.1*	6.92*	.0298*
321-36A	--	--	61.3	--	--	3.19	--
321-36B	29.7	1303.7	187.0	1.45	63.6	9.12	.023
321-37B	17.6	231.9	45.7	0.955*	12.57*	2.48*	.0106*
321-37E	32.9	48.7	12.6	2.09	3.1	.802	.0193
321-37F	3.4	44.7	9.37	.192	2.52	.528	--
321-37Q	7.8	65.1	15.6	.46	3.8	.9	.014
321-39	23.7	224.1	43.2	1.37*	13.0*	2.5*	.012*
321-40	--	23.0	2.8	--	1.18*	.14*	.013*
321-42A	12.6	73.9	20.6	.65	3.83	1.07	.012
321-42B	8.5	48.7	17.9	4.6*	2.6*	.96*	.012*
321-43A	22.7	49.7	14.0	1.3*	2.8*	.79*	.017*
321-43B	4.5	33.1	9.1	.24*	1.7*	.47*	.019*
321-46B	5.4	69.1	16.6	.28*	3.6*	.85*	.015*
321-48B	11.4	88.7	20.0	.6*	4.6*	1.0*	.014*
321-50B	40.8	769.9	123.0	2.1*	39.5*	6.3*	.011*
321-51	20.5	255.0	38.2	1.1*	13.8*	2.1*	--
321-51A	--	--	--	--	--	--	.013*
322-1A	9.11	135.0	26.2	.52	7.76	1.5	.012
322-1B	8.67	--	--	.62*	--	--	.016*
322-3A	28.5	265.1	26.9	1.63	15.2	1.55	.008
322-11A	9.4	30.4	6.5	.50	--	--	.010*
322-11B	9.23	112.2	12.1	.53*	2.09*	.45*	.010*
322-12A	12.1	77.3	9.1	.62	5.80	.62	.011
322-12B	13.3	144.0	--	.72	4.2	.49	.011
322-13A	20.9	238.9	--	1.1	7.55	--	.009
322-15B	19.9	140.9	29.1	1.07	12.8	--	.010
322-16B	12.4	--	14.4	.69	7.84	1.62	.011
322-17B	7.8	--	--	.42	--	.77	.018
322-18A	56.1	964.8	162.7	3.02	51.9	8.76	.006

Sample #	$E_s/\rho_{app.}$ in($\times 10^{-6}$)	$\sigma_{cs}/\rho_{app.}$ in($\times 10^{-3}$)	$\sigma_{UTS}/\rho_{app.}$ in($\times 10^{-3}$)	$E_s\left(\frac{\rho_{real}}{\rho_{app.}}\right)$ psi($\times 10^{-6}$)	$\sigma_{cs}\left(\frac{\rho_{real}}{\rho_{app.}}\right)$ psi($\times 10^{-3}$)	$\sigma_{UTS}\left(\frac{\rho_{real}}{\rho_{app.}}\right)$ psi($\times 10^{-3}$)	$\rho\left(\frac{\rho_a}{\rho_{He}}\right)$ Ω-cm($\times 10$)
322-19B	11.56	145.75	14.4	.65	8.16	.804	.014
322-20	27.3	317.6	50.7	1.55	18.0	2.88	.008
322-21	19.8	124.9	27.7	1.04	6.54	1.45	.011
322-22A	--	129.0	37.4	--	6.9	2.0	--
322-22B	--	161.7	37.0	--	8.71	1.99	--
322-23B	--	--	135.7	--	--	7.895	--
322-24A	--	--	40.7	--	--	2.22	--
322-24B	--	--	43.2	--	--	2.48	--
322-25A	52.7	782.0	109.4	2.82	41.8	5.85	.006
322-25A	46.6	619.0	68.25	2.76	36.7	4.04	.007
322-26	57.6	766.8	101.7	--	--	--	--
322-27A	52.7	831.7	87.7	2.7	42.7	4.5	.005
322-28A	--	547.6	94.0	--	28.5	4.89	.006
322-29A	28.5	445.4	68.36	1.5	23.5	3.6	.009
322-30	25.7	87.3	27.17	1.32	4.48	1.29	.011
322-31B	9.63	74.2	14.56	.55	4.24	.831	.015
322-32	13.5	114.5	17.4	.78	6.62	1.005	.011
322-33	23.4	108.2	51.46	1.37	6.33	3.01	.010
322-34	39.5	495.6	142.1	1.91	24.0	6.88	.007
322-35	24.4	424.2	47.8	1.26	21.9	2.47	.012
322-36	40.6	723.4	117.6	2.13	37.9	6.16	.006
322-37	16.7	131.2	41.8	.87	6.83	2.175	.011
322-38	35.27	423.1	93.65	2.14	25.7	5.68	.007
322-39	33.8	473.8	137.9	1.89	26.53	7.72	.007
322-40	39.9	468.74	120.9	2.29	28.1	6.94	.005
322-41	31.8	372.7	98.46	1.83	21.4	5.66	.008
322-42A3	33.8	414.0	114.2	--	--	--	--
322-42A4	29.4	601.1	43.25	--	--	--	--
322-42B1	28.9	414.7	82.2	1.5	21.6	4.28	.009
322-42B2	32.1	486.8	81.9	1.69	25.7	4.32	.009
322-42B3	33.7	735.5	117.9	1.78	38.8	6.22	.0135
322-42B4	29.36	511.6	44.9	1.6	27.9	2.45	.007
322-42B5	30.9	--	--	--	--	--	--

Sample #	$E_s/\rho_{app.}$ in($\times 10^{-6}$)	$\sigma_{cs}/\rho_{app.}$ in($\times 10^{-3}$)	$\sigma_{UTS}/\rho_{app.}$ in($\times 10^{-3}$)	$E_s\left(\dfrac{\rho_{real}}{\rho_{app.}}\right)$ psi($\times 10^{-6}$)	$\sigma_{cs}\left(\dfrac{\rho_{real}}{\rho_{app.}}\right)$ psi($\times 10^{-3}$)	$\sigma_{UTS}\left(\dfrac{\rho_{real}}{\rho_{app.}}\right)$ psi($\times 10^{-3}$)	$\rho\left(\dfrac{\rho_a}{\rho_{He}}\right)$ Ω-cm($\times 10$)
322-42B₆	35.8	621.8	46.5	1.93	33.5	2.5	.010
322-45	22.95	228.2	68.86	1.43	14.2	4.28	.010
322-48	17.5	87.9	40.4	.94	4.7	2.16	.013
322-49A	27.7	—	—	1.46	—	—	.008
322-50	21.2	—	—	1.17	—	—	.007
322-61	14.96	—	—	.79	—	—	.010
322-62	34.9	—	—	1.88	—	—	.006
322-63	46.8	—	—	2.64	—	—	.005
322-63A	57.45	—	—	3.1	—	—	.005
322-64	54.23	—	—	3.13	—	—	.005
322-64B	56.25	—	—	3.27	—	—	.005
322-67	43.0	—	—	2.55	—	—	.005
322-67B	44.9	—	—	2.29	—	—	.006
322-68	19.8	—	—	1.09	—	—	.009
322-68A	--	—	—	—	—	—	.009
322-69	16.8	—	—	.9	—	—	.009
322-69A	16.1	—	—	.96	—	—	.010
322-70	15.2	—	—	.79	—	—	.011
323-2	40.8	—	—	2.14	—	—	.006
323-2A	45.0	—	—	2.34	—	—	.006
323-3A	60.7	—	—	3.36	—	—	.005
323-4	19.5	—	—	1.04	—	—	.0093
323-4A	19.5	—	—	1.04	—	—	.0095

TABLE 11   Comparison of Ultimate Strength
                  Determined by Direct Tension
                       vs. Disc Rupture

Sample #	Direct Tension	Disc Rupture
317-38	3780 psi	5100 psi
318-59	4600 psi	4153 psi
321-16B	5306 psi	4705 psi
321-36A	4081 psi*	2462 psi
321-50B	3780 psi	5228 psi
322-23B	3163 psi	4050 psi
322-24A	1367 psi	1279 psi
322-24B	1122 psi	1279 psi

*Broke in Grip

TABLE 12   Comparison of Sonic Modulus
                      and Mechanical Modulus

Sample #	HTT Temp.°C	Mechanical Modulus	Sonic Modulus
317-8	2000	1.27×10^6	1.82×10^6
317-26	2000	0.38×10^6	0.31×10^6
317-42	2000	1.4×10^6	1.5×10^6
317-46	2000	1.59×10^6	1.27×10^6
318-17	2000	1.16×10^6	1.18×10^6
318-52	2000	2.0×10^6	1.69×10^6
321-12	2000	1.01×10^6	1.22×10^6

TABLE 13   Sonic Modulus vs. Pyrolysis
                          Temperature

$$psi\,(\times 10^{-6})$$

Sample #	700°C	800°C	900°C	1000°C	1577°C	1800°C	2000°C
318-59 #1L	1.02	--	--	2.16	1.95	1.77	1.46
318-59 #2L	1.06	--	--	2.07	2.10	1.82	1.76
318-60L	.93	--	--	--	1.82	1.77	1.70
321-11L	.75	--	--	2.37	1.68	1.72	1.58
321-11CL	.73	--	--	1.75	1.75	1.72	1.66
321-12L	.66	--	--	1.49	2.03	1.23	1.18
321-13 #1L	.80	--	--	1.84	1.77	1.73	1.75
321-13 #2L	.82	--	--	1.84	--	1.79	1.72
321-13 #3L	.88	--	--	1.91	--	1.75	1.72
321-15 #1	.81	--	1.69	1.92	1.91	1.84	1.69
321-15 #2	--	1.53	--	1.96	2.01	1.86	1.71
321-15L	--	1.69	--	2.06	1.875	1.86	1.79
321-16A	--	1.60	--	1.88	1.87	1.70	1.55
321-16AL	--	1.57	--	1.97	1.87	1.67	1.58
321-16B	--	1.68	--	1.87	1.68	1.55	1.48
321-17B	.80	--	1.80	2.12	1.96	1.91	1.81
321-18A	--	1.63	--	2.2	2.14	2.09	1.98
321-18B #1	--	1.73	--	1.48	1.86	1.81	1.73
321-18B #2	--	1.52	--	1.97	2.09	1.74	1.73
321-18BL	--	1.56	--	1.60	1.90	1.83	1.75
321-19A	--	1.53	--	2.03	1.96	1.89	1.83
321-19B #1	.75	--	3.27	1.58	1.78	1.49	1.49
321-19B #2	--	1.32	--	1.69	1.61	1.61	1.55
321-19BL	--	1.40	--	2.15	1.63	1.64	1.55

TABLE 14   Resistivity vs. Pyrolysis Temperature

Ω-cm($\times$10)

Sample #	800°C	900°C	1000°C	1577°C	1800°C	2000°C
318-59 #1L	--	--	.499	.102	.083	.110
318-59 #2L	--	--	.522	.099	.081	.060
318-60L	--	--	.523	.0108	.016	.170
321-11L	--	--	.643	.116	.120	.120
321-11CL	--	--	.471	.098	.090	.170
321-12L	--	--	.542	.148	.120	.06
321-13 #1L	--	--	.506	.120	.170	.100
321-13 #2L	--	--	.521	.106	.160	.110
321-13 #3L	--	--	.490	.111	.110	.110
321-15 #1	--	.143	.014	.0302	.015	.015
321-15 #2	.448	--	.029	.0319	.015	.015
321-15L	.324	--	..10	.115	.170	.110
321-16A	.279	--	.014	.029	.015	.015
321-16AL	.366	--	.170	.089	.120	.100
321-16B	.445	--	.030	.0328	.017	.017
321-17B	--	.083	.080	.0357	.018	.018
321-18A	.238	--	.047	.0333	.017	.017
321-18B #1	.611	--	.059	.0334	.016	.016
321-18B #2	.302	--	.03	.0325	.016	.016
321-18BL	.374	--	.160	.114	.110	.110
321-19A	.317	--	.031	.0332	.017	.017
321-19B #1	--	.171	.017	.0368	.018	.018
321-19B #2	.302	--	.03	.0325	.016	.016
321-19BL	.355	--	.150	.081	.110	.110